8-1-1975

Hydrography and Hydrodynamics of Virginia Estuaries VI: Mathematical Model Studies of Water Quality of the Rappahannock Estuary

A. Y. Kuo
Virginia Institute of Marine Science

A. Rosenbaum
Virginia Institute of Marine Science

P. V. Hyer
Virginia Institute of Marine Science

C. S. Fang
Virginia Institute of Marine Science

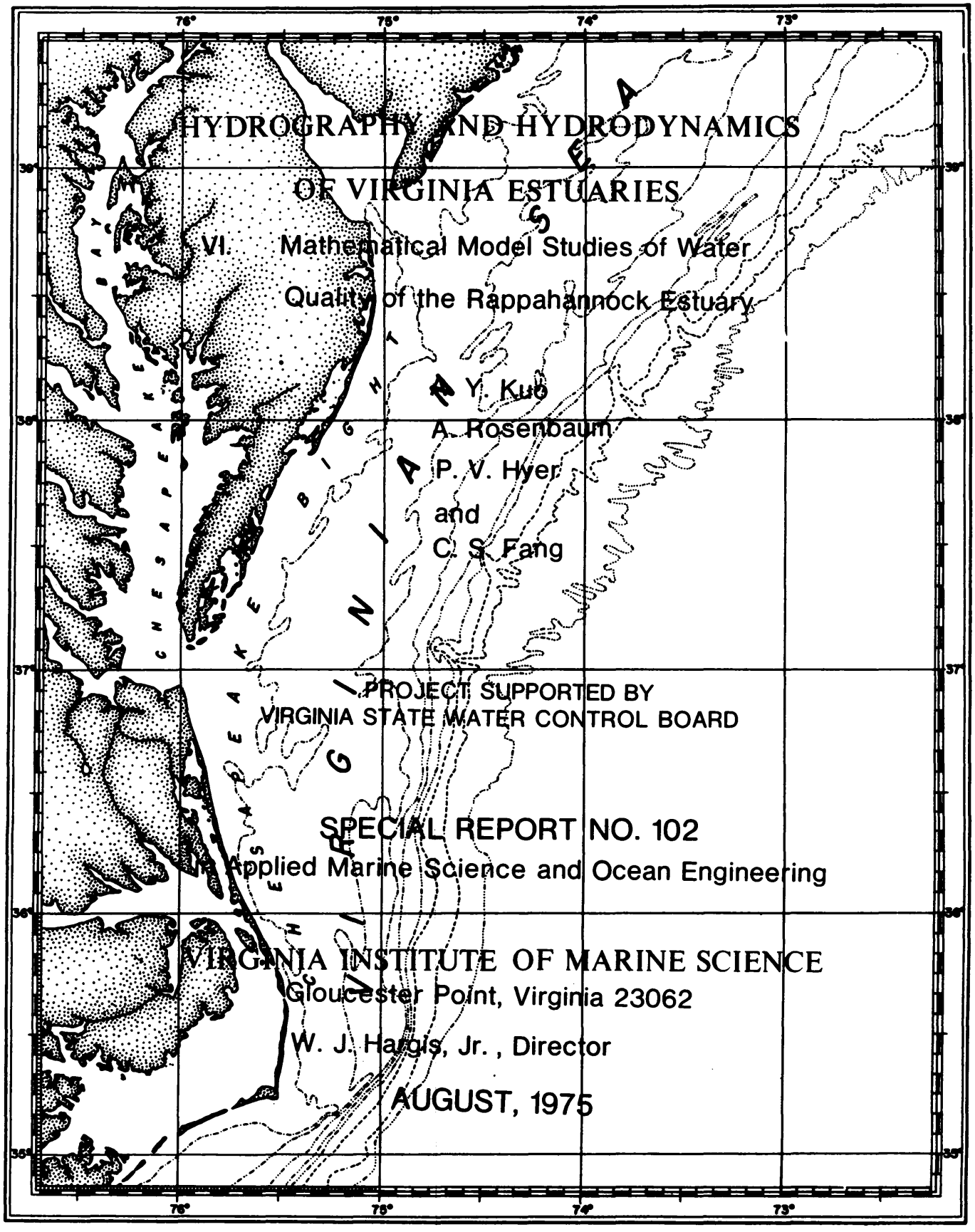

HYDROGRAPHY AND HYDRODYNAMICS OF VIRGINIA ESTUARIES

VI. Mathematical Model Studies of Water Quality of the Rappahannock Estuary

Y. Kuo

A. Rosenbaum

P. V. Hyer

and

C. S. Fang

PROJECT SUPPORTED BY
VIRGINIA STATE WATER CONTROL BOARD

SPECIAL REPORT NO. 102

In Applied Marine Science and Ocean Engineering

VIRGINIA INSTITUTE OF MARINE SCIENCE

Gloucester Point, Virginia 23062

W. J. Hargis, Jr., Director

AUGUST, 1975

HYDROGRAPHY AND HYDRODYNAMICS OF VIRGINIA ESTUARIES

VI. Mathematical Model Studies of Water Quality of the Rappahannock Estuary

by

A. Y. Kuo
A. Rosenbaum
P. V. Hyer
and
C. S. Fang

PREPARED UNDER

THE COOPERATIVE STATE AGENCIES PROGRAM

FOR

VIRGINIA STATE WATER CONTROL BOARD

Project Officers

Dale Jones
Michael Bellanca

Virginia State Water Control Board

Special Report No. 102

in Applied Marine Science and

Ocean Engineering

Virginia Institute of Marine Science
Gloucester Point, Virginia 23062

William J. Hargis, Jr.
Director

August, 1975

TABLE OF CONTENTS

LIST OF TABLES

LIST OF FIGURES

ACKNOWLEDGEMENTS

The comments and suggestions of Messrs. Dale Jones, Mike Bellanca, Drs. Wen Kao and Jack Hyden of the State Water Control Board are greatly appreciated.

We thank Mr. John Jacobson for his supervision of the field study and Mrs. Shirley Crossley for her patient typing of this report. We appreciate the efforts of Ms. Terrell Markle in proofreading and preparation of the figures.

The funding of this project is a joint program supported by Virginia State Water Control Board and Virginia Institute of Marine Science through the Cooperative State Agencies Program.

ABSTRACT

In Summer, 1973 an extensive field program was conducted in the Rappahannock Estuary from Windmill Point to Tappahannock. Time series data in three spatial dimensions were collected for dissolved oxygen, salinity, temperature, and current velocity. In addition, the rate of dispersal of a batch of dye was observed. These data, combined with the results of an earlier similar study of the reach from Tappahannock to Fredericksburg, were used to calibrate and verify three one-dimensional, time dependent mathematical models. One of these models predicts the intratidal distribution of dissolved oxygen, biochemical oxygen demands and salinity. This model employs an implicit scheme for numerical time integration. The other two models, one with implicit scheme and the other with explicit scheme, are non-tidal and are used to predict the long-term intrusion of salinity under the influence of mean advection and tidal mixing. The long-term salinity models have been applied to investigate the salinity concentration changes for the proposed Salem Church Dam project.

I. Summary & Conclusions

1. The Rappahannock Drainage Basin is relatively unpopulated, and agricultural in nature. Petrochemicals, commercial fishing and fish processing are important to the region. Recreational water uses are also important. The region is characterized by hot summers and mild, wet winters.

2. An hydrographic survey was conducted in July, 1973, at nine transects between the entrance and Tappahannock. Time series data on salinity, temperature, dissolved oxygen and tidal current were collected at one to three stations on each transect. During the same period of time a batch release of dye was made near Tappahannock and daily slack water runs were conducted to collect dye and hydrographic samples.

3. This survey complements a similar one conducted in 1970 for the reach between Fredericksburg and Tappahannock.

4. Data on long-term variations were collected by means of monthly or semi-monthly slack water runs. On each slack water run, salinity, temperature, biochemical oxygen demand and dissolved oxygen were sampled at thirty-three transects.

5. Time-series data from the intensive field surveys reveal tidal periodicity in salinity and in some cases tidal periodicity in dissolved oxygen concentration.

6. Slack water run data indicate that the upstream limit of salt water intrusion at high water slack varies approximately between mile 62 (Leedstown) during low flow and mile 46 (Mulberry Pt.) during high flow. Surface salinity at Tappahannock varies from 1 part per thousand during high flow to 7 parts per thousand during low flow.

7. Critical conditions for oxygen depletion, namely high water temperature and low freshwater discharge were found to occur during the months of August and September.

8. Two critical reaches have been identified. a.) The first is immediately downstream of Fredericksburg, where (at the time of the 1970 survey) high man-made loading from the Fredericksburg STP and an FMC Corp. plant depressed the cross-sectional average dissolved oxygen level below 4.0 parts per million. 1973 and 1974 data show an improvement in dissolved oxygen in this reach. Under conditions of high temperatures and low freshwater discharge comparable to those of 1970, a minimum cross-sectional average dissolved oxygen concentration of less than 5.0 ppm was observed only once. This improvement may be associated with the lower reported man-made loading. b) The second critical reach

is near the mouth, where a combination of non-point source loading from intensive fishing activity and restraint of vertical mixing by natural geographic features produces dissolved oxygen values of 2.0 or less at depths of 10 meters or more.

9. Two types of models have been completed and verified for the Rappahannock River:

i. Tidal-time model for DO, BOD and salinity;

ii. Long-term tidal average model for salinity.

II. INTRODUCTION

A previous report of the estuarine modeling project being carried out under the Cooperative State Agencies program (Fang, et al., 1972) concentrated on the tidal Rappahannock upstream of Tappahannock. That portion of the estuary was studied intensively in the summer of 1970 and models were produced for that reach only. The work upon which this report is based was undertaken in order to study the remainder of the Rappahannock estuary. The necessary field work was performed in the summer of 1973 and models were produced of the entire tidal Rappahannock. This report concerns the 1973 field study and the extension of models to cover the entire Rappahannock.

The models reported on in this report are as follows: a real-time, intra-tidal model of dissolved oxygen, carbonaceous biochemical oxygen demand (BOD), nitrogenous BOD and salinity; two tidal average salinity intrusion models, one based on an explicit integration scheme and the other on an implicit integration scheme.

This study is a part of our continuous program of development and evaluation of mathematical modeling techniques and of the application of such models and techniques to studies of tidal tributaries and coastal waters of Virginia under the Cooperative State Agencies Program.

III. DESCRIPTION OF STUDY AREA

Downstream of Tappahannock, the Rappahannock drainage basin is a coastal plain, fairly level and low lying, with several marshes bordering the river and its tributaries (see figure 1). The river basin is accordingly broad and shallow, except for a central channel. A sill at the river mouth with a depth of approximately thirty feet confines the channel to form a basin with a maximum depth of seventy feet.

The Rappahannock is classified as a moderately mixed estuary in which the removal of salt at the surface is compensated for by a net advection upstream at the bottom. Nichols (1972) has observed the effects of this circulation on the distribution of suspended sediment. There seems to be a zone of maximum turbidity at the upstream limit of saline intrusion, apparently caused by the convergence of bottom water.

Since the estuary empties into Chesapeake Bay, salinity in the estuary is moderated by remoteness from the ocean and the effect of freshwater flow in other tributaries to the Bay, especially the Susquehanna. Salinity at the mouth of the Rappahannock rarely exceeds twenty parts per thousand.

The tidal wave takes approximately 9 hours to propagate upstream from the mouth at Windmill Point to the fall line at Fredericksburg, The tide undergoes certain changes as it propagates. The mean tide range increases from 1.2 feet

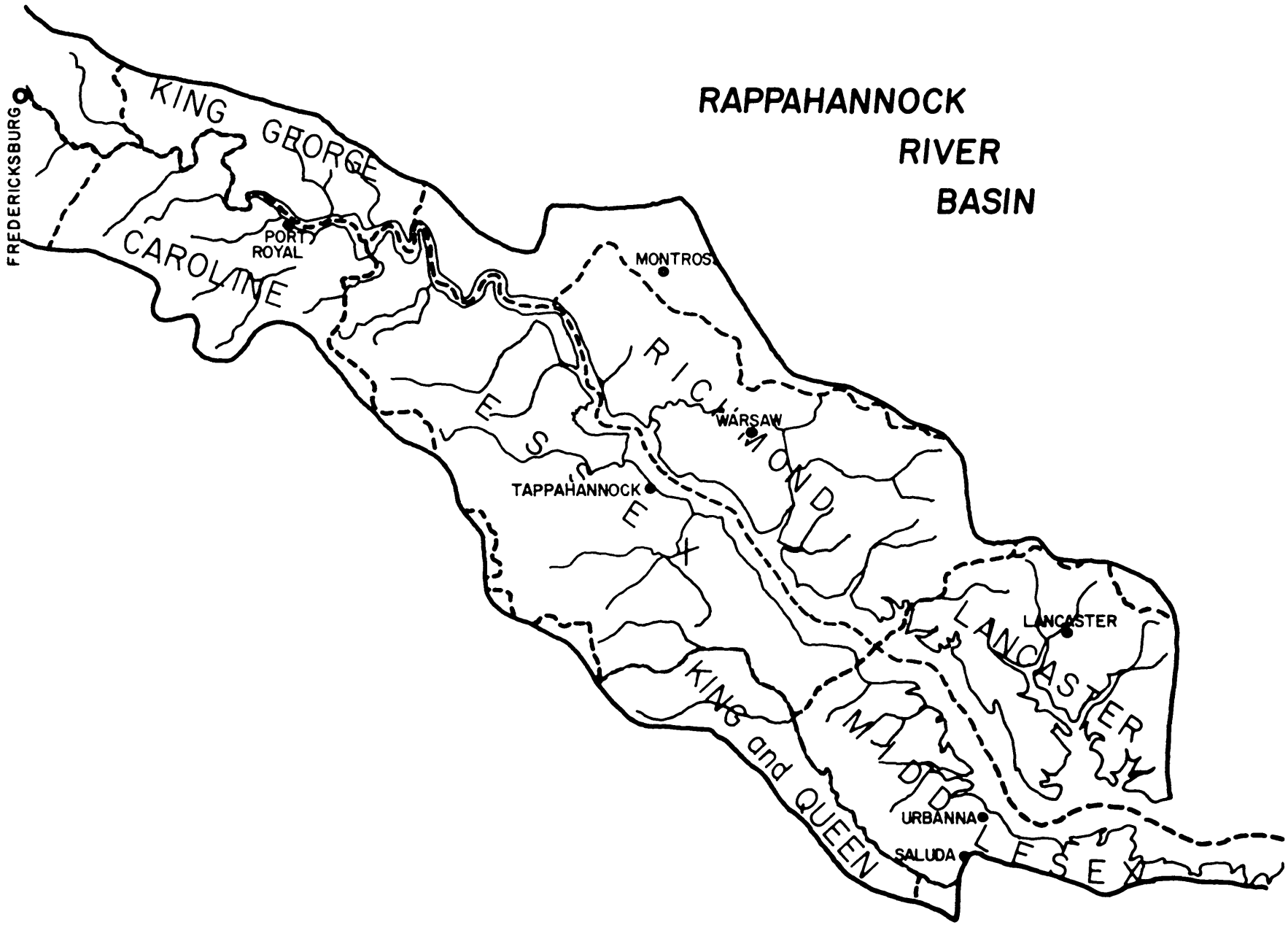

Figure 1. The Rappahannock River Estuary of Virginia. (From Planning Bulletin 219, Volume I. Division of Water Resources)

near the river mouth to 1.8 feet at Bowlers Rock, then decreases slightly to 1.5 feet at Leedstown, and increases again to 2.8 feet at Fredericksburg. The mean tidal current increases from 1.0 feet per second near the mouth to 2.2 feet per second at Tappahannock, then decreases again to 1.2 feet per second at Port Royal. Another evident change is the transition away from a pure traveling wave. At Orchard Point, near the mouth of the Rappahannock maximum ebb occurs less than 1.5 hours before low water. At Port Royal, however, this time difference is more than two hours.

The climate of the region is classified as humid subtropical. Solar insolation tends to be quite strong in the summer, leading to considerable warming of the river water. Through the combined effects of evapotranspiration and low freshwater input, there is a period of low flow, usually overlapping the period of very warm river water. At the opposite end of the hydrologic cycle, heavy spring rains produce high river flow which, in this saline system, causes considerable density stratification.

The salinity distribution in the Rappahannock makes a large portion of the estuary and its tidal tributaries favorable for growing oysters, i.e. salinity is high enough to allow oysters to grow, yet low enough to discourage the most serious predators, namely oyster drills and MSX. Oyster culture activity frequently implies an oyster processing industry along the shores of the river in which it occurs, and there are several processing houses on the Rappahannock estuary. Other commercial fisheries are active

in the Rappahannock. There is a resort industry based on sport fishing in the Rappahannock. Along most of the river shores agricultural, timber land and summer and permanent housing sites predominate. There is also a farm on the shores of the Rappahannock devoted to the raising of ducks for market.

Being principally rural in nature, the drainage basin supports farming and lumbering. The main crops grown are corn and soybeans. The mainstay of the lumber industry is the loblolly pine, used mainly for the production of paper.

IV. HYDROGRAPHIC SURVEY

1. Description of Surveys

To provide the necessary data for construction and verification of the mathematical models, a number of field programs were carried out. An intensive field survey was conducted in July, 1973, when nine transects were occupied between Windmill Point and Tappahannock. Three stations were occupied at hourly intervals at each transect, for three days, and one overnight period. Figure 2 shows the transects occupied and figure 3 depicts the distances upstream schematically. Conductivity and temperature measurements and dissolved oxygen and dye samples were taken at two-meter intervals from surface to bottom. Simultaneously, current meters were in place at three or more depths at each station taking twenty-minute averages of water speed and direction.

Concurrently with this intensive field study, a dye dispersion study was conducted. Four barrels of DuPont Rhodamine WT (250 lbs. of 20% solution per barrel) were released near evening slack before ebb on July 18 at buoy BW"R12". This buoy is approximately 43 miles upstream of the river mouth and about 1000 feet downstream of the bridge at Tappahannock. The dye was poured into the prop wash from a boat moving across the stream, in order to mix the dye into the water and create an initial distribution which was mixed in the lateral and vertical directions.

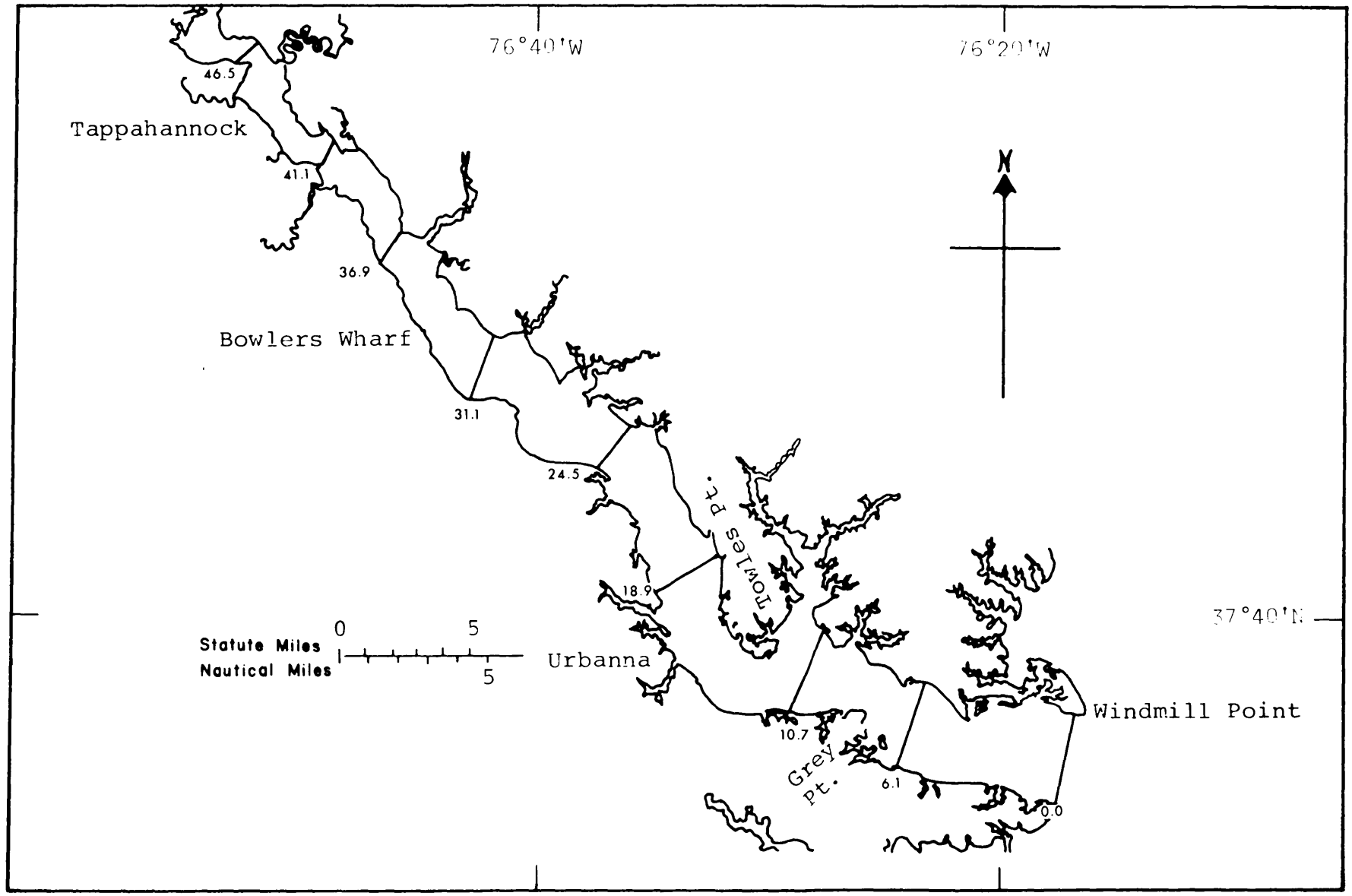

Figure 2. Locations of transects occupied during intensive field survey, 1973.

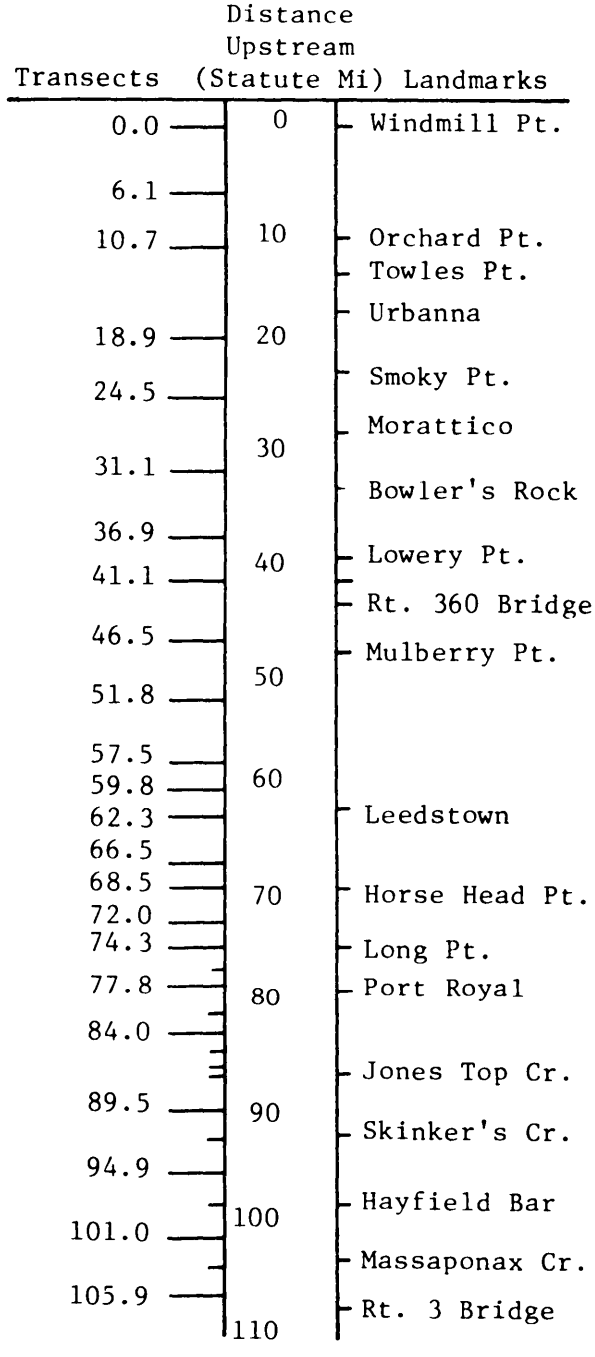

Figure 3. Locations of Rappahannock stations with respect to landmarks.

Such an initial distribution of dye will undergo one-dimensional dispersion in the longitudinal direction.

Dye samples were collected on slack water runs for more than two weeks after the initial dye release. Samples were also collected at the anchor stations. Surface, middle and bottom waters were sampled.

These studies complement similar ones carried out in 1970 in the reach from Tappahannock to Fredericksburg (Fang, et al., 1972).

A bathymetric survey was made in 1973 by the U. S. Army Corps of Engineers. One hundred and two bottom profiles were collected.

A program of monthly slack water runs has been going on since August, 1970. In these runs, dissolved oxygen and biochemical oxygen demand samples and temperature and conductivity measurements are taken at two-meter intervals from surface to bottom. The slack water stations generally coincide with the intensive field survey transects.

2. Instrumentation and Analysis

Dissolved oxygen samples were collected with a Frautschy bottle and stored in 125 ml glass sample bottles and "pickled" in the field. The samples were titrated in the laboratory using the Azide modification of the modified Winkler Method. Biochemical oxygen demand (BOD) samples were collected in Frautschy bottles and transferred to 500 ml dark bottles. These samples were then incubated for five days at $20^{o}C$ and analyzed for DO content using the Modified Winkler Method.

Conductivity and temperature were measured using an InterOcean Model 513 CTD. Salinity was calculated from conductivity and temperature according to laboratory calculations. Occasional spot-check salinity samples were stored in 125 ml sample bottles and analyzed in the laboratory using a Beckman RS-7A salinometer. These data for the intensive field study are presented graphically in Appendix A.

Dye samples were analyzed in the laboratory using a Turner Associates fluorometer. Calibration standards were made up from using a sample of concentrated dye and Rappahannock River water collected before the dye release. By successive dilution, standard samples were prepared which covered the range of dye concentrations from more than one part per million (visible to the naked eye) down to 0.05 parts per billion, which is about the threshold of the fluorometer and too weak to be seen by eye. Calibration curves were made up from these standards. Observed dye concentrations are presented in Appendix B. The concentrations at slack tides were plotted against distance in figures B1 to B14. The curves represent data from slack water runs in which data were collected at top, middle and bottom of the channel. The points represent cross-sectional averages from data collected at anchor stations at which data were also collected at side channels or shoals. The

cross-sectional average concentration of transects were plotted against time in figures B15 to B19.

Dye samples were analyzed in the laboratory using a Turner Associates fluorometer. Results of the dye study are shown graphically in Appendix B.

All hydrographic data were keypunched in a standard format, edited and stored in a magnetic disk data file.

Cross-sectional areas were determined by planimetry of the bottom profile data and adjusted to mean sea level. Channel widths were determined from Geological Survey 7.5 minute quadrangles. Reach lengths were determined from Coast & Geodetic Survey navigation charts.

Current meter data were collected by means of Braincon film-recording current meters. These meters were equipped with a vane for indicating current direction and a Savonious rotor for determining speed. An internal camera recorded the current direction, meter tilt and total number of rotor revolutions over a twenty-minute period. The photographic film was developed and analyzed using a scanner interfaced with a tape recorder. Speed and direction were calculated from the digitized data. The longitudinal component of velocity was calculated for each frame and cross-section averages of tidal current were calculated for each twenty-minute period, weighting each station according to depth. Tidal fluxes were calculated by

multiplying average tidal current by cross-sectional area at mean sea level. The results of these calculations are shown in Appendix C. Ebb currents are positive and flood currents are negative in these figures.

Tidal volume and drainage area figures have been worked out for Chesapeake Bay and all its tributaries by Cronin (1971) & Seitz (1971) of CBI. Accumulated drainage area and geometrical data for the tidal Rappahannock are summarized in Table 1.

Table 1

Geometric Data for Rappahannock River

Distance Upstream (statute miles)	Conveyancy Area (ft^2)	Cross-Section Area (ft^2)	Transect Mean Depth (ft)	Accumulated Drainage Area (mi^2)
109.70	900.00	900.00	3.00	1616.23
108.70	1400.00	1400.00	4.00	1620.00
107.90	1772.50	1772.50	4.27	1624.45
107.10	2180.40	2180.40	8.55	1630.20
106.60	3162.00	3162.00	12.78	1633.49
105.80	3339.60	3339.60	9.93	1639.24
105.10	3625.30	3625.30	11.51	1644.17
104.30	4934.00	4934.00	13.61	1649.92
103.90	3034.30	3034.30	9.63	1653.21
103.30	3919.50	3919.50	11.04	1658.65
102.80	4018.50	4018.50	10.44	1663.72
102.10	3488.40	3488.40	8.23	1671.32
101.70	4752.90	4752.90	11.32	1676.39
101.10	3686.20	3686.20	8.99	1682.72
100.60	4904.90	4904.90	11.41	1687.79
100.10	4438.60	4438.60	12.16	1694.12
99.60	4473.90	4536.40	9.32	1699.19
99.00	3776.00	3856.00	10.94	1705.52
98.50	4148.20	4310.20	11.06	1711.86
98.00	4871.30	4871.30	10.83	1716.92
97.30	4679.90	4679.90	9.13	1722.18
96.80	5773.60	5773.60	15.00	1725.37
96.50	4940.30	4940.30	10.08	1727.77
95.90	5693.30	5693.30	8.97	1731.76
95.20	4674.50	4674.50	8.90	1736.55
94.70	5681.50	5681.50	9.16	1740.54
94.30	5985.30	5985.30	21.76	1742.93
93.40	5630.80	5630.80	17.33	1749.32
92.70	6148.50	6148.50	11.71	1754.11
92.10	5803.30	6153.30	8.41	1758.10
91.50	6595.60	6595.60	18.58	1758.70
91.10	6521.50	6521.50	10.85	1759.18
90.60	8426.10	8426.10	24.42	1759.66
89.80	6874.70	6874.70	10.04	1760.53
89.10	6197.80	6522.80	16.31	1761.22
88.70	8073.20	8073.20	21.53	1761.70
88.20	6956.80	6956.80	16.66	1762.18
87.50	8075.10	8075.10	9.91	1762.90
86.60	7834.60	7834.60	19.00	1763.86
86.10	8487.90	8555.90	12.04	1764.91
85.60	8277.00	9252.00	15.92	1766.95
84.90	9020.30	9127.80	12.11	1769.36
84.00	9530.90	9530.90	21.78	1772.65
83.50	8916.00	8916.00	13.31	1774.28
82.80	8057.80	8057.80	21.78	1776.69

Table 1 (cont'd)

Distance Upstream (statute miles)	Conveyancy Area (ft^2)	Cross-Section Area (ft^2)	Transect Mean Depth (ft)	Accumulated Drainage Area (mi^2)
82.20	11258.50	11258.50	22.29	1778.72
81.30	9006.00	9110.00	14.30	1782.01
80.40	9695.50	9761.50	16.03	1787.01
79.60	10608.70	11562.70	9.56	1795.97
78.80	11309.00	12113.00	13.80	1805.00
78.10	12491.00	12491.00	9.30	1813.00
77.30	10583.00	12983.00	10.70	1822.00
76.50	12762.00	13095.00	24.80	1831.00
75.90	11886.00	11886.00	14.90	1837.00
75.20	16691.00	17807.00	10.80	1845.00
74.50	16120.00	16120.00	15.00	1849.00
73.20	16050.00	16051.00	22.00	1857.00
72.30	16623.00	16623.00	29.40	1863.00
71.50	16836.00	20179.00	13.40	1867.00
70.40	22659.00	27459.00	23.90	1874.00
69.70	17030.00	17800.00	18.90	1878.00
68.70	24372.00	24372.00	35.80	1884.00
68.10	18064.00	18064.00	25.60	1889.00
67.50	19180.00	19375.00	16.80	1894.00
67.00	20398.00	20398.00	15.50	1897.00
66.30	23159.00	23335.00	14.20	1903.00
65.40	21889.00	23329.00	13.50	1910.00
64.60	25080.00	25850.00	13.80	1917.00
63.60	25886.00	26321.00	11.50	1925.00
62.90	24133.00	24661.00	37.10	1927.00
61.80	22792.00	22891.00	31.20	1929.00
61.30	27797.00	29017.00	14.00	1930.00
60.60	22927.00	23599.00	23.60	1931.00
59.90	24670.00	24670.00	21.30	1932.00
59.40	29953.00	30793.00	22.70	1932.00
58.70	33304.00	34318.00	13.50	1933.00
58.20	31903.00	31903.00	22.20	1934.00
56.70	31245.00	31245.00	11.80	1939.00
55.30	28253.00	31054.00	22.70	1944.00
54.00	28965.00	30585.00	19.30	1949.00
53.10	32446.00	34550.00	13.90	1953.00
51.90	31161.00	32245.00	15.00	1958.00
50.70	31016.00	40936.00	13.20	1972.00
49.50	39650.00	39650.00	11.80	1985.00
47.40	40145.00	40145.00	10.40	2009.00
45.90	63278.00	63278.00	15.40	2029.00
44.80	43684.00	53434.00	7.20	2057.00
43.60	55343.00	55343.00	8.90	2086.00
41.10	59763.00	61653.00	9.10	2150.00
39.00	71888.00	71888.00	9.40	2204.00
36.20	105393.00	105393.00	8.90	2281.00
34.80	93560.00	96216.00	10.40	2318.00
31.60	136855.00	136855.00	10.40	2342.00

Table 1 (cont'd)

Distance Upstream (statute miles)	Conveyancy Area (ft^2)	Cross-Section Area (ft^2)	Transect Mean Depth (ft)	Accumulated Drainage Area (mi^2)
28.90	144068.00	144068.00	12.20	2359.00
25.90	188284.00	188284.00	12.50	2407.00
23.00	258029.00	258029.00	17.40	2455.00
19.50	287866.00	287866.00	19.00	2503.00
15.80	294324.00	301344.00	25.60	2535.00
13.00	287038.00	291038.00	30.50	2541.00
9.30	380048.00	399403.00	29.50	2587.00
7.00	415308.00	420308.00	32.40	2594.00
3.70	357018.00	369258.00	34.20	2602.00
0.70	399722.00	406562.00	22.50	2607.00

V. WATER QUALITY MODEL STUDY

The implicit scheme water quality model of upper tidal Rappahannock (Fang, et.al., 1972) was extended to cover the whole length of the tidal Rappahannock River. The model is a one-dimensional, real-time, intra-tidal model. The model was refined to treat the carbonaceous and nitrogenous biochemical oxygen demands separately. The finite difference formulation has been modified for a more efficient numerical integration. The description of the model is presented in the following in its entirety.

1. Basic Principle of the Model

The model is based on the equation describing the mass-balance of a dissolved or suspended substance in a water body. To facilitate the numerical computation, the river is divided into a number of volume elements, called reaches, by a series of lateral transects perpendicular to its axis. The concentration of a substance is represented by an average value within the volume element. Changes in the amounts of a substance with respect to time in a particular reach may be due to:

(1) advection and dispersion which physically transport materials into or out of the reach through the bounding transects,

(2) biochemical decay or creation of the substance within the reach,

(3) addition or removal of the substance due to external sources or sinks.

These mechanisms may be expressed mathematically to formulate a mass-balance equation for substances such as sea salt, oxygen, biochemically degradable material, or any form of nutrients.

Considering the mth reach of the river bounded by the mth and (m+1)th transects as shown in the sketch below:

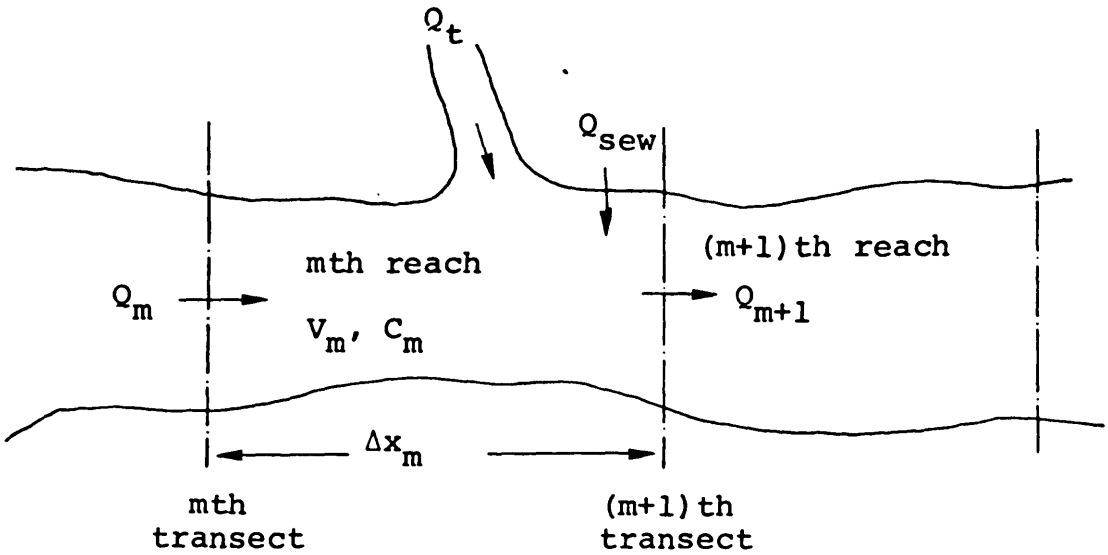

the time rate of change of the total amount of a particular substance within the reach may be expressed as:

$$\frac{\partial}{\partial t}(C_m V_m) = Q_m C_m^* - Q_{m+1} C_{m+1}^* + \left(EA\frac{\partial C}{\partial x}\right)_{m+1} - \left(EA\frac{\partial C}{\partial x}\right)_m + SO_m \qquad (1)$$

where

t = time,

x = the distance along the river axis,

C_m = the volume average concentration of the mth reach,

V_m = the volume of the mth reach,

Q_m = the flow rate of water through the mth transect,

C_m^* = the concentration of the water, flowing through the mth transect,

E_m = dispersion coefficient at the mth transect,

A_m = the cross-sectional area of the mth transect,

SO_m = external sources or sinks.

Of the terms on the right hand side of the equation (1), the first two represent advective transport, the next two represent dispersive transport, the last represents the internal decay and creation, plus the external addition and removal of which the mathematical expressions are different for different substances.

The time rate of change of water volume may be expressed as

$$\frac{\partial V_m}{\partial t} = Q_m - Q_{m+1} + Q_\ell \tag{2}$$

where $Q_\ell = Q_t + Q_{sew}$, and

Q_t = discharge from tributaries,

Q_{sew} = discharge from human activities such as sewage flow.

Substituting equation (2) into equation (1) and dividing the resulting equation by V_m, it is obtained

$$\frac{\partial C_m}{\partial t} = \frac{Q_m}{V_m}(C_m^* - C_m) - \frac{Q_{m+1}}{V_m}(C_{m+1}^* - C_m) + \frac{1}{V_m}\left(EA\frac{\partial C}{\partial x}\right)_{m+1} - \frac{1}{V_m}\left(EA\frac{\partial C}{\partial x}\right)_m + \frac{1}{V_m}(SO_m - Q_\ell C_m) \tag{3}$$

2. Finite Difference Approximation in Time Domain

With proper initial and boundary conditions, equation (3) may be integrated with respect to time to obtain the temporal variations of concentration within each reach of the river. To solve the equation with a digital computer, it is integrated numerically over successive

finite time intervals. At each integration step over a time increment, the various parameters, such as flow rates, dispersion coefficients, etc., should assume representative values during this particular time interval. An implicit scheme is used to formulate the finite difference equation, i.e., the concentration at the end of the time step as well as that at the beginning of the time step is used to express the right hand side of equation (3).

Equation (3) is approximated by the following finite difference form,

$$\frac{C'_m - C_m}{\Delta t} = \frac{1}{2}\left\{\frac{Q'_m}{V'_m}(C^{*\prime}_m - C'_m) + \frac{Q_m}{V_m}(C^*_m - C_m)\right\}$$
$$- \frac{1}{2}\left\{\frac{Q'_{m+1}}{V'_m}(C^{*\prime}_{m+1} - C'_m) + \frac{Q_{m+1}}{V_m}(C_{m+1} - C_m)\right\}$$
$$+ \frac{E'_{m+1}A'_{m+1}}{V'_m}\frac{C'_{m+1} - C'_m}{\Delta x_m + \Delta x_{m+1}} + \frac{E_{m+1}A_{m+1}}{V_m}\frac{C_{m+1} - C_m}{\Delta x_m + \Delta x_{m+1}}$$
$$- \left(\frac{E'_m A'_m}{V'_m}\frac{C'_m - C'_{m-1}}{\Delta x_m + \Delta x_{m-1}} + \frac{E_m A_m}{V_m}\frac{C_m - C_{m-1}}{\Delta x_m + \Delta x_{m-1}}\right)$$
$$+ \overline{\frac{1}{V_m}(SO_m - Q_\ell C_m)} \qquad (4)$$

where Δt is the time increment. The primed and unprimed variables designate the parameters evaluated at the end and beginning of time interval respectively, and the over bar represents the average value over the time interval.

The concentration, C^*_m, of the water flowing through the mth transect is calculated as a weighted average of the concentrations in the adjacent reaches, C_{m-1} and C_m. Thus

$$C^*_m = \alpha\, C_{m-1} + (1-\alpha)C_m \qquad (5)$$

$$C^{*\prime}_m = \alpha' C'_{m-1} + (1-\alpha')C'_m \qquad (6)$$

where the weighting factors α and α' depend on the direction of flow through the transect,

$$0.5 \leq \alpha \leq 1 \qquad \text{if } Q_m \geq 0$$

$$0 \leq \alpha \leq 0.5 \qquad \text{if } Q_m < 0$$

and

$$0.5 \leq \alpha' \leq 1 \qquad \text{if } Q_m' \geq 0$$

$$0 \leq \alpha' \leq 0.5 \qquad \text{if } Q_m' < 0$$

Similarly,

$$C^*_{m+1} = \alpha_2 C_{m+1} + (1-\alpha_2) C_m \tag{7}$$

$$C^{*'}_{m+1} = \alpha'_2 C'_{m+1} + (1-\alpha'_2) C'_m \tag{8}$$

and

$$0.5 \leq \alpha_2 \leq 1 \qquad \text{if } Q_{m+1} < 0$$

$$0 \leq \alpha_2 \leq 0.5 \qquad \text{if } Q_{m+1} \geq 0$$

$$0.5 \leq \alpha'_2 \leq 1 \qquad \text{if } Q'_{m+1} < 0$$

$$0 \leq \alpha'_2 \leq 0.5 \qquad \text{if } Q'_{m+1} \geq 0$$

Substituting equations (5), (6), (7) and (8) into equation (4), it is obtained that

$$\begin{aligned} C'_m - C_m = {} & \frac{\Delta t}{2}\left\{\frac{Q'_m}{V'_m}\alpha'(C'_{m-1} - C'_m) + \frac{Q_m}{V_m}\alpha(C_{m-1} - C_m)\right\} \\ & - \frac{\Delta t}{2}\left\{\frac{Q'_{m+1}}{V'_m}\alpha'_2(C'_{m+1} - C'_m) + \frac{Q_{m+1}}{V_m}\alpha_2(C_{m+1} - C_m)\right\} \\ & + \frac{E'_{m+1}A'_{m+1}}{V'_m}\cdot\frac{\Delta t}{\Delta x_m + \Delta x_{m+1}}(C'_{m+1} - C'_m) \\ & + \frac{E_{m+1}\cdot A_{m+1}}{V_m}\cdot\frac{\Delta t}{\Delta x_m + \Delta x_{m+1}}(C_{m+1} - C_m) \\ & + \frac{E'_m \cdot A'_m}{V'_m}\cdot\frac{\Delta t}{\Delta x_m + \Delta x_{m-1}}(C'_m - C'_{m-1}) \\ & + \frac{E_m \cdot A_m}{V_m}\cdot\frac{\Delta t}{\Delta x_m + \Delta x_{m-1}}(C_m - C_{m-1}) + \frac{\Delta t}{V_m}(SO_m - Q_\ell C_m) \end{aligned} \tag{9}$$

Defining

$$ADV_m = \frac{\Delta t}{2} \cdot \frac{AC_m}{V_m}$$

$$ADV2_m = \frac{\Delta t}{2} \quad \frac{AC_{m+1}}{V_m}$$

$$DIF_m = \frac{\Delta t}{\Delta x_m + \Delta x_{m-1}} \cdot \frac{E_m \cdot A_m}{V_m}$$

$$DIF2_m = \frac{\Delta t}{\Delta x_m + \Delta x_{m+1}} \cdot \frac{E_{m+1} \cdot A_{m+1}}{V_m}$$

$Q_m = AC_m \cdot U_m$

$Q_{m+1} = AC_{m+1} \cdot U_{m+1}$

U_m = advective velocity

AC_m = conveyancy cross-sectional area

and similarly for the primed variables, equation (9) becomes

$$\begin{aligned} & C'_m (1-\alpha'_2 U'_{m+1} \cdot ADV2'_m + \alpha' U'_m \cdot ADV'_m + DIF'_m + DIF2'_m) \\ = \; & C'_{m+1} (-\alpha'_2 U'_{m+1} \cdot ADV2'_m + DIF2_m) + C'_{m-1} (\alpha' U'_m \cdot ADV'_m \\ & + DIF'_m) + C_m (1+\alpha_2 U_{m+1} \cdot ADV2_m - \alpha U_m \cdot ADV_m \\ & - DIF2_m - DIF_m) + C_{m+1} (-\alpha_2 U_{m+1} \cdot ADV2_m + \\ & DIF2_m) + C_{m-1} (\alpha U_m \cdot ADV_m + DIF_m) \\ & \overline{\qquad\qquad\qquad\qquad\qquad\qquad\qquad\qquad\qquad\qquad} \\ & + \frac{\Delta t}{V_m} (SO_m - Q_\ell C_m) \end{aligned} \tag{10}$$

Equation (10) is further simplified to

$$\begin{aligned} & (1+COE_m) C'_m = COE2_m \cdot C'_{m+1} + COE1_m \cdot C'_{m-1} \\ & + CON_m \cdot C_m + CON2_m \cdot C_{m+1} + CON1_m \cdot C_{m-1} \\ & \overline{\qquad\qquad\qquad\qquad\qquad\qquad\qquad\qquad\qquad\qquad} \\ & + \frac{\Delta t}{V_m} (SO_m - Q_\ell C_m) \end{aligned} \tag{11}$$

where

$$COE_m = \alpha' U'_m \cdot ADV'_m - \alpha'_2 U'_{m+1} \cdot ADV2'_m + DIF'_m + DIF2'_m$$

$$COE1_m = \alpha' U'_m \cdot ADV'_m + DIF'_m$$

$$COE2_m = -\alpha_2' U'_{m+1} \cdot ADV2'_m + DIF2'_m$$

$$CON_m = 1 - \alpha U_m \cdot ADV_m + \alpha_2 U_{m+1} \cdot ADV2_m - DIF_m - DIF2_m$$

$$CON1_m = \alpha U_m \cdot ADV_m + DIF_m$$

$$CON2_m = -\alpha_2 U_{m+1} \cdot ADV2_m + DIF2_m$$

3. Application to Water Quality Parameters

Equation (11) may be applied to any dissolved or suspended substance which is of interest in the problem of water quality. The following paragraphs describe the application to some of the most important water quality parameters.

(i) Salinity, S

$$SO_m = Q_t S_t + Q_{sew} \cdot S_{sew}$$

where S_t and S_{sew} are salinities of tributary inflow and point source discharge respectively. Therefore:

$$SO_m - Q_\ell S_m = Q_t (S_t - S_m) + Q_{sew} (S_{sew} - S_m)$$

In a tidal estuary, the tributary inflow may be positive or negative, depending on the phase of tide, with an average value over tidal cycle Q_f, the freshwater inflow of the tributary. Without the detailed information about the time variation of Q_t over tidal cycle, the net effect of tributary inflow may be approximated as the dilution of salt water in the reach by the freshwater inflow Q_f. Therefore, the last term of equation (11) becomes

$$\frac{\Delta t}{V_m} \{- Q_f S_m + Q_{sew} (S_{sew} - S_m)\}$$

and equation (11) becomes

$$S'_m = a_m S'_{m+1} + b_m S'_{m-1} + c_m \qquad (12)$$

where

$$a_m = \frac{COE2_m}{1+COE_m}$$

$$b_m = \frac{COE1_m}{1+COE_m}$$

$$c_m = \{S_m(CON_m - \frac{Q_{sew}+ Q_f}{V_m} \cdot \Delta t) + S_{m+1} \cdot CON2_m + S_{m-1}\ CON1_m + \frac{\Delta t}{V_m} \cdot Q_{sew} \cdot S_{sew})\}/(1 + COE_m)$$

(ii). Substances with the First Order Decay

e.g. CBOD = carbonaceous biochemical oxygen demand

NBOD = nitrogenous biochemical oxygen demand

$$SO_m = - k_c \cdot CBOD_m \cdot V_m + CBODP_m + CBODNP_m + Q_t \cdot CBOD_t$$

where k_c is the decay rate, $CBODP_m$ and $CBODNP_m$ are the point source and non-point source respectively, and $CBOD_t$ is the concentration of tributary inflow. The net effect of tributary inflow resulting from the freshwater input may be estimated in the same way as the case of salinity, and thus,

$$\frac{\Delta t}{V_m}\ (\overline{SO_m - Q_\ell \cdot CBOD_m}) = - \frac{\Delta t}{2} k_c\ (CBOD'_m + CBOD_m) + \frac{\Delta t}{V_m} \{(CBODP_m + CBODNP_m) + Q_f(CBODBG - CBOD_m) - Q_{sew} \cdot CBOD_m\}$$

where CBODBG is the concentration of CBOD in the freshwater input. Thus, equation (11) becomes

$$CBOD'_m = a_m \cdot CBOD'_{m+1} + b_m \cdot CBOD'_{m-1} + c'_m \qquad (13)$$

where

$$a_m = \frac{COE2_m}{1+COE_m+\frac{\Delta t}{2} k_c}$$

$$b_m = \frac{COE1_m}{1+COE_m+\frac{\Delta t}{2} k_c}$$

$$c_m = \{CBOD_m \ (CON_m - \frac{\Delta t}{2} k_c - \frac{Q_f + Q_{sew}}{V_m} \cdot \Delta t)$$

$$+ CBOD_{m+1} \cdot CON2_m + CBOD_{m-1} \cdot CON1_m$$

$$+ \frac{\Delta t}{V_m} \cdot Q_f \cdot CBODBG + \frac{\Delta t}{V_m} (CBODP_m + CBODNP_m)\}/$$

$$(1 + COE_m + \frac{\Delta t}{2} k_c)$$

(iii). Dissolved Oxygen, D.O.

$$SO_m = - k_c \cdot CBOD_m \cdot V_m - k_n \cdot NBOD_m \cdot V_m + f \cdot Ah_m \cdot$$

$$(DOS_m - DO_m) - BEN_m + PHOTO_m + Q_t \cdot DO_t + Q_{sew} \cdot DO_{sew}$$

where

k_n = decay rate of NBOD,

f = oxygen exchange coefficient,

Ah_m = total surface area of the reach,

DOS_m = saturated oxygen content,

BEN_m = benthic demand,

PHOTO = net addition of oxygen due to photosynthesis and respiration,

DO_t = oxygen content of tributary inflow,

DO_{sew} = oxygen content of point source discharge.

The net effect of tributary inflow resulting from the freshwater input may be estimated with the same way as salinity and, thus

$$\frac{\Delta t}{V_m}(SO_m - Q_\ell \cdot DO_m) = -k_c \cdot \Delta t \cdot CBOD_m - k_n \cdot \Delta t \cdot NBOD_m$$

$$+ \frac{\Delta t}{2} \frac{Ah_m}{V_m} \{f(DOS_m - DO_m) + f'(DOS'_m - DO'_m)\}$$

$$- \frac{\Delta t}{V_m}(BEN_m - PHOTO_m) + \frac{\Delta t}{V_m}\{Q_f(DOBGD - DO_m)$$

$$+ Q_{sew}(DO_{sew} - DO_m)\}$$

where DOBGD is the DO content of freshwater inflow from tributary. Thus, equation (11) becomes

$$DO'_m = a_m \cdot DO'_{m+1} + b_m \cdot DO'_{m-1} + c_m \qquad (14)$$

where

$$a_m = \frac{COE2_m}{1 + COE_m + \frac{\Delta t}{2} k'_2}$$

$$b_m = \frac{COE1_m}{1 + COE_m + \frac{\Delta t}{2} k'_2}$$

$$c_m = \{DO_m(CON_m - \frac{\Delta t}{2} k_2 - \frac{Q_f + Q_{sew}}{V_m} \cdot \Delta t)$$

$$+ DO_{m+1} \cdot CON2_m + DO_{m-1} \cdot CON1_m$$

$$+ \frac{\Delta t}{V_m}(Q_f \cdot DOBGD + Q_{sew} \cdot DO_{sew})$$

$$- k_c \cdot \Delta t \cdot CBOD_m - k_m \cdot \Delta t \cdot NBOD_m$$

$$+ \frac{\Delta t}{2} k_2 \cdot DOS_m + \frac{\Delta t}{2} k'_2 \cdot DOS'_m$$

$$- \frac{\Delta t}{2} \cdot BEN_m + \frac{\Delta t}{V_m} \cdot PHOTO_m\}/(1+COE_m + \frac{\Delta t}{2} k'_2)$$

$k_2 = \frac{f}{V_m} \cdot Ah_m$, the reaeration coefficient.

4. Method of Solution

Because of advective and dispersive transport across the transects bounding each end of a particular reach of the estuary, the concentration of a substance in one reach will depend on the concentrations in two adjacent reaches. This interdependence of concentrations at neighboring reaches is manifested in equation (12), (13), or (14). Therefore, the equation cannot be solved for the concentration at the mth reach by itself. Equations must be written for every reach of the estuary and solved for the concentrations in every reach simultaneously.

Suppose that the total length of the estuary to be modeled is divided into N reaches. (N-2) equations will be obtained by writing equation (12), (13), or (14) for m = ML+1 to m = MU-1, where the MLth and MUth reaches are the most upstream and downstream ones, respectively. Since there are (N-2) equations for N unknowns, two boundary conditions must be specified. The principal operation of numerical computations in the model is then to compute the concentrations in each reach at time $t_o + \Delta t$ with a given initial concentration field at time t_o and appropriate boundary conditions. The computed concentration field at $t_o + \Delta t$ will then be used as the initial condition to compute the concentration field at time $t_o + 2\Delta t$, and so forth. Each computation cycle will advance the time by the increment of Δt. Within each computation cycle, the (N-2) simultaneous equations are solved by an elimination method.

Taking the equation for salinity as an example, S'_{ML+1} may be expressed in terms of S'_{ML+2} through equation (12) with m = ML+1, and boundary condition S'_{ML} given, i.e.

$$S'_{ML+1} = a_{ML+1}S'_{ML+2} + b_{ML+1}S'_{ML} + C_{ML+1} \tag{15}$$

where the only unknown on the right hand side of the equation is S'_{ML+2}. Equation (15) may, in turn, be substituted back into equation (12) with m = ML+2, and thus one arrives at an expression for S'_{ML+2} in terms of S'_{ML+3}. In general, there exists the following relation

$$S'_m = P_m S'_{m+1} + O_m \tag{16}$$

where the recursion coefficients P_m and O_m may be calculated from the upstream boundary condition S'_{ML}.

With subscript m-1, equation (16) becomes

$$S'_{m-1} = P_{m-1}S'_m + O_{m-1}$$

Substituting this expression for S'_{m-1} in equation (12), it becomes

$$S'_m = a_m S'_{m+1} + b_m (P_{m-1}S'_m + O_{m-1}) + c_m$$

or

$$S'_m = \frac{a_m}{1 - b_m \cdot P_{m-1}} S'_{m+1} + \frac{b_m O_{m-1} + c_m}{1 - b_m \cdot P_{m-1}} \tag{17}$$

The comparison between equations (16) and (17) gives

$$\left.\begin{aligned} P_m &= \frac{a_m}{1 - b_m \cdot P_{m-1}} \\ O_m &= \frac{b_m \cdot O_{m-1} + c_m}{1 - b_m \cdot P_{m-1}} \end{aligned}\right\} \tag{18}$$

Since S'_{ML} is a known quantity, the comparison between equation (15) and (16) with m = ML+1 gives

$$P_{ML+1} = a_{ML+1}$$

$$O_{ML+1} = b_{ML+1} \cdot S'_{ML} + c_{ML+1}$$

and thus

$$P_{ML} = O, \; O_{ML} = S'_{ML}$$

In summary, the recursion coefficients and equation are

$$P_{ML} = O, \; O_{ML} = S'_{ML}$$

$$P_m = \frac{a_m}{1 - b_m \cdot P_{m-1}}$$

$$O_m = \frac{c_m + b_m \cdot O_{m-1}}{1 - b_m \cdot P_{m-1}} \quad \Big\} \qquad (18)$$

and

$$S'_m = P_m S'_{m+1} + O_m, \qquad (16)$$

with m = ML+1, ML+2, ---, MU-1.

Then, the order of numerical computations is

(1) calculate the recursion coefficients by applying equations (18) repeatedly with m = ML+1, ML+2, ---, MU-1, and

(2) with S'_{MU} given as the downstream boundary condition, the salinity of the interior reaches is calculated by applying equation (16) repeatedly with m = MU-1, MU-2, ---, ML+1

5. Evaluation of Parameters

(i) Velocity U: In an estuary, the current velocity may be divided into two parts,

$$U_m(t) = UF_m + Ut_m(t) \tag{19}$$

where UF is the non-tidal component generated by freshwater discharge and Ut is the oscillating tidal component. In this model, the tidal current is approximated by a sinusoidal function of time with period T and phase ϕ

$$Ut_m(t) = UT_m \sin\{\frac{2\pi}{T} t + \phi_m\} \tag{20}$$

where UT is the amplitude. UT_m and ϕ_m are obtained from field data. The non-tidal component UF is calculated by the equation

$$UF_m = \frac{Q_m}{AC_m} \tag{21}$$

where Q_m is the freshwater discharge from a drainage area upstream of the mth transect; Q_m is estimated from the record of a stream gauge station located upstream of the tidal limit, with freshwater discharge assumed to be proportional to drainage area.

(ii) Dispersion Coefficient E: The dominant mechanism of longitudinal dispersion is the interaction between turbulent diffusion and shearing current. Taylor's (1954) formulation of one-dimensional dispersion has been successfully modified and extended to homogeneous estuaries (Holley, et.al., 1970; Harleman, 1971). The dispersion coefficient in the freshwater portion of a tidal estuary may be expressed as

$$E = \nu n |U| R^{5/6} \tag{22}$$

where n is Manning's friction coefficient, $|U|$ is the absolute value of velocity, R is hydraulic radius, and ν is a constant

on the order of 100. It is known that the presence of density stratification due to salinity intrusion enhances the vertical shear while suppressing the turbulence, and therefore, increases the dispersion coefficient. Equation (22) is modified to

$$E = \nu n|U|R^{5/6}(1 + \nu'S) \tag{23}$$

where ν' is a constant and S is the salinity. ν' is determined by the model calibration, i.e. adjusting ν' until the model results agree satisfactorily with the salinity distribution measured in the field.

(iii). Reaeration Coefficient k_2: O'Connor and Dobbins (1956) presented a theoretical derivation of the reaeration coefficient, in which fundamental turbulence parameters were taken into account. They derived the following formula

$$(k_2)_{20} = \frac{(D_c U)^{1/2}}{H^{3/2}} \tag{24}$$

where D_c is the molecular diffusivity of oxygen in water, U and H are the cross-sectional mean velocity and depth respectively, and $(k_2)_{20}$ is the reaeration coefficient at $20^{o}C$. This formula has been shown to give a satisfactory estimate of k_2 for a reach of river with cross-sectional mean depth and velocity more or less uniform throughout the reach. In case the cross-section varies appreciably within a single reach, there is no reason to expect a satisfactory estimate from the formula by using the values of U and H at the two bounding transects of the reach. Therefore, equation

(24) is modified as stated in the following paragraph.

Assuming that the O'Connor and Dobbins formula is valid locally then

$$f = k_2 h = \frac{(D_c u)^{1/2}}{h^{1/2}} \tag{25}$$

where f is the exchange coefficient, i.e., the exchange rate of oxygen through unit water surface area, u is the local depth-mean velocity and h is local depth. M, the exchange rate of oxygen through the water surface over an entire reach is

$$M = \int_{Ah} f\ (DOS - DO)\, dAh \tag{26}$$

where Ah is the total surface area over a reach. By definition of k_2,

$$M = (k_2)_{20} V(DOS - DO) \tag{27}$$

thus,

$$(k_2)_{20} = \frac{D_c^{1/2}}{V} \int_{Ah} \frac{u^{1/2}}{h^{1/2}}\, dAh = D_c^{1/2} \left\langle \frac{u^{1/2}}{h^{1/2}} \right\rangle \frac{Ah}{V}$$

$$= D_c^{1/2} \left\langle \frac{u^{1/2}}{h^{1/2}} \right\rangle \frac{1}{\langle h \rangle} \tag{28}$$

where < > indicates the average over the surface area Ah, and <h> is the mean depth of the reach. Since the velocity data are available only at the end transects of a reach, no true $\left\langle \frac{u^{1/2}}{h^{1/2}} \right\rangle$ may be estimated. In this model, the average value $\frac{U^{1/2}}{H^{1/2}}$ at the two end-transects is used.

To adjust k_2 for temperatures other than 20°C, Elmore and West's (1961) formula is used

$$k_2 = (k_2)_{20} \cdot 1.024^{(\theta-20)} \qquad (29)$$

where θ is the water temperature in centigrade degrees.

(iv). Photosynthesis and Respiration, PHOTO: The amount of oxygen produced by photosynthesis varies with the intensity of sunlight, the turbidity of water and the density of plant population. Moreover, the same plants extract oxygen from the water for respiration. This combined oxygen source and sink is assumed constant with respect to time. The magnitude is allowed to vary from reach to reach and an array is provided in the computer program for input data in mg/ℓ/day. If more complete information is available, the time varying functional form of this oxygen source and sink may be specified.

(v). BOD Decay Rates: k_c and k_n

The decay rates of CBOD (carbonaceous biochemical oxygen demand) and NBOD (nitrogenous biochemical oxygen demand) were determined by the model calibration, i.e., adjustment of decay rates until the model results agree satisfactorily with the CBOD and NBOD distribution measured in the field. The decay rates also depend on water temperature; the following formulas are used for this temperature dependence,

$$k_c = (k_c)_{20} \cdot 1.047^{(\theta-20)}$$

$$k_n = (k_n)_{20} \cdot 1.017^{(\theta-20)}$$

(vi). Saturated Oxygen Content, DOS

The saturation concentration of dissolved oxygen depends on temperature and salinity. From tables of saturation concentration (Carritt and Green, 1967) a polynomial equation was determined by a least-squares method.

$$DOS = 14.6244 - 0.367134\theta + 0.0044972\theta^2 - 0.0966S + 0.002050\theta S + 0.0002739S^2$$

where S is salinity in parts per thousand and DOS is in mg/liter.

(vii). Benthic Oxygen Demand, BEN

The bottom sediment of an estuary may vary from deep deposits of sewage or industrial waste origin to relatively shallow deposits of natural material of plant origin and finally to clean rock and sand. The oxygen consumption rate of the bottom deposits must be determined with field measurements. Field data were used wherever they are available. A value of 1.0 $gm/m^2/day$ at 20^oC is typical average for most estuaries. The temperature effect was simulated by (Thomann, 1972).

$$BEN = (BEN)_{20} \cdot 1.065^{(\theta-20)}$$

where $(BEN)_{20}$ is the benthic demand at 20^oC.

6. Segmentation of the River

The tidal portion of the Rappahannock River (extending 110 miles from the mouth at the Chesapeake Bay to the fall line at Fredericksburg) is divided into 102 reaches. The lengths of the reaches increase from 0.5 miles

at the upstream portion to about 3.5 miles near the river mouth. The geometries of the transects were measured by U. S. Corps of Engineers in 1973. Table 1 lists the geometric data and distances from the river mouth.

Table 2 is a list of the major point sources of pollutants. The model reach numbers indicate the numbers of reaches into which the point sources discharge. The average discharge rates represent the average of 1973 and 1974 data furnished by Tidewater regional office of the State Water Control Board. Various factors estimated from field data were applied to convert 5-day BOD to ultimate carbonaceous BOD. In cases where nitrogen data were not available, the nitrogenous BOD was estimated for the model simulations described in the next section. Figure 4 shows the locations of these major point sources.

7. Model Calibration and Verification

The field data collected during the intensive field survey in July, 1973 were used for model calibration. The graphical summary of the salinity, temperature and dissolved oxygen is presented in Appendix A. The cross-sectional average tidal currents were calculated and presented in Appendix C; these tidal currents data were used as input data to the model to simulate tidal advection. The freshwater discharge information was obtained from Water Resources Data of Virginia, 1973. For the model calibration run, a freshwater

Source	Model Reach Number	Approximate Distance From Mouth (statute miles)	Design Flow(^{o}) or Average Flow(x) (MGD)	Average $CBOD_u$ (lbs/day)	Average (or estimate) $NBOD_u$ (lbs/day)
Fredericksburg STP	4	107.0	2.4^{o}	712.0	1302.0
FMC Corp-Fredericksburg	5	106.6	5.7^{x}	941.0	220.0
Tappahannock	88	42.6	0.106^{x}	75.90	76.8
Tidewater Memorial Hospital-Tappahannock	88	42.6	0.032^{x}	16.13	32.0
Urbanna	98	15.8	0.025^{o}	37.95	36.6
Barnhardt Farms	98	15.3	1.0^{x}	740.90	743.4
Tides Inn	100	9.3	0.020^{o}	6.05	6.4
Tides Golf Lodge	100	9.3	0.025^{o}	8.47	8.6

Table 2. Major Point Sources of Pollutants on the Tidal Rappahannock River

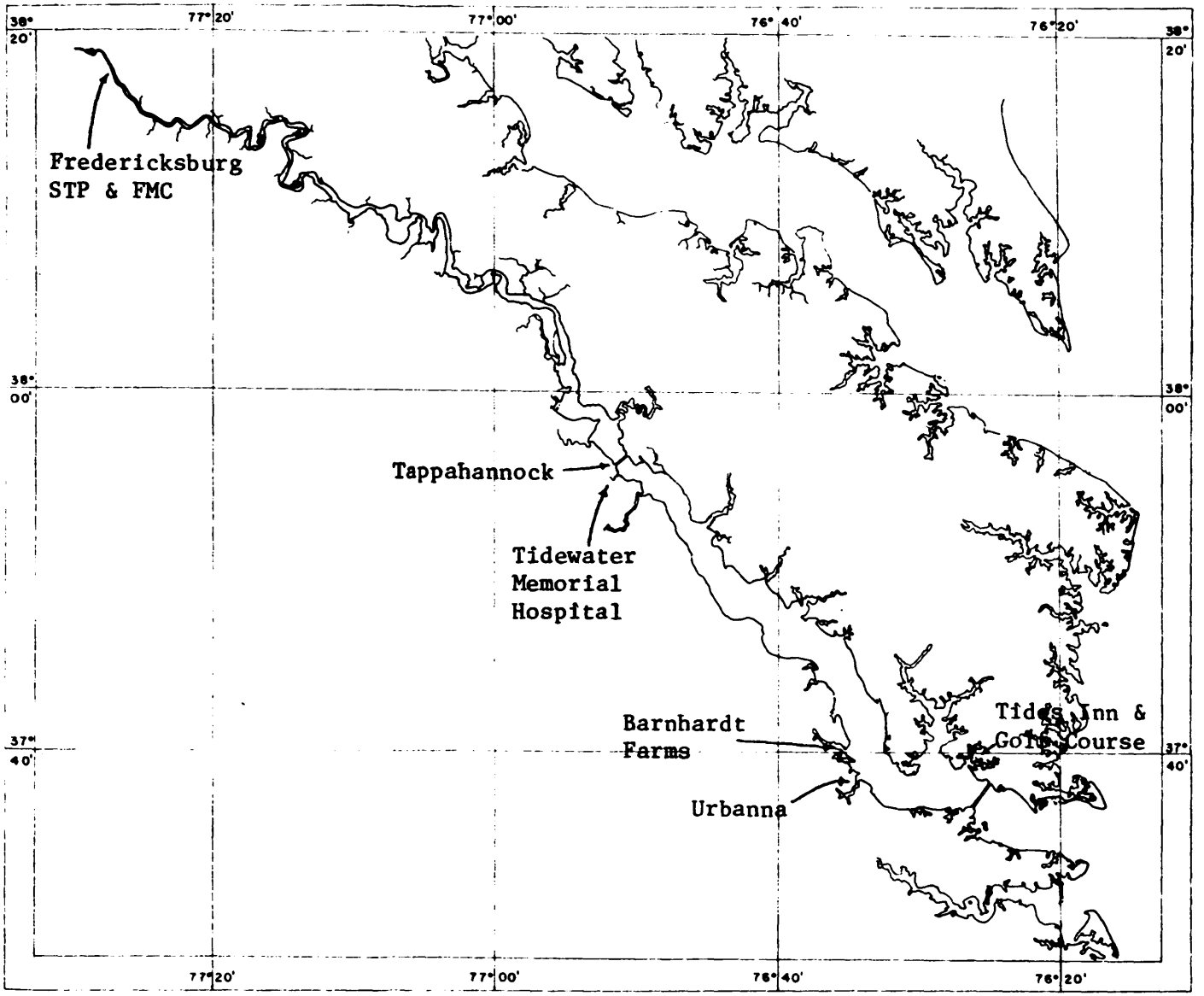

Figure 4. Locations of major point sources of pollutants along the tidal Rappahannock.

discharge at Fredericksburg of 1040 cfs was used, which is the average value of the 25-day period from July 1 to July 25.

Since the field data cover only the lower part of the river, the model was run to simulate the part of the river from reach number 50 to reach number 102. The model results are compared with the salinity field data for the calibration of the parameter υ' for the dispersion coefficient (eqn. (23)). Figure 5 shows the comparison with $\upsilon' = 0$. Each of the observed data points in the figure represents the average value over the cross-section and sampling period. The curve represents the model result of the longitudinal salinity distribution averaged over a tidal cycle.

To calibrate the weighting factor (eqns. (5) and (6)) of the advective term for the BOD-DO part of the model, the model was run to simulate an instantaneous dye release. The model results are shown in figures B1 to B12 with $\alpha = 0.7$. In order to match the peak concentrations with field data, a decay rate of 0.05/day was assumed. The figures show that the model results agree well with the field data for the downstream side of the concentration curves. The model predicts a stronger upstream dispersion than that indicated by field data. This may be attributed to the absorption of dye in the highly turbid water near the head of salt intrusion. Figure 5 shows that salinity decreased to zero near mile 50 from the river mouth. According to Nichols (1973) a turbidity maximum is expected at the bottom

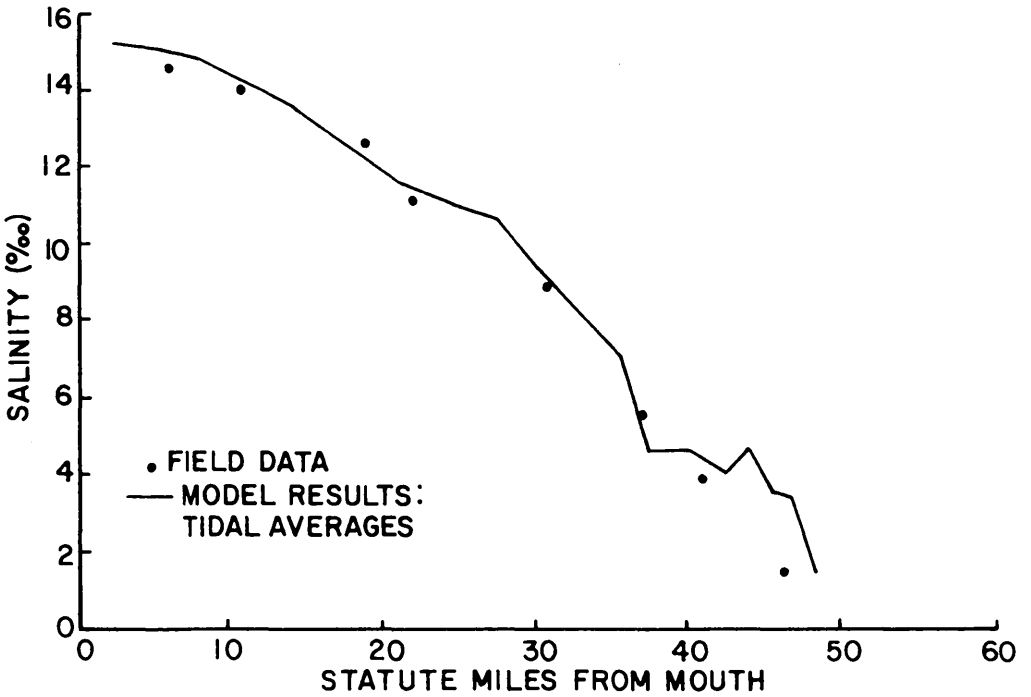

Figure 5. Longitudinal salinity distribution, July, 1973. (The data points represent the values averaged over cross-section and tidal cycles).

layer of water in this region. This turbid water will absorb some of the dye as it disperses upstream with bottom layer of saline water.

Figure 6 shows the comparison of DO distribution along the river. Field data indicate that a DO minimum existed in reaches between 10 and 25 miles from river mouth. It is suspected that the critical DO in these reaches was due primarily to a combination of great depth, which impedes vertical mixing and reaeration, and non-point sources of pollution, very likely associated with the intense fishing activity in this area during this season. Large commercial menhaden fishing vessels have been observed discharging large volumes of fish oil in this area (Hargis, et al. 1975). Non-point pollutant discharges of 0.120 mg $CBOD_u$/l/day and 0.048 mg $NBOD_u$/l/day were assumed for this part of the estuary. Non-point pollutant discharges of 0.075 mg $CBOD_u$/l/day and 0.030 mg $NBOD_u$/l/day were assumed for the remainder of the estuary in order to simulate pollution associated with normal land runoff.

The field data also indicate that reaches upstream of mile 40 are supersaturated with dissolved oxygen. Moreover, previously reported data (Fang, et al. 1972) suggest a diurnal variation in dissolved oxygen concentrations in sections of the estuary. Both these conditions are indicative of photosynthetic oxygen production. The area from mile 40 to mile 79 contains quite a bit of marshland along the shores, which might account for the indications of significant

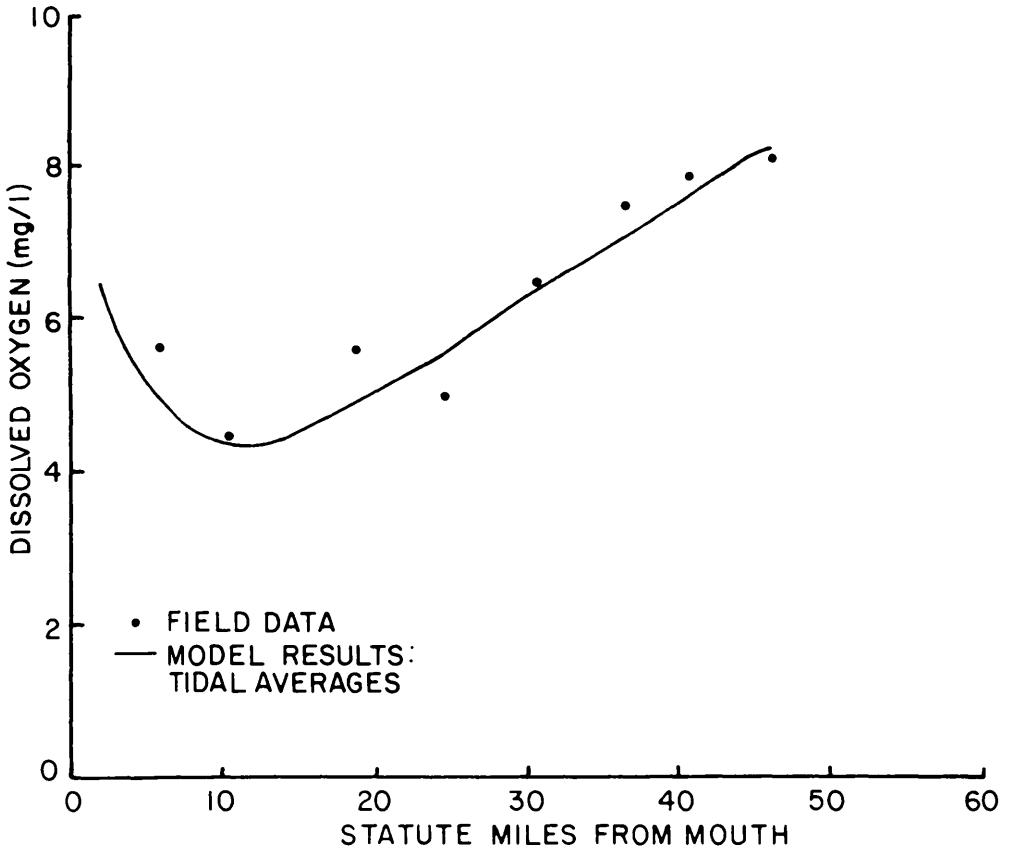

Figure 6. Longitudinal distribution of dissolved oxygen, July, 1973. (The field data points represent values averaged over the cross-section and tidal cycles.)

photosynthetic activity. A photosynthetic oxygen production rate of 1.5 gm/m^2/day, therefore, was assumed for this area of the estuary.

The model was also run to simulate the whole length of the tidal Rappahannock and its results were compared with the slack water run data of September 26, 1973. Figure 7 shows the comparison of longitudinal salinity distribution. A value of 3 was used for ν' in determining the dispersion coefficient according to equation (23). Figures 8 & 9 show the comparison of DO distribution. A survey by Environmental Protection Agency in 1970 reported benthic demand of 1.7 - 3.0 gm/m^2/day in river reaches below fall line. Therefore, in the application of the model, a benthic demand of 1.5 gm/m^2/day was assumed for river reaches between fall line and mile 85.

The field data indicate that the DO at reaches between miles 10 and 25 improved considerably from July to September while no reduction in waste discharges from point sources was noted. The improvement may have resulted from the abatement of much of the fishing activity observed in the summer season. Figure 8 shows the comparison of DO field data with model predictions for this hypothesis. Non-point source discharges in these reaches were assumed to have decreased to 0.045 mg $CBOD_u$/l/day and 0.018 mg $NBOD_u$/l/day. Upstream photosynthetic oxygen production was also assumed to have decreased somewhat to values of 0.5 gm/m^2/day from mile 40 to mile 60 and 1.0 gm/m^2/day from mile 60 to mile 79.

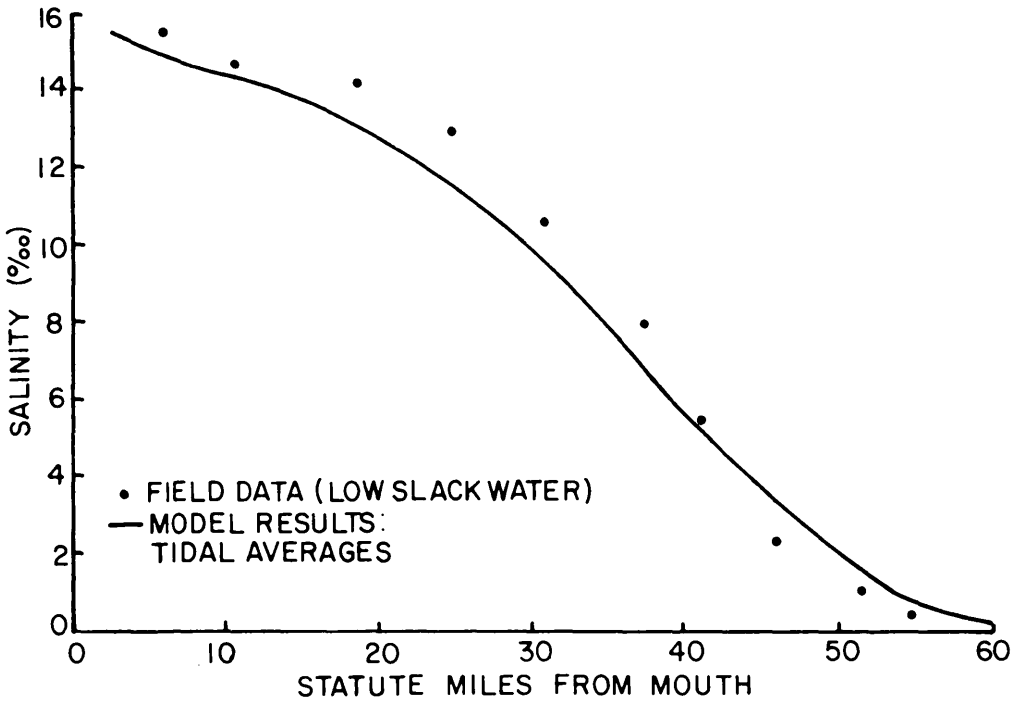

Figure 7. Longitudinal salinity distribution, September 26, 1973. (The field data points represent values averaged over cross-section and tidal cycles.)

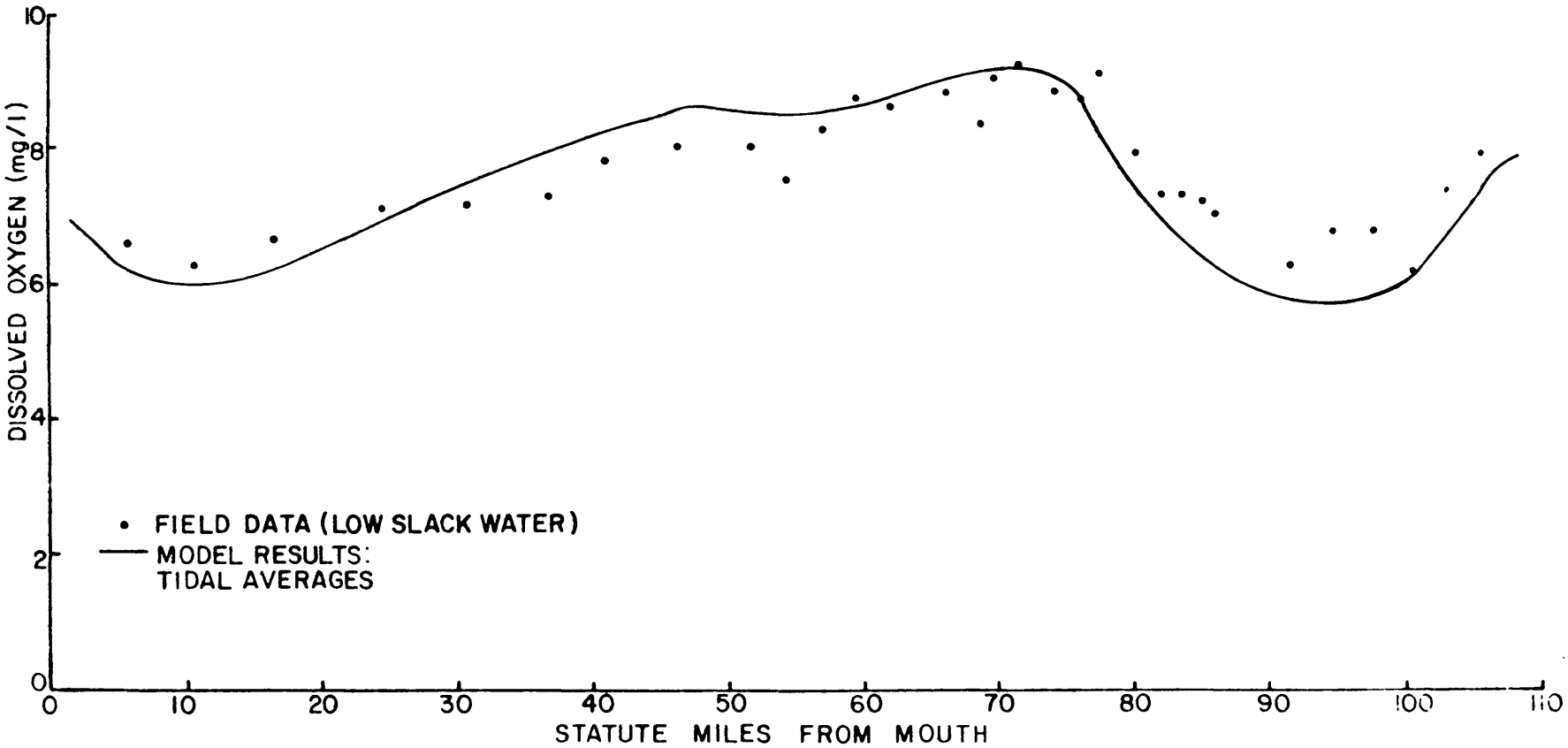

Figure 8. Longitudinal distribution of dissolved oxygen, September 26, 1973 under hypothesis of decreased non-point pollution near mouth. (The field data points represent values averaged over the cross-section.)

Another possible explanation for the improvement in DO near the mouth is increased photosynthetic activity in that area. On September 12, two weeks prior to this observation, red tides were observed in the mouth of the estuary (Hargis, et al., 1975). Comparative data on phytoplankton density or chlorophyll concentrations in this area, however, are not available for the days under discussion here. Figure 9 shows the comparison of DO field data with model predictions for the hypothesis of increased photosynthetic activity near the mouth. Non-point source discharges were assumed to be the same as those for the July run, while photosynthetic oxygen production was assumed to be 1.0 $gm/m^2/day$ from the mouth to mile 20 and from mile 60 to mile 79, and 0.5 $gm/m^2/day$ from mile 20 to mile 60.

A third possibility is some combination of these two hypotheses.

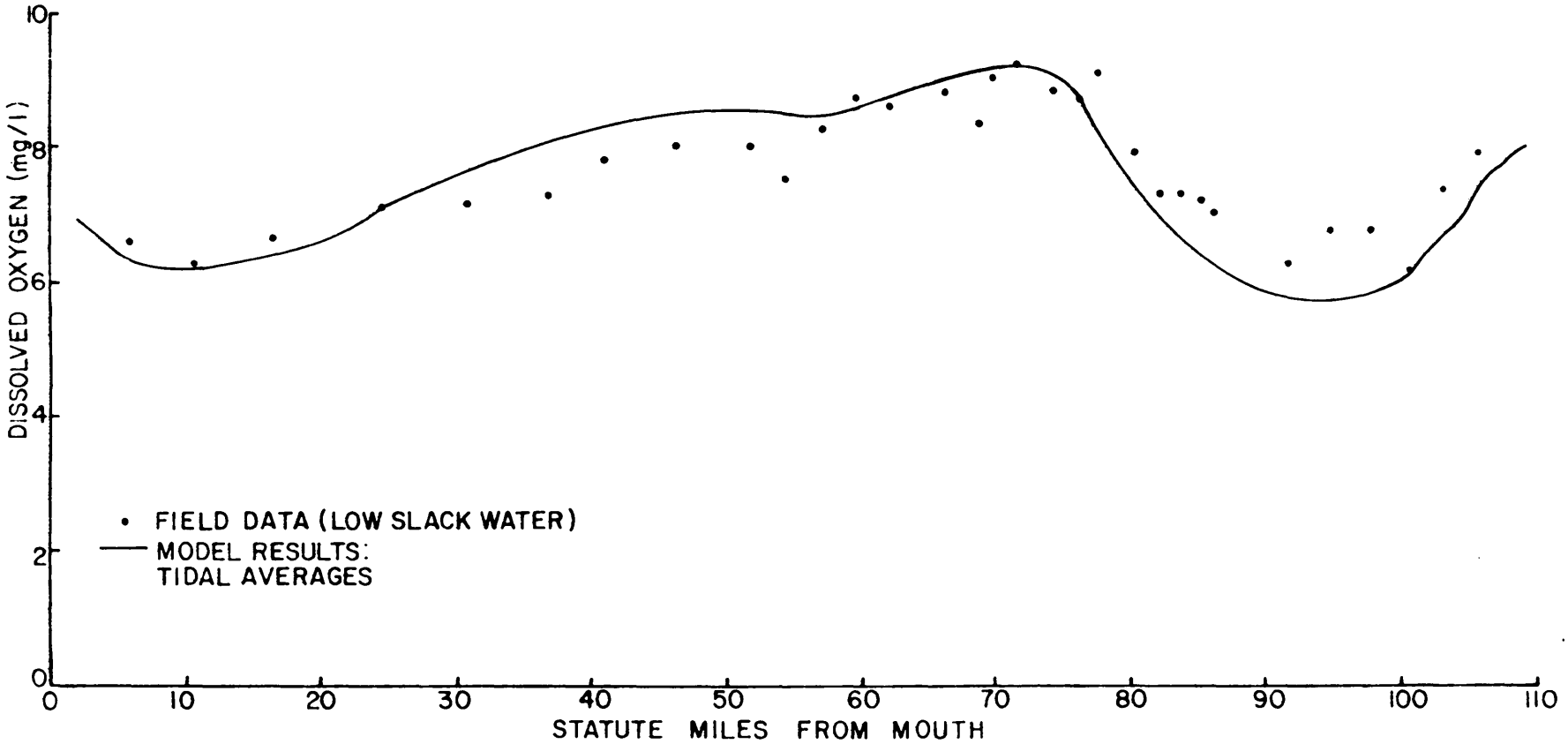

Figure 9. Longitudinal distribution of dissolved oxygen, September 26, 1973 under hypothesis of increased photosynthetic activity near mouth. (The field data points represent values averaged over the cross section.)

8. Manual for Program User

The following is a list of all the input data needed to be specified to run the model. The values of those variables designated by asterisk are constant for a particular estuary and, therefore, should not be altered from run to run.

A. Main Program

(1a) ML, MU: station numbers of upstream boundary and downstream boundary respectively, ML<MU.

(1b) DRAIN: total drainage area, in square miles, at transect ML

Format: (2I10, F10.0)

(2a) TMAX: the integral number of tidal cycles the program is to be run; in general, 40 tidal cycles will be sufficient to reach an equilibrium state.

*(2b) DTT: the time increment in tidal cycle.

(2c) NRNM: the number of simulations under which the program is to be executed in a single run,

NRNM $\geq$ 1.

FORMAT: (2F10.0, I5)

(3a) NP: the number of times the calculated concentration fields are to be printed.

(3b) TT(I), I=I, NP: number of tidal cycles after computation begins at which the concentration fields are to be printed. All the numbers should be integral multiples of DTT, and TT(NP) should equal TMAX.

Format: (I5, 5X, (7F10.0)).

(4a) DNB: the number of hours from 0600 to computation starting time; DNB is to take into account the phase of diurnal variation in photosynthesis and respiration.

(4b) TB: the number of hours from low water slack at the most upstream transect to computation starting time; TB may be set to zero for most cases.

Format: (7F10.0)

*(5a) BETA: weighting factor for advection of sea salt.

*(5b) ALPHA: weighting factor for advection of oxygen and biochemical oxygen demand (BOD).

Format: (7F10.0).

B. Hydral Subroutine

(1) TITLE: a title describing the particular section of estuary to be modeled.

Format: (1X, 35A2)

(2) NDG, NS, NAME: data group number, number of points in the group, and some description of the contents. in order to exit the subroutine set NDG ≥ 99.

Format: (2I5, 30A2)

(a) Data group 1.

NS is the number of transects of interest starting with transect number 1, NS ≥ MU + 1.

(i) DIST(I), I=1, NS: distance of transect from mouth, in statute miles.

Format: (7F10.0)

(ii) ARCO(I), I=1, NS: conveyance area or cross-sectional area of the transect in the main channel of flow, in square feet.

Format: (7F10.0)

(iii) ART(I), I=1, NS: total cross-sectional area of the transect including stagnant shoals which merely store water, in square feet.

Format: (7F10.0)

(iv) VOL(I), I=1, NS: volume of reach up to mean tide level, in cubic feet; VOL (NS) may be arbitrarily specified.

Format (6E12.0)

(v) H1(I), I=1, NS: transect depth, in feet.

Format (7F10.0)

(vi) HA(I), I=1, NS: average reach depth in feet. HA(NS) may be arbitrarily specified.

Format: (7F10.0)

(vii) ARD(I), I=1, NS: drainage area increment over the Ith reach, in square miles. ARD(NS) may be arbitrarily specified.

Format: (7F10.0)

(b) Data Group 2.

NS is the number of transects of interest starting with transect 1, NS $\geq$ MU + 1.

*(i) PHA(I), I=1, NS: phase difference of tide at Ith transect relative to transect 1, in hours.
Format: (7F10.0)

*(ii) UT(I), I=1, NS: tidal velocity at each transect, in feet per second.
Format: (7F10.0)

(iii) S(I), I=1, NS: initial salinity of each reach, in parts per thousand
Format: (7F10.0)

C. Input Subroutine

(1) TITLE: a title describing the particular run of the program.
Format: (1X, 35A2)

(2) NDG, NS, NAME: input data group number, number of points in the group, and some description of the contents
In order to exit the subroutine set NDG ≥ 99.
Format: (2I5, 30A2)

(a) Data Group 1.
NS is the number of data sets to be read.

(ia) DISCH: freshwater discharge at transect ML, in cubic feet per second.

(ib) FC: manning friction coefficient

(ic) AK, TK: empirical constants relating dispersion coefficient to the salinity and the salinity gradient respectively; AK ≥ 0, TK ≥ 0.
Format: (7F10.0)

(ii) CBODLA, NBODLA, DOLA, SLA: concentrations of carbonaceous BOD, nitrogenous BOD, dissolved oxygen, and salinity respectively in lateral freshwater inflow; in milligrams per liter for BOD and DO; in parts per thousand for salinity.

(iii) CBODU, CBODD: carbonaceous BOD levels of reaches ML and MU, respectively, in milligrams per liter.

Format: (7F10.0)

(iv) NBODU, NBODD: nitrogenous BOD levels of reaches ML and MU, respectively, in milligrams per liter.

Format: (7F10.0)

(v) DOU, DOD: dissolved oxygen concentrations of reaches ML and MU, respectively in milligrams per liter.

Format: (7F10.0)

(vi) SU, SD: salinity of reach ML and estimated maximum salinity of reach MU respectively, in parts per thousand.

Format: (7F10.0)

(b) Data Group 2.

NS is the number of reaches of interest starting with reach 1.

(i) CBOD(I), I=1, NS: the initial carbonaceous BOD concentrations in each reach, in milligrams per liter.

Format: (14F5.0)

(ii) NBOD(I), I=1, NS: the initial nitrogenous BOD concentrations in each reach, in mg/liter.

Format (14F5.0)

(iii) DO(I), I=1, NS: the initial dissolved oxygen concentrations in each reach, in mg/liter.

Format: (14F5.0)

NOTE: This data group need not be specified by the user. Default values are as follows:

CBOD(I), I=1, NS: 0.5
NBOD(I), I=1, NS: 0.5
DO(I), I=1, NS: 7.0

(c) Data Group 3.

NS is the number of reaches into which point sources of wastewater are introduced.

K, QWAST(K), CBODP(K), NBODP(K), DOWAST(K), SP(K): reach number, flow rate of wastewater in cubic feet per second, flow rate of carbonaceous BOD in pounds per day, flow rate of nitrogenous BOD in pounds per day, concentration of dissolved oxygen in wastewater in mg/liter, salinity concentration in wastewater in parts per thousands.

Format: (I5, 5X, 5F10.0)

NOTE: This data group need not be specified, or data may be specified for any subset of reaches. Default values are zero for each QWAST(I), CBODP(I), NBODP(I), DOWAST(I), SP(I).

(d) Data Group 4.

NS is the number of reaches of interest starting with reach 1 or NS is 1 if values are to be uniform throughout the estuary.

TEMP(I), I=1, NS: water temperature of reach in degress centigrade.

Format: (14F5.0)

NOTE: This data group must always be immediately followed by data groups 5 and 6, respectively.

(e) Data Group 5.

NS is the number of reaches of interest starting with reach 1 or NS is 1 if values are to be uniform throughout the estuary.

(i) CKC(I), I=1, NS: decay coefficient of carbonaceous BOD at 20^{o} centigrade in each reach (base e), in unit of 1/day.

Format: (14F5.0)

(ii) TCCKC: temperature coefficient for CKC.

Format: (F10.0)

(iii) CKN(I), I=1, NS: decay coefficient of nitrogenous BOD at 20^{o} centigrade in each reach (base e), in unit of 1/day.

Format: (14F5.0)

(iv) TCCKN: temperature coefficient for CKN

Format (F10.0)

NOTE: This data group must always be immediately followed by data group 6.

(f) Data Group 6.

NS is the number of reaches of interest starting with reach 1 or NS is 1 if values of both subgroups are to be uniform throughout the estuary.

(i) CBODNP(I), I=1, NS

Format: (7F10.0)

(ii) NBODNP(I), I=1, NS

Format: (7F10.0)

The CBOD and NBOD concentrations in each reach, resulting from non-point sources, in mg/liter.

(g) Data Group 7.

NS is the number of reaches of interest, starting with reach 1.

PHOTO(I), I=1, NS: the rate of photosynthetic-respiration in each reach, in grams of dissolved oxygen per square meter per day.

Format: (7F10.0)

NOTE: This data group need not be specified.

Default values are 0.0 for each reach.

(h) Data Group 8.

NS is the number of reaches of interest starting with reach 1.

(i) BEN(I), I=1, NS: the benthic oxygen demand at $20^{o}C$ in each reach in grams per square meter per day.

Format: (14F5.0)

(ii) TCBEN: temperature coefficient for benthic oxygen demand.

Format: (F7.0)

NOTE: This data group need not be specified. Default values are 0.0 for each reach.

NOTE: In Data Groups 2 through 8, the variables with I < ML may be specified arbitrarily.

In case more than one simulation is to be executed in one run, i.e., NRNM ≥ 2, the input data for INPUT subroutine may be repeated. Only those data groups for which the values are to be altered need to be specified, with the following exceptions: If data group 4 is specified, groups 5 and 6, respectively must immediately follow or if group 5 is specified, group 6 must immediately follow. In any case, after data for the first simulation, TITLE for the INPUT subroutine must be specified, an NDG ≥ 99 must be specified to exit the subroutine. Therefore, for each simulation after the first a minimum of two data cards are required.

NOTE: All BOD values are ultimate BOD values, rather than 5-day.

VI. SALT INTRUSION MODEL STUDY

Two mathematical models were developed and verified for use to predict the intrusion of salt water. These are tidal average models designed to simulate the intrusion of salt water over several months under the action of mean advection by freshwater discharge and dispersion by tidal current. One of the models is based on the program DECS-III (Pence, et.al., 1968) which uses explicit scheme for numerical integration. The other was developed in VIMS and employed implicit scheme for numerical integration. Both models were described in an earlier report (Fang, et.al., 1972). In this previous report, a description was given of the models and an account of the verification for the reaches from Fredericksburg to Tappahannock. Since that time, the models have been extended to the mouth of the Rappahannock, and the verification period has been extended in time to include a dry autumn condition followed by a wet spring. The models have also been applied to study certain aspects of the flow release schedule planned for the proposed Salem Church Dam Project.

1. Model Verification

The continuing slack water runs conducted by VIMS were used to verify the salinity intrusion models. The period for verification extended from August, 1970 to May, 1971, and so included both a dry period and a wet period.

It was found that time constant dispersion coefficients tended to exaggerate the flushing that occurred during periods of high flow. Following the suggestion of Paulson (1970), dispersion coefficients were weighted with the square root of fresh water. Empirically the following form was found to work better.

$$E \alpha \sqrt{1 + Q_f/Q_r}$$

where E is the dispersion coefficient and Q_f is the fresh-water discharge, and Q_r is an empirical constant.

Figures 10 to 17 show the results of the verification. In these figures, the dotted and solid lines represent the results of models using explicit scheme and implicit scheme respectively, and the circles represent the vertical averages of slack water observed salinity concentrations.

2. Model Application

Having been verified for the entire Rappahannock River, these salinity models were put to use in solving a particular problem that arose concerning the downstream reaches of the Rappahannock.

Large areas of river bottom in the Rappahannock River downstream of Towle's Point would be excellent for oyster production were it not for the oyster diseases prevalent in this area. Because of the high salinity of the overlying waters, MSX has a permanent foothold. Before Hurricane Agnes helped reduce their number, oyster drills

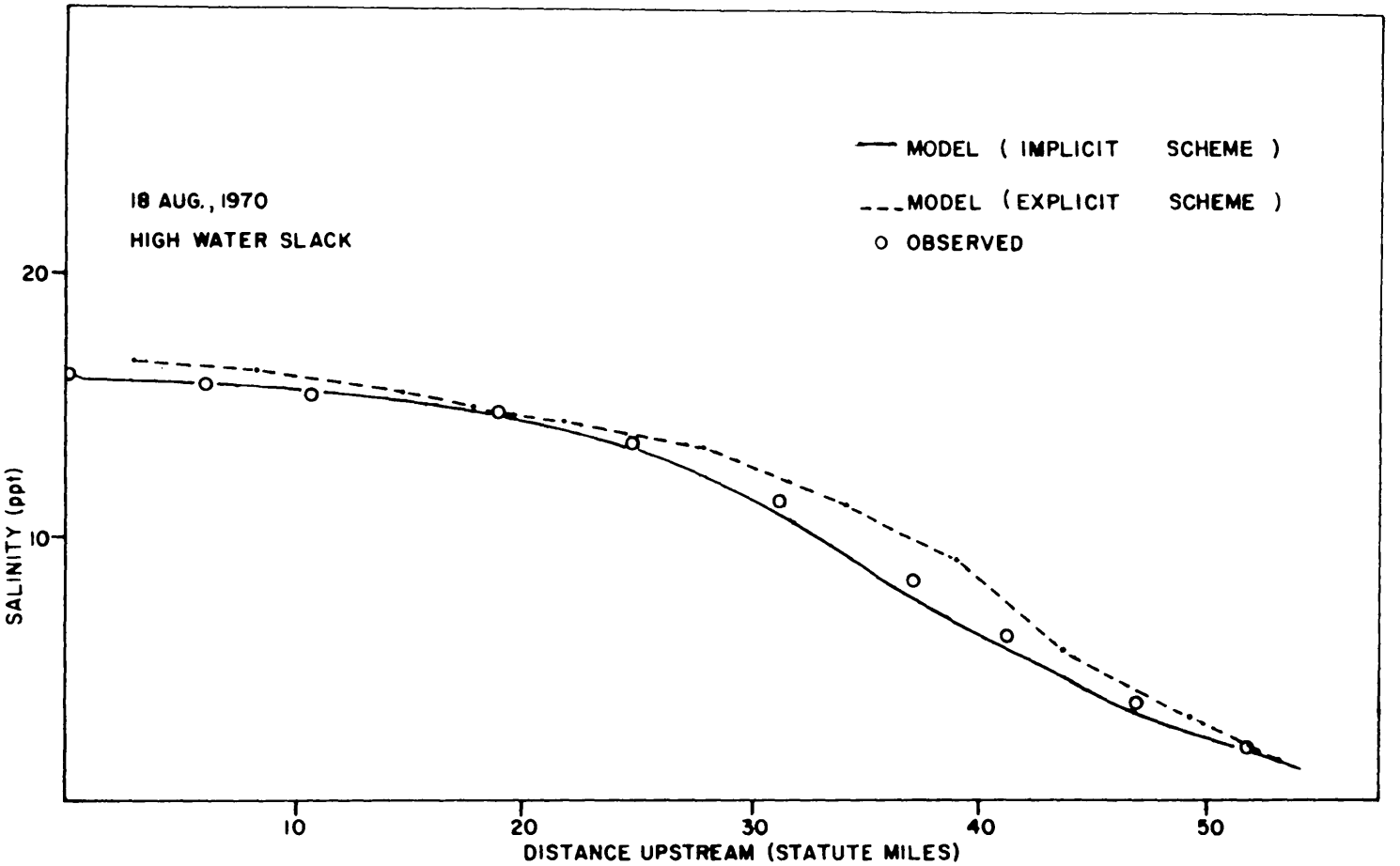

Figure 10. Longitudinal salinity distribution, August 18, 1970.

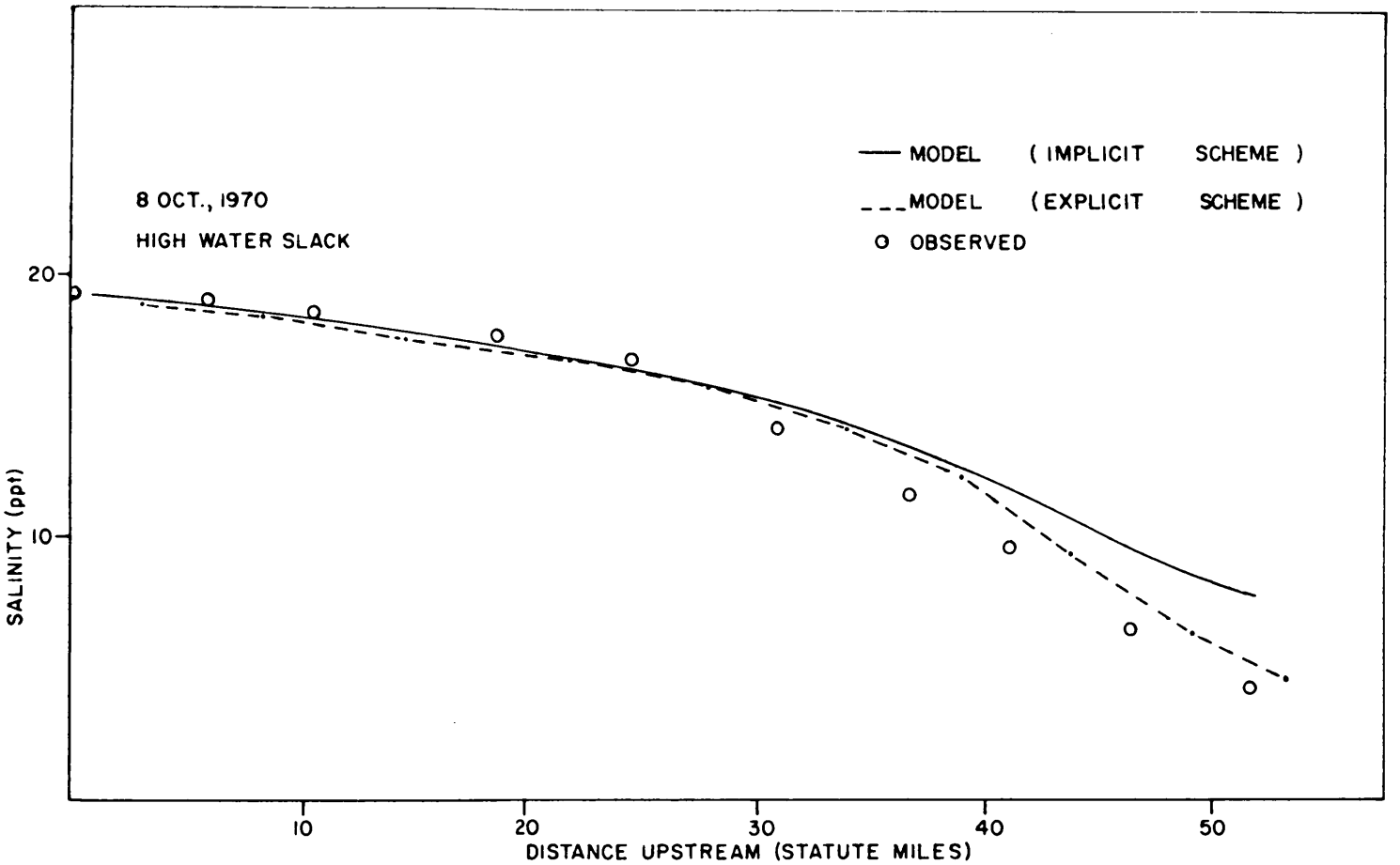

Figure 11. Longitudinal salinity distribution, October 8, 1970.

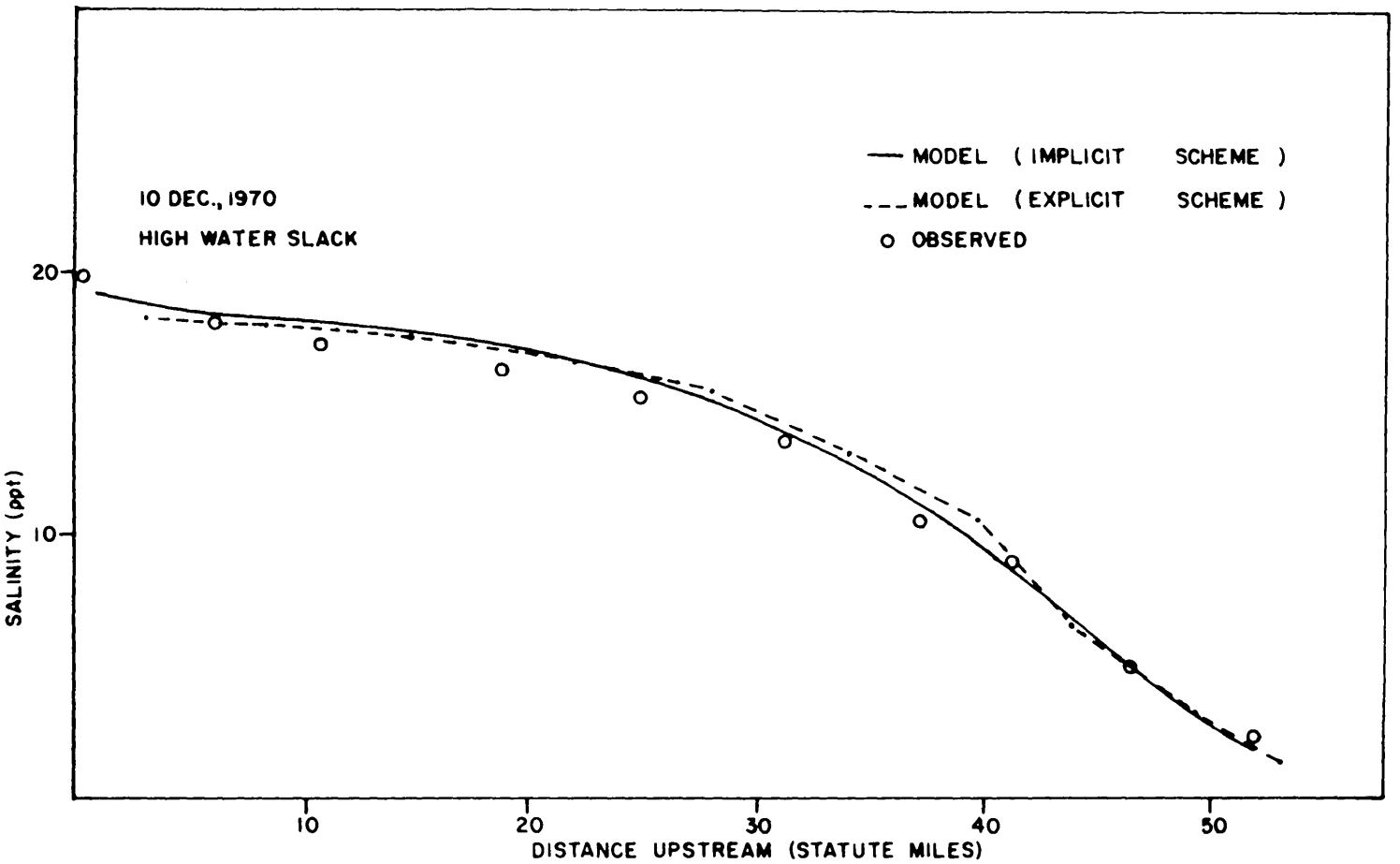

Figure 12. Longitudinal salinity distribution, December 10, 1970.

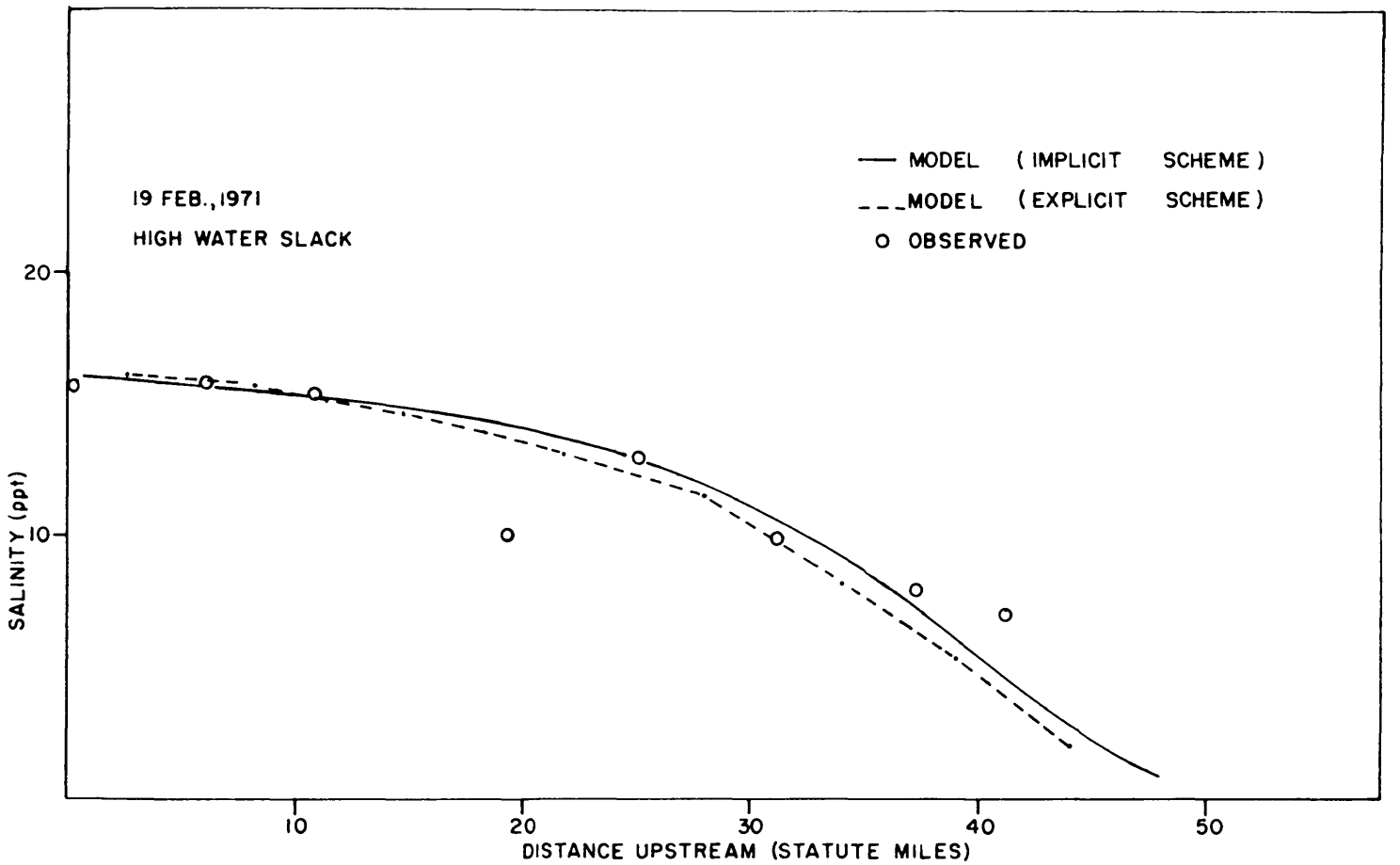

Figure 13. Longitudinal salinity distribution, February 19, 1971.

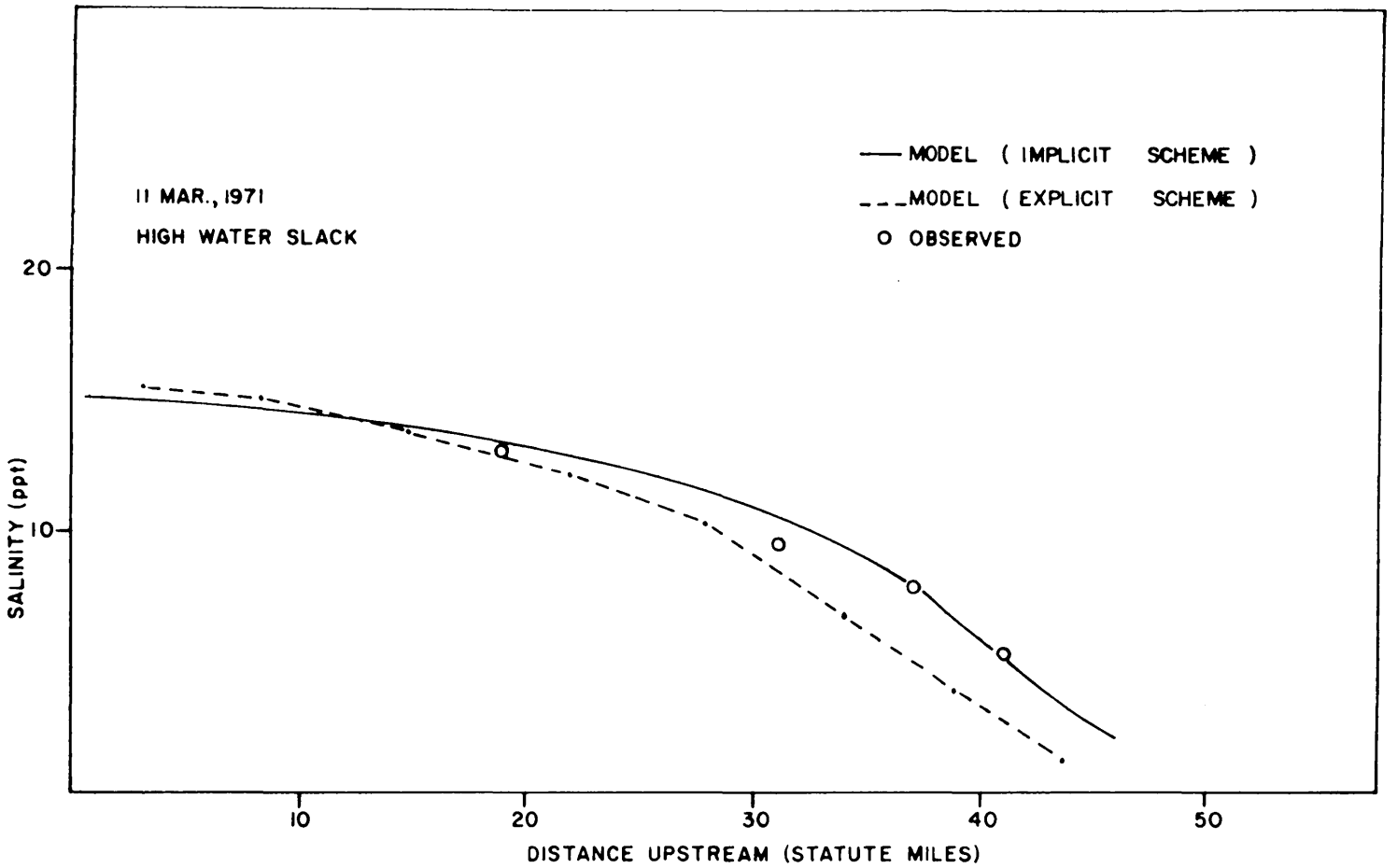

Figure 14. Longitudinal salinity distribution, March 11, 1971.

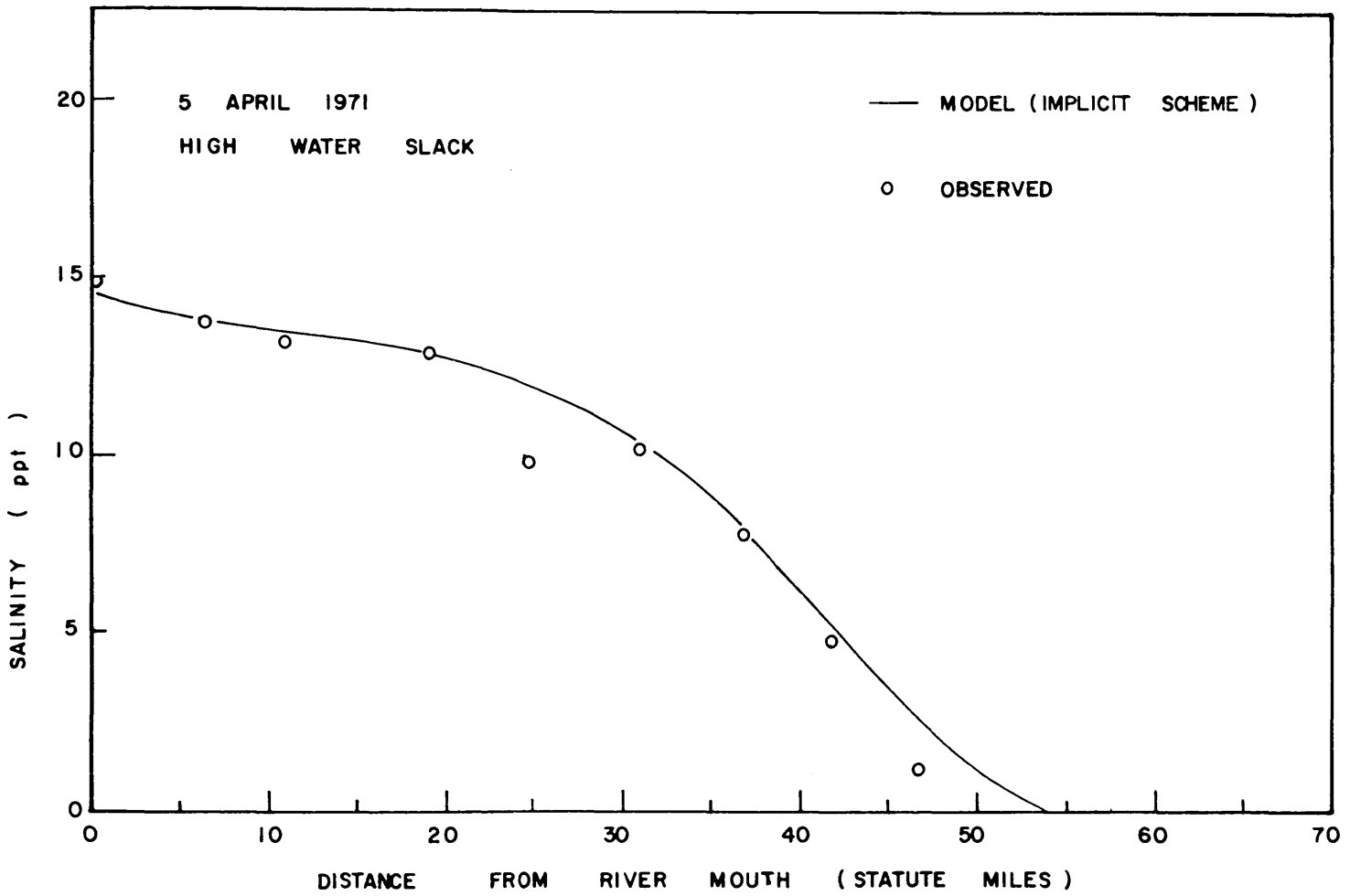

Figure 15. Longitudinal salinity distribution, April 5, 1971.

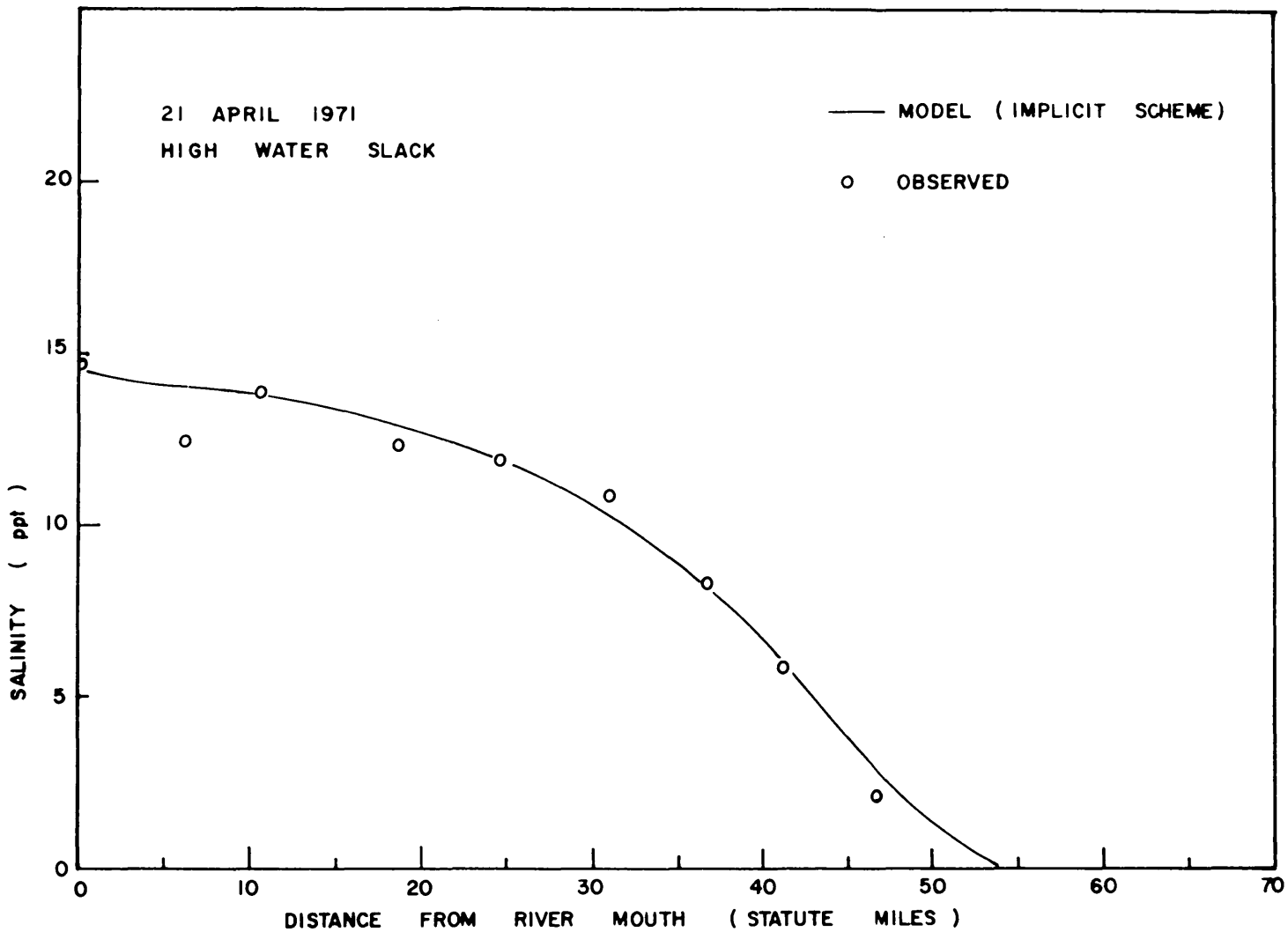

Figure 16. Longitudinal salinity distribution, April 21, 1971.

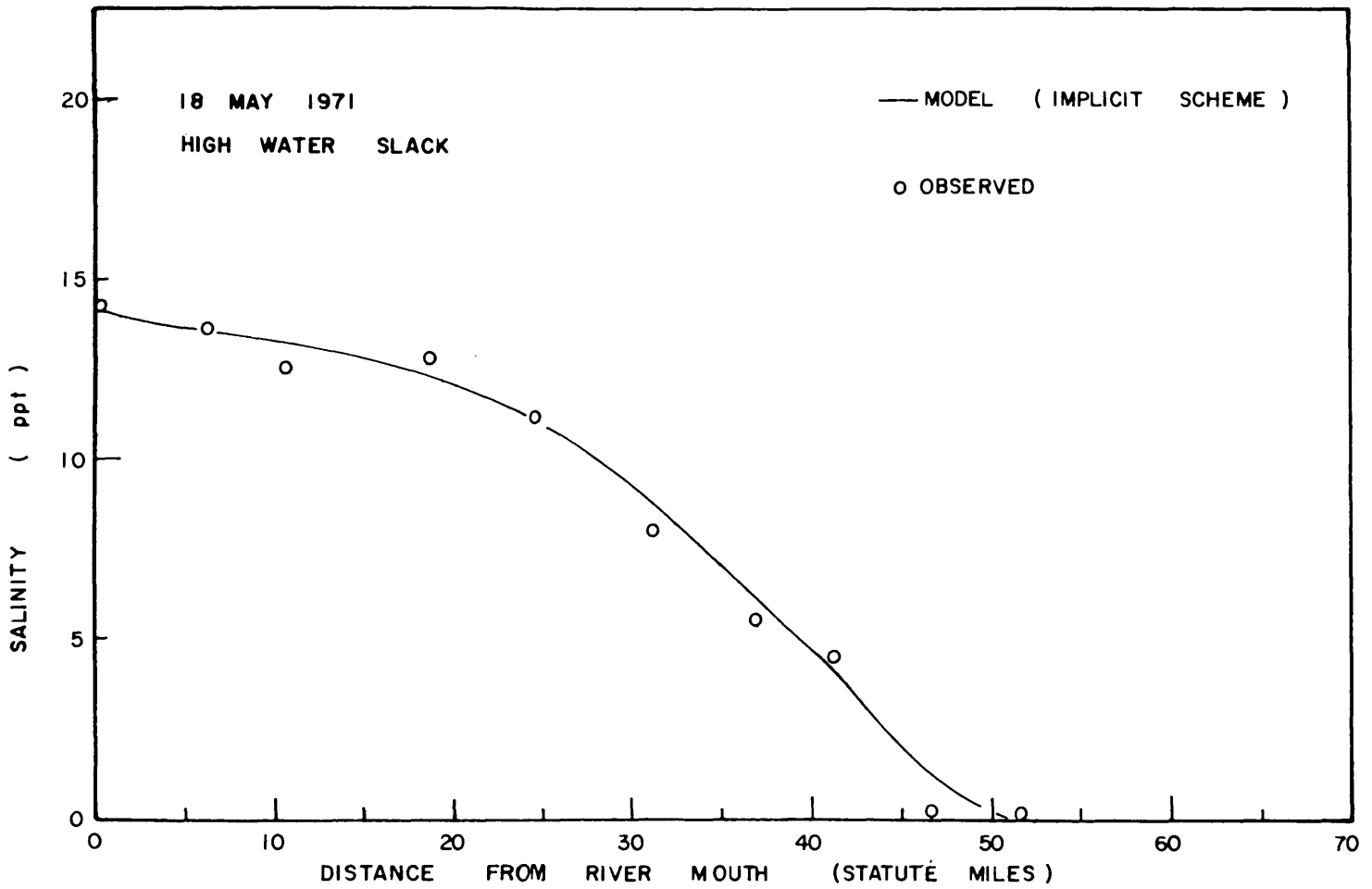

Figure 17. Longitudinal salinity distribution, May 18, 1971.

also were strong in this area. Drills have affected the economics of commercial planting of oysters downstream of Towle's Point in a negative fashion. As a consequence of MSX and drills which thrive in waters of higher salinity (above 15 ppt) oyster culture there has not been possible. The Corps of Engineers proposed to use the Salem Church Dam to control the salinity in such a way as to make oyster culture economically feasible downstream of Towle's Point, and thus derive an economic benefit. The necessary conditions for disease control are a temperature of at least $20^{o}C$ and salinity less than ten parts per thousand for twenty days.

Several proposed controlled flow release schedules were tested by means of the mathematical models to see if these conditions could be achieved in a wet year. Mathematical model tests were run to compare the natural hydrograph of 1960 with a hypothetical controlled release for that year. The results from the two models are essentially identical. A sample result is shown in figure 18. The solid line represents simulated natural salinity at the end of May, 1960. The dashed curve represents the salinity distribution to be expected had Salem Church Dam been in operation and had it been discharging 8000 cfs for three weeks prior to this date. As can be seen, the difference between these curves decreases in the downstream direction. The decrease in salinity downstream of Towle's Point is not large enough to achieve the necessary conditions for disease control.

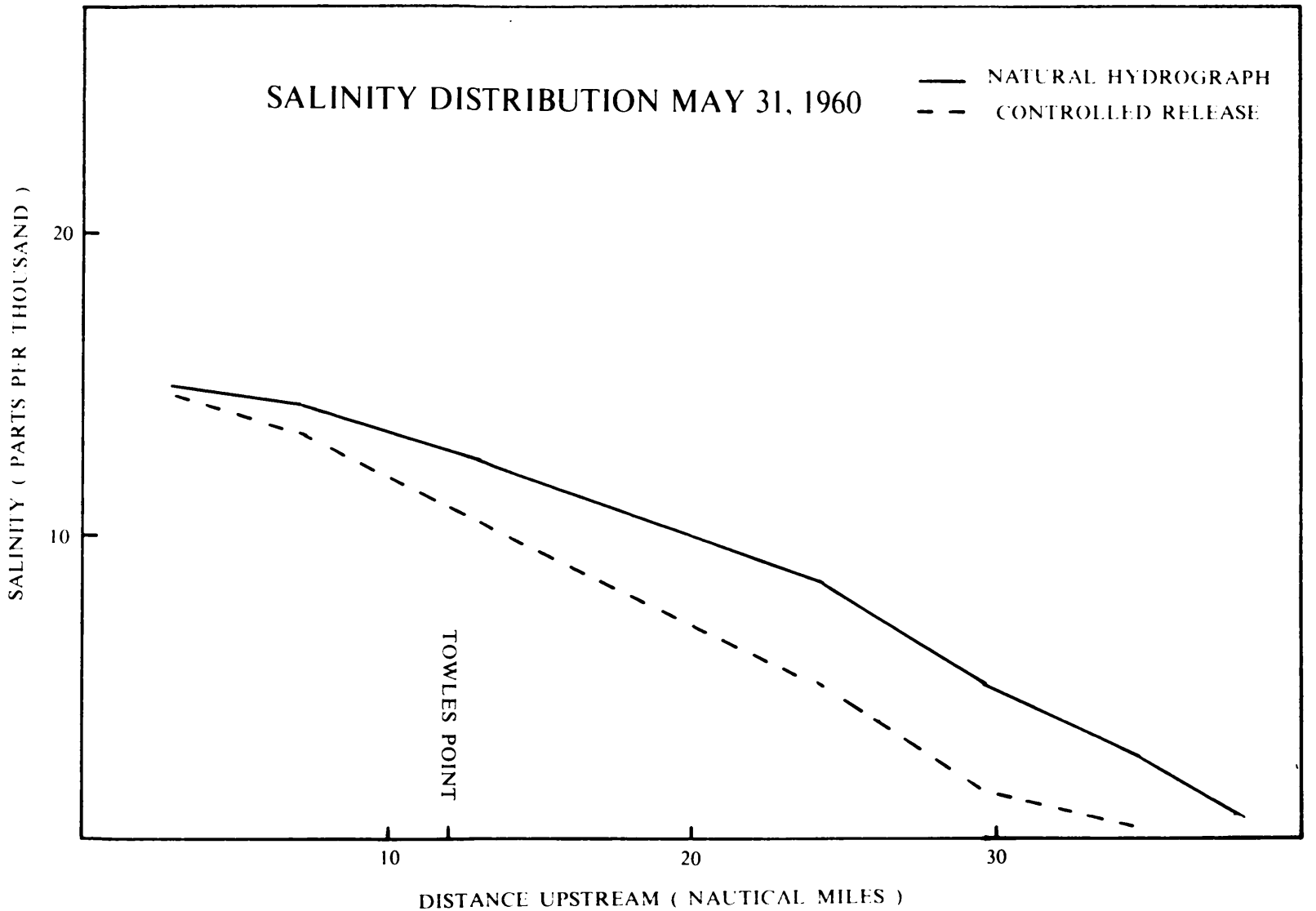

Figure 18. Effects of controlled freshwater release on salinity distribution.

References:

Carritt, D. E. and E. J. Green. 1967. New Tables for Oxygen Saturation of Sea Water. J. Mar. Res. 25(2).

Cronin, W. B. 1971. Volumetric, Areal, and Tidal Statistics of the Chesapeake Bay Estuary and its Tributaries. CBI Special Rep. 20, Ref. 71-2.

Elmore, H. L. and W. F. West. 1961. Effect of Water Temperature on Stream Reaeration. Proc. ASCE, 87(SA6).

Fang, C. S., P. V. Hyer, A. Y. Kuo and W. J. Hargis, Jr. 1972. Hydrography and Hydrodynamics of Virginia Estuaries. Part III. Studies of the Distribution of Salinity and Dissolved Oxygen in the Upper Tidal Rappahannock River. Special Rep. No. 25. Va. Inst. of Mar. Sci.

Hargis, W. J., D. Oberholtzer, and M. M. Nichols. 1975. Southern Chesapeake Bay water color and circulation analysis. Va. Inst. of Mar. Sci.

Harleman, D. R. F. 1971. One-Dimensional Models in Estuarine Modeling: An Assessment. Tracor, Inc.

Holley, E. R., D. R. F. Harleman, and H. B. Fischer. 1970. Dispersion in Homogeneous Estuary Flow. Proc. ASCE, 96 (HY8).

O'Connor, D. J. and W. E. Dobbins. 1956. Mechanics of Reaeration in Natural Streams. Proc. ASCE 82(SA2).

Paulson, R. W. 1970. Variation of the Longitudinal Dispersion Coefficient in the Delaware River Estuary as a Function of Freshwater Inflow. Water Resources Res., Vol. 6, No. 2.

Pence, G. D., Jr., J. M. Jeglic and R. V. Thomann. 1968. Time-Varying Dissolved Oxygen Model. J. Sanitary Eng. Div. Proc. ASCE, Vol. 94, No. SA2.

Seitz, R. C. 1971. Drainage Area Statistics for the Chesapeake Bay Freshwater Drainage Basin. CBI Special Rep. 19.

Taylor, G. I. 1954. The Dispersion of Matter in Turbulent Flow through a Pipe. Proc. Roy. Soc. of London, A223.

Nichols, M. and G. Poor. 1967. Sediment Transport in a Coastal Plain Estuary. J. Waterways and Harbors Division. Proc. ASCE, Vol. 93, No. WW4.

Thomann, R. V. 1972. System Analysis and Water Quality Management. Environmental Research and Applications, Inc. New York, N. Y.

APPENDIX A

Graphical Summary of
Results of Intensive Field Survey

July, 1973

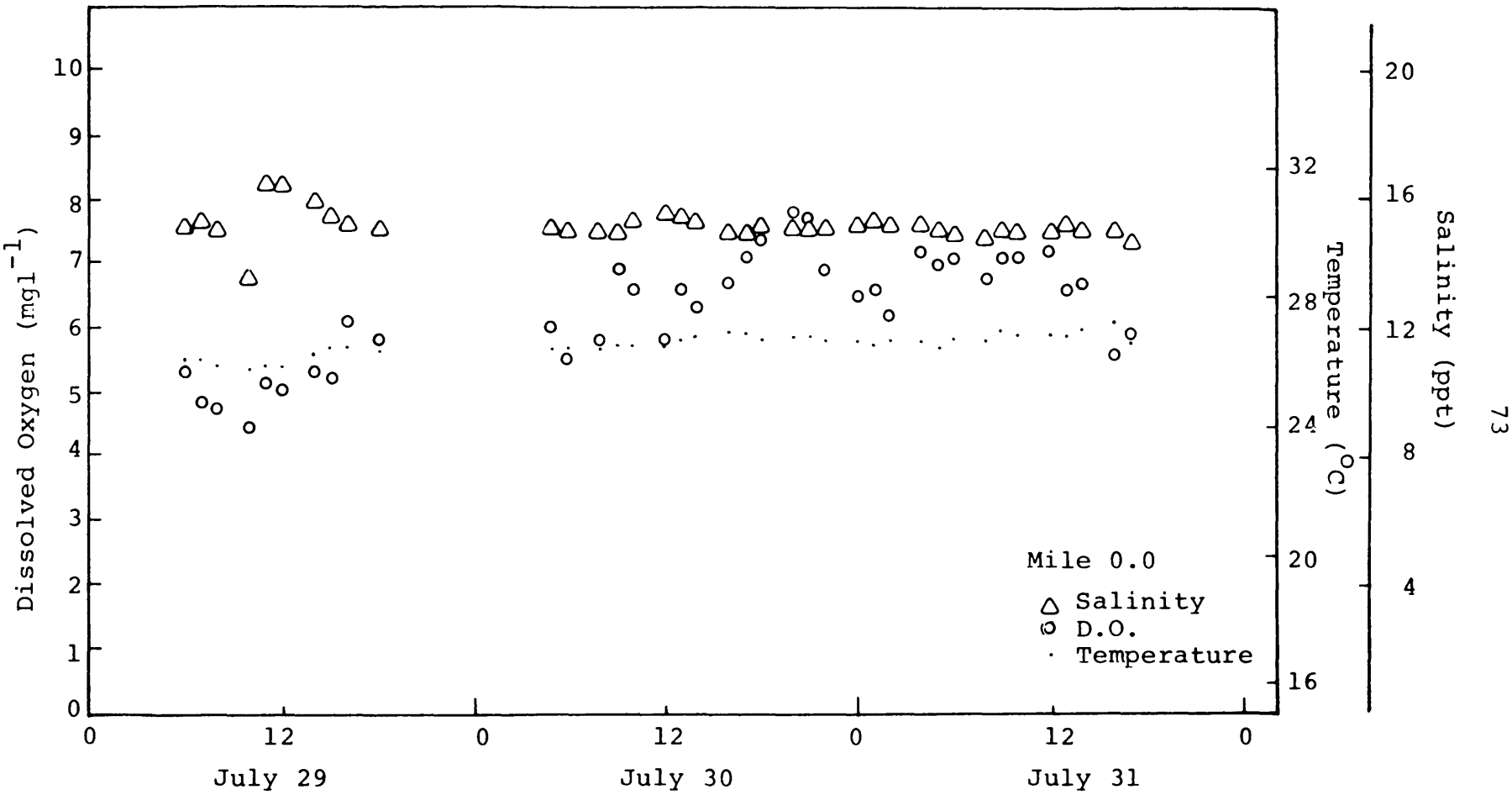

Figure A1. Observed Water Quality Parameters, Mile 0.0.

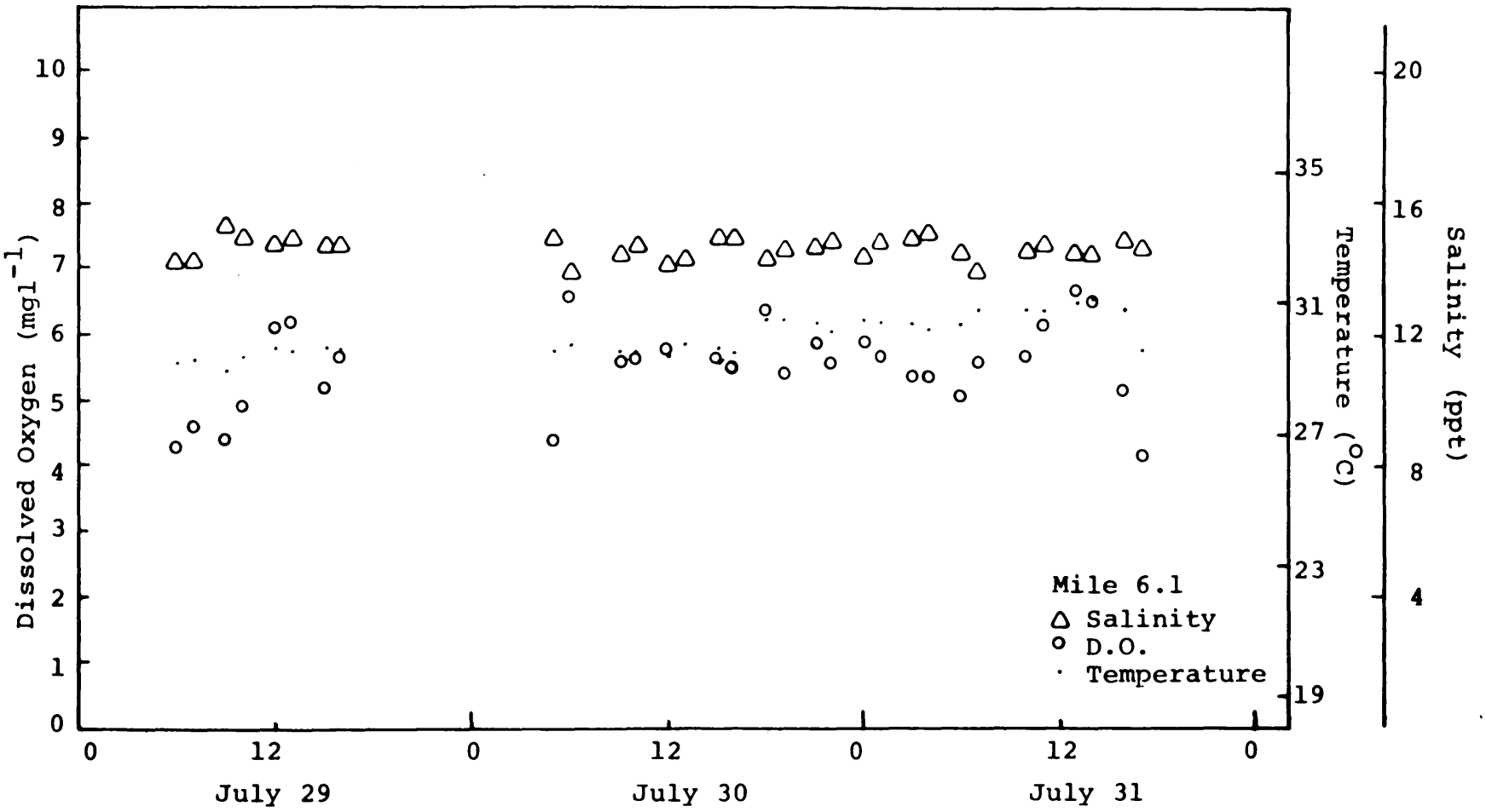

Figure A2. Observed Water Quality Parameters, Mile 6.1.

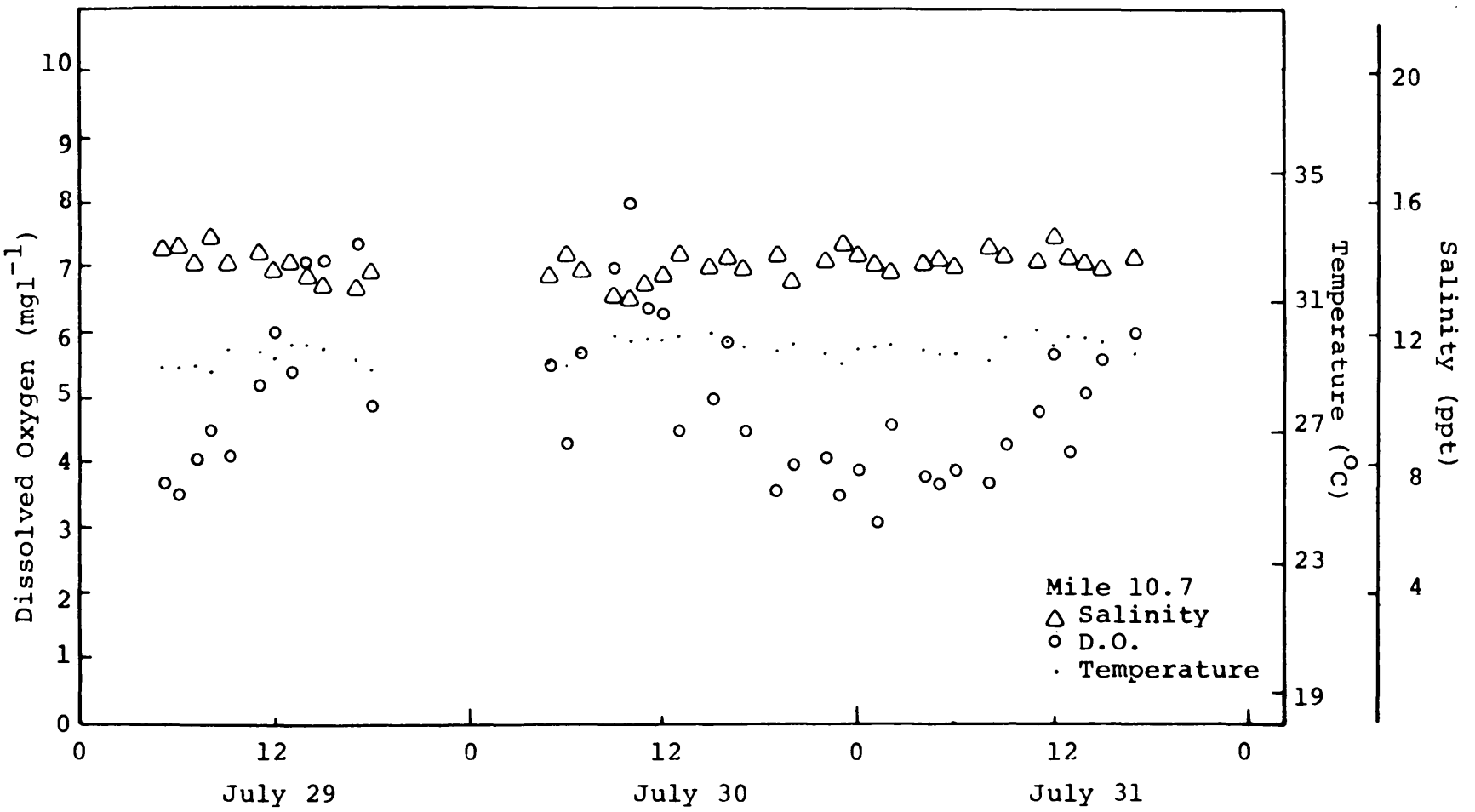

Figure A3. Observed Water Quality Parameters, Mile 10.7.

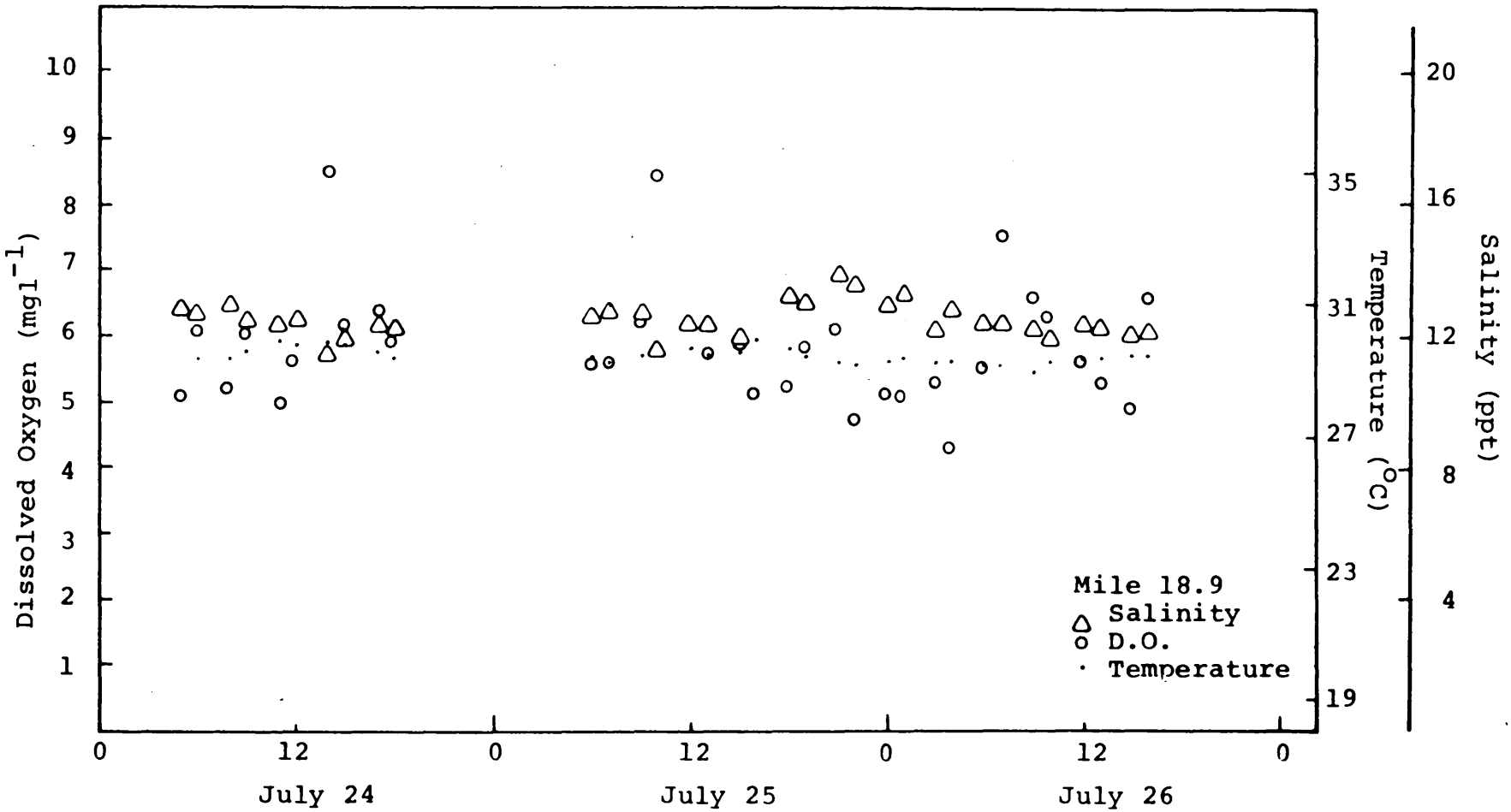

Figure A4. Observed Water Quality Parameters, Mile 18.9.

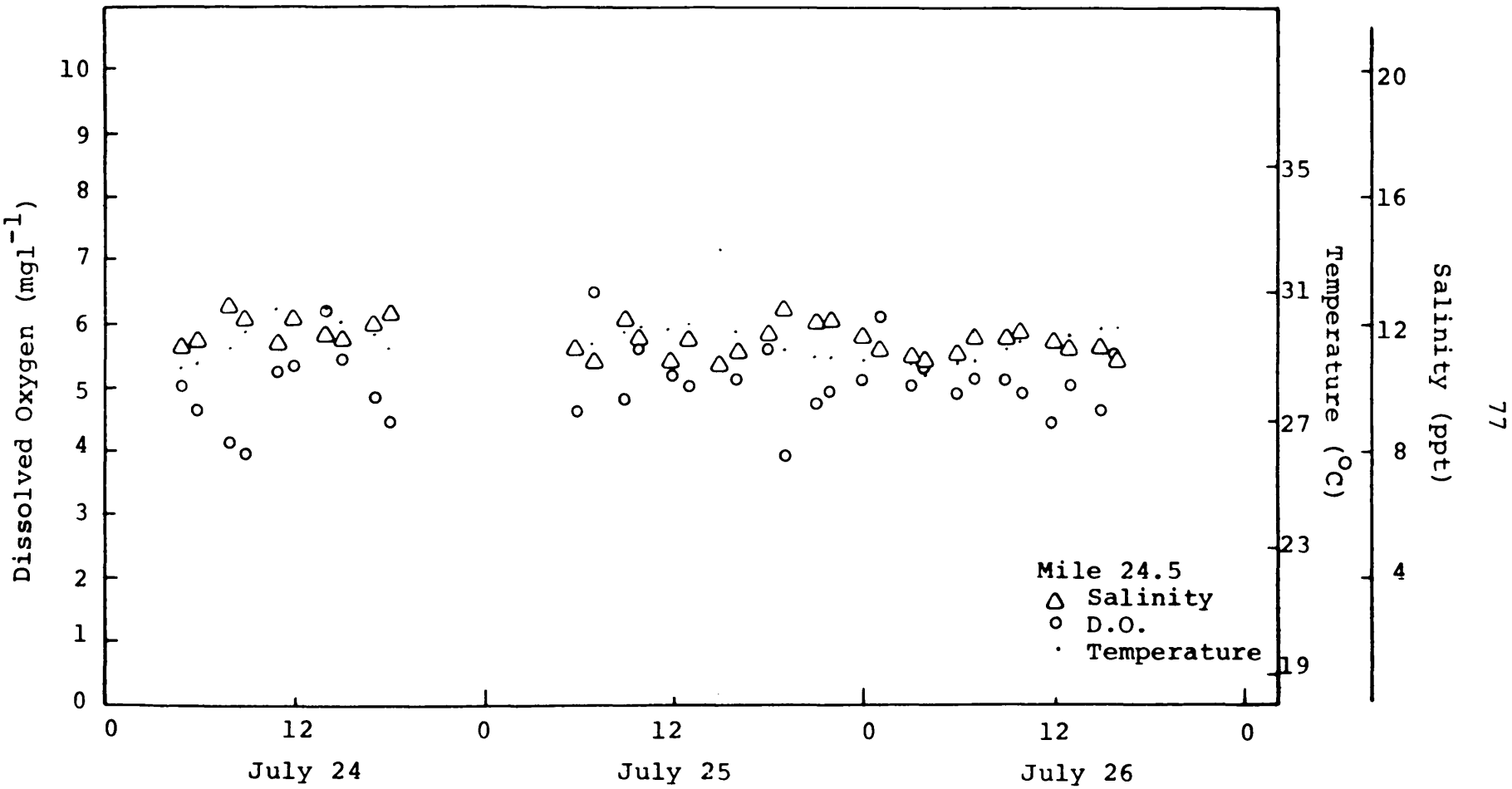

Figure A5. Observed Water Quality Parameters, Mile 24.5.

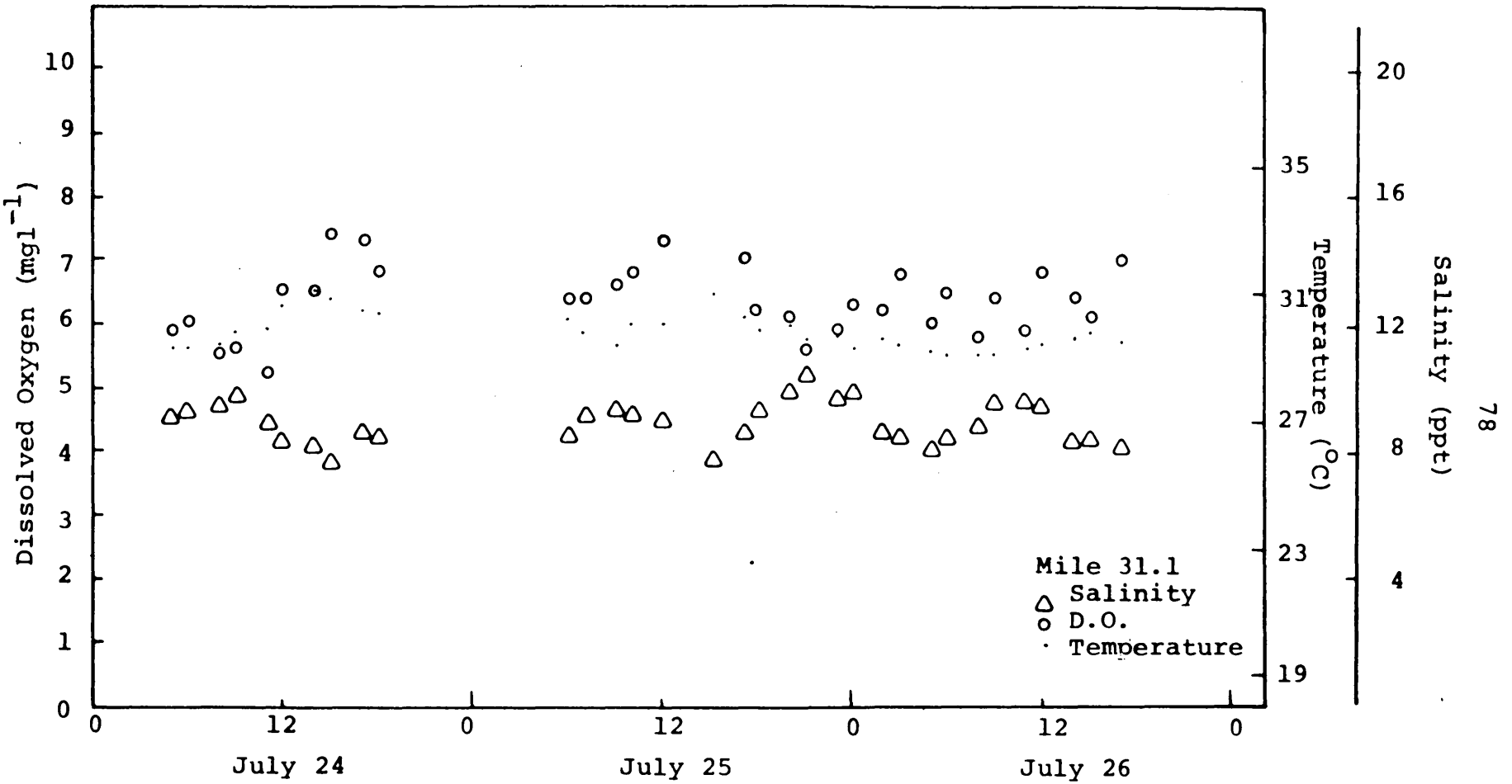

Figure A6. Observed Water Quality Parameters, Mile 31.1.

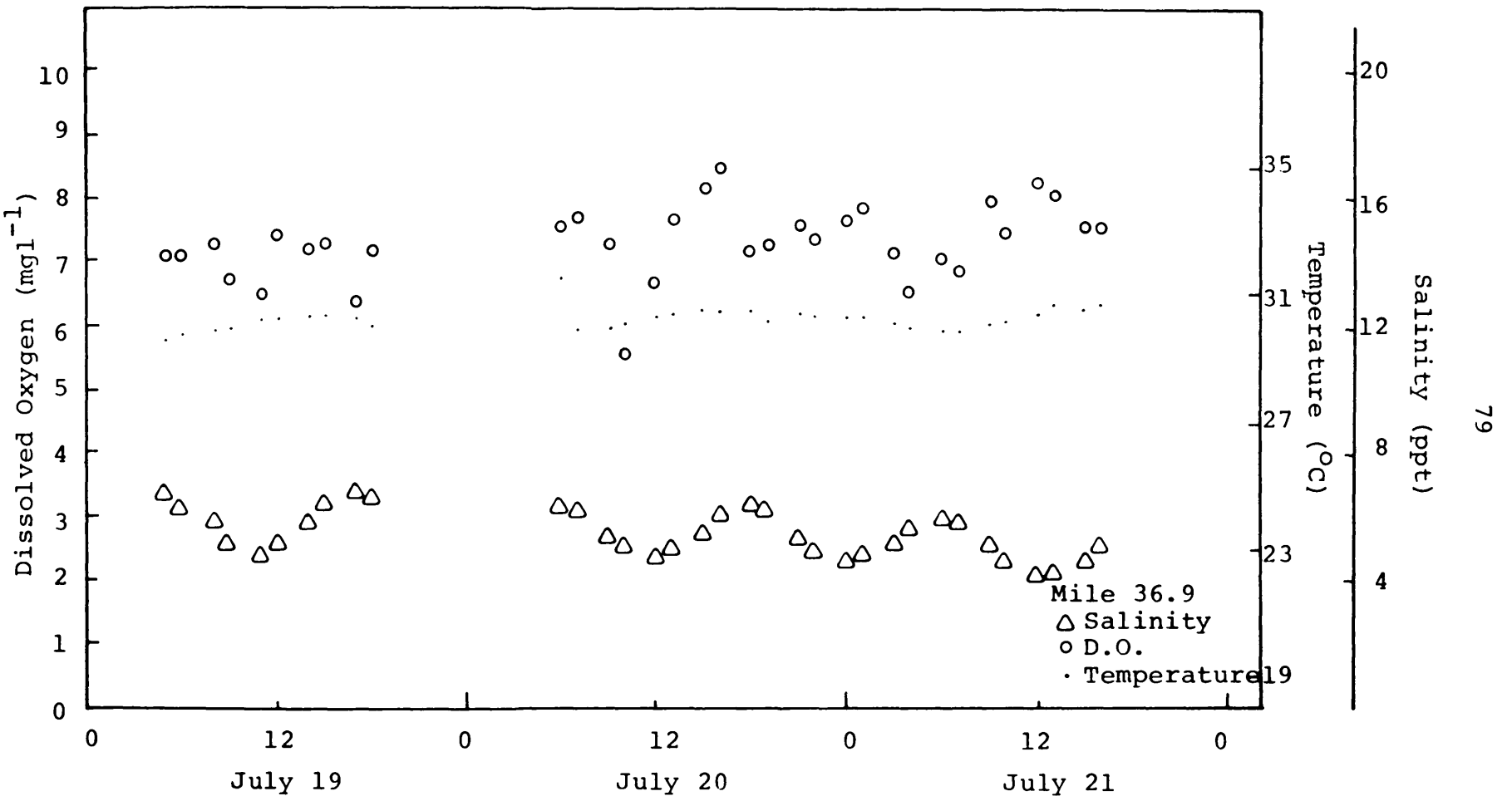

Figure A7. Observed Water Quality Parameters, Mile 36.9.

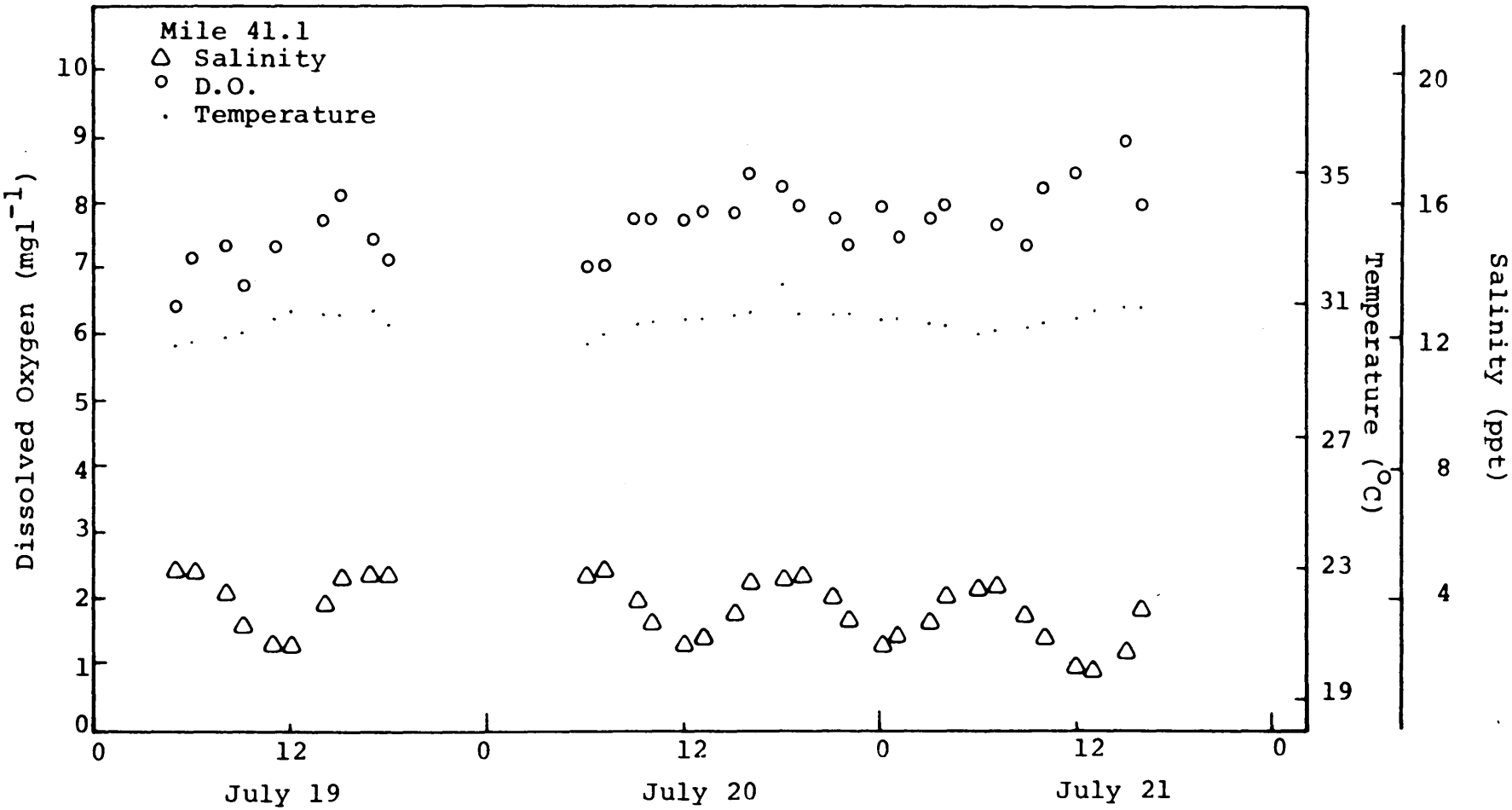

Figure A8. Observed Water Quality Parameters, Mile 41.1.

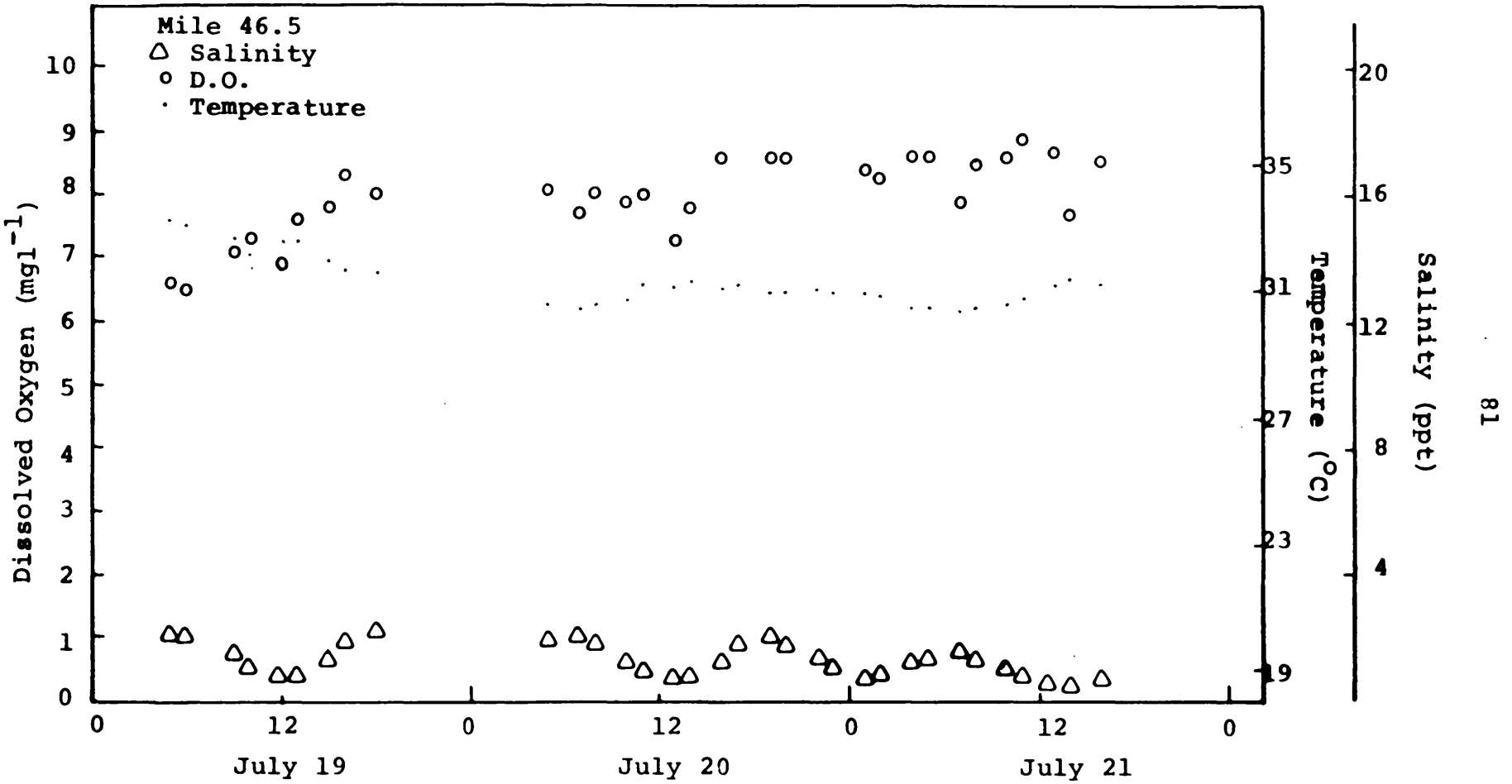

Figure A9. Observed Water Quality Parameters, Mile 46.5.

APPENDIX B

Graphical Summary of
Distribution of Dye Following Release

July, 1973

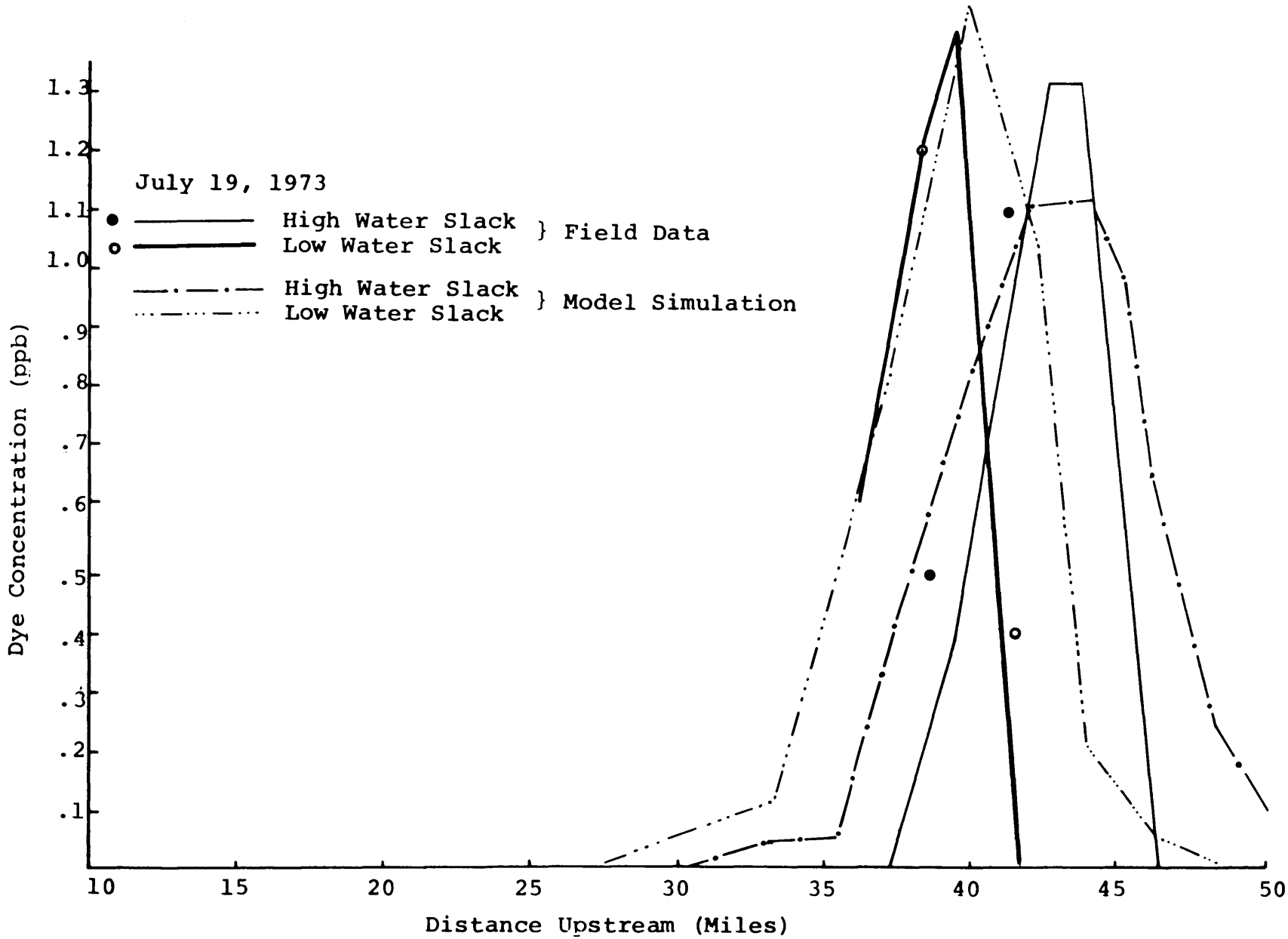

Figure B1. Longitudinal Dye Distribution, July 19.

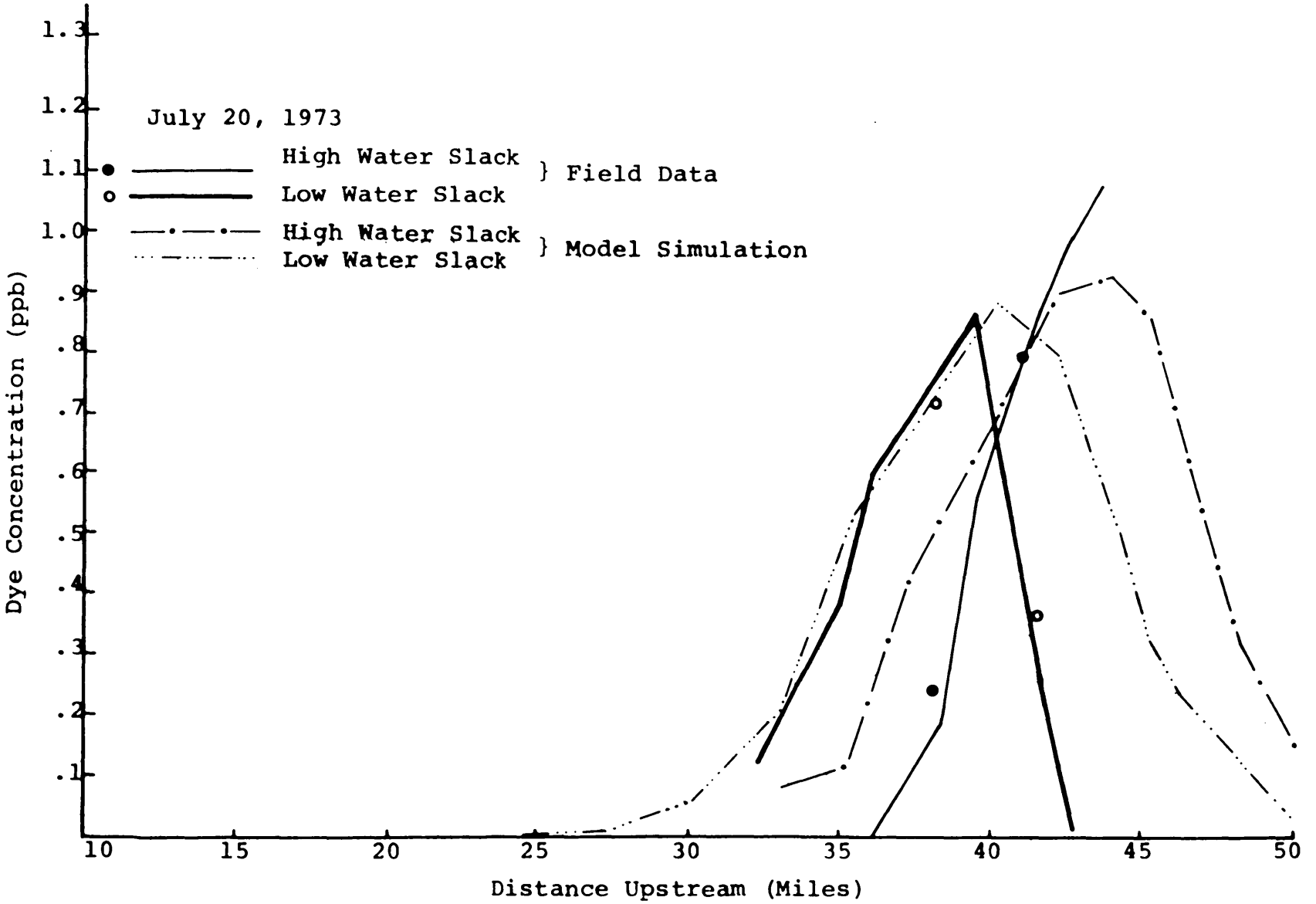

Figure B2. Longitudinal Dye Distribution, July 20.

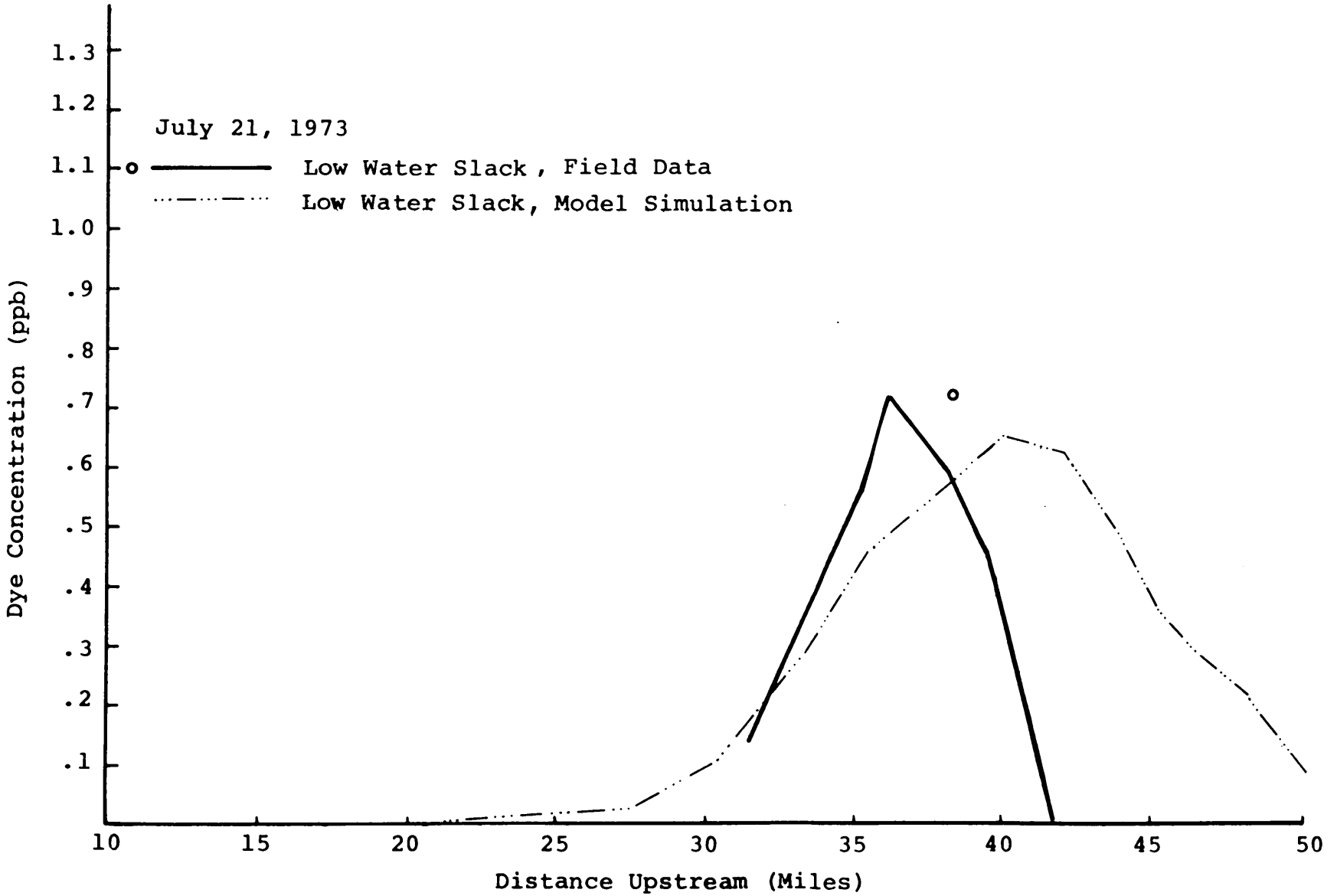

Figure B3. Longitudinal Dye Distribution, July 21.

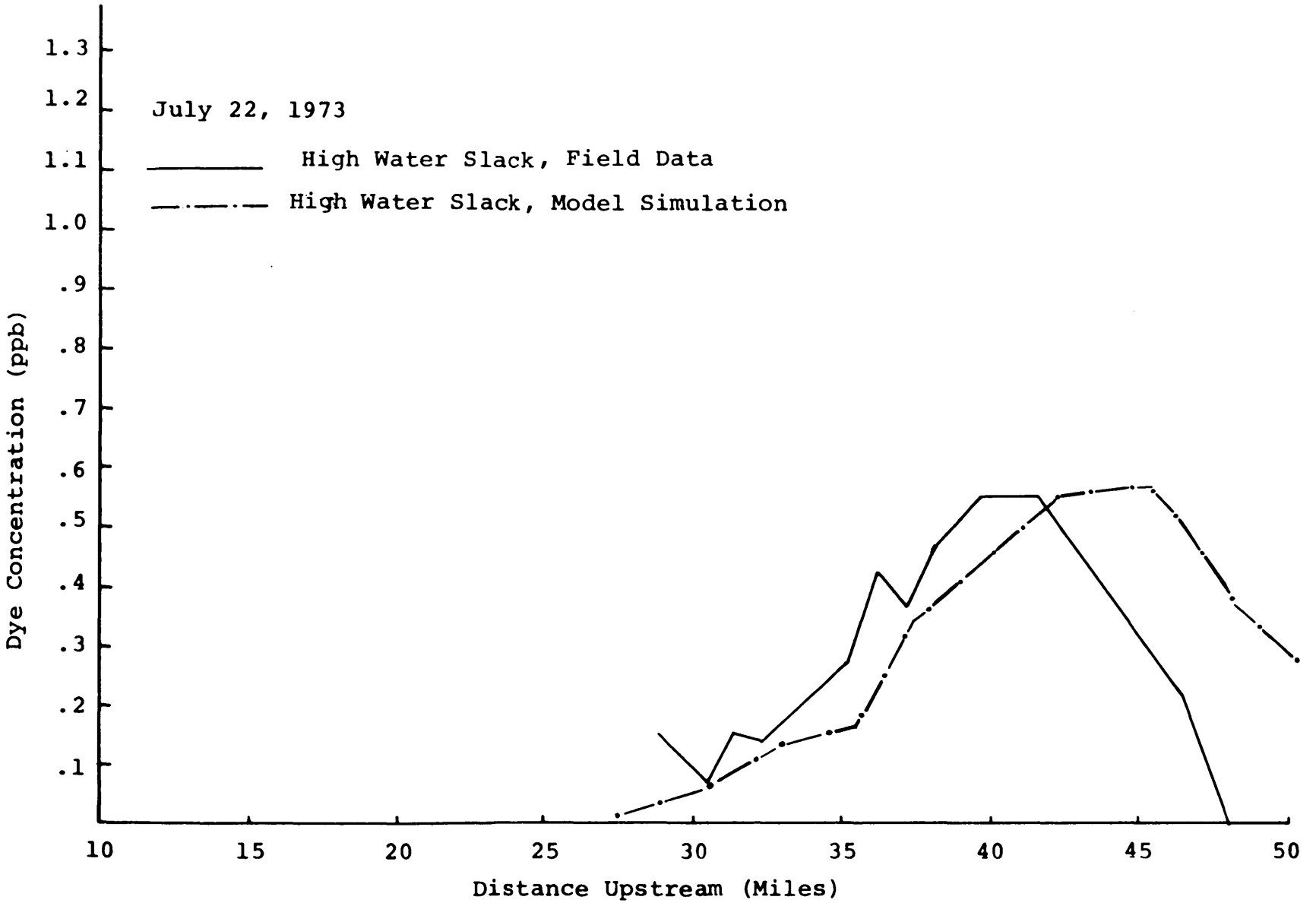

Figure B4. Longitudinal Dye Distribution, July 22.

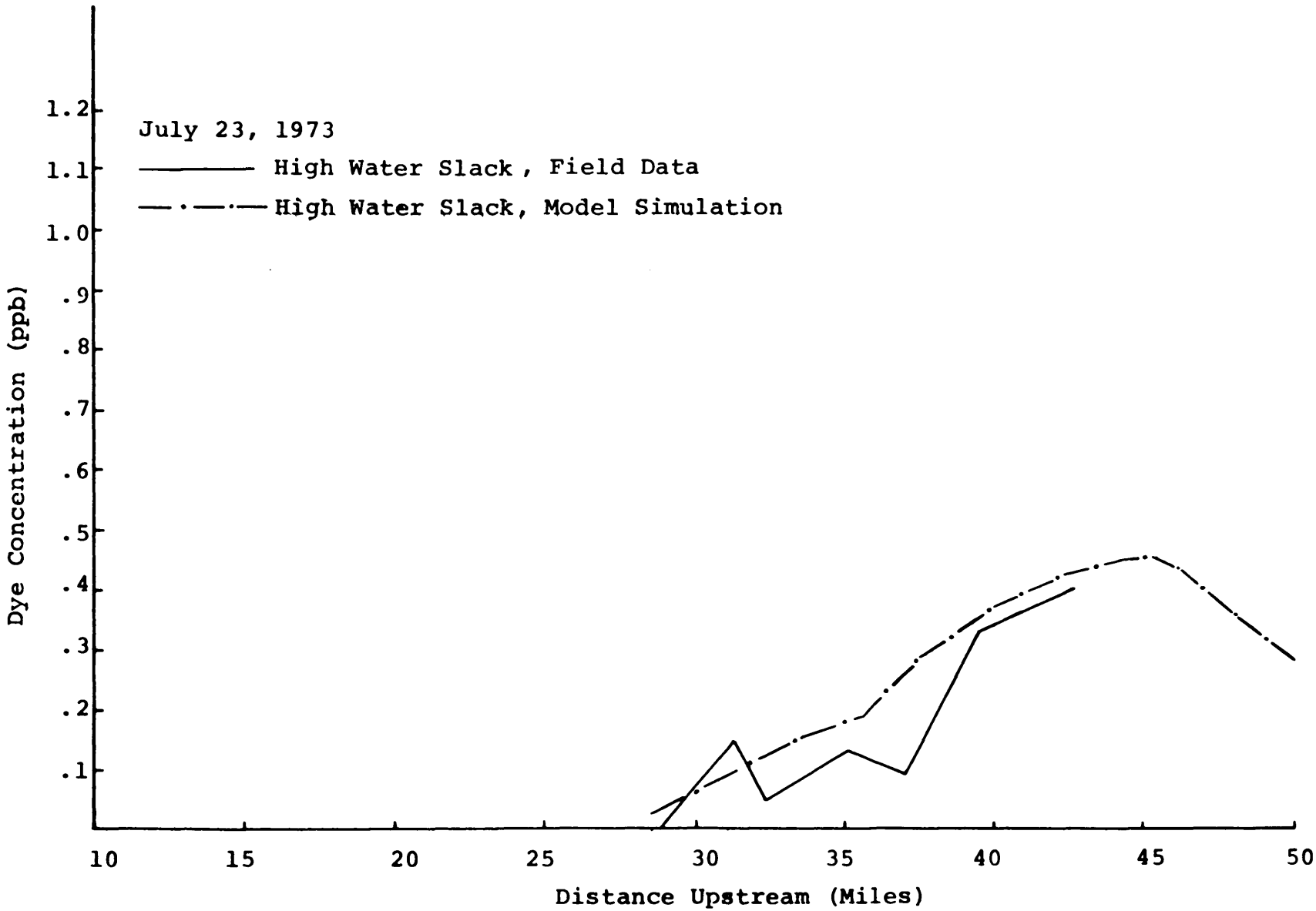

Figure B5. Longitudinal Dye Distribution, July 23.

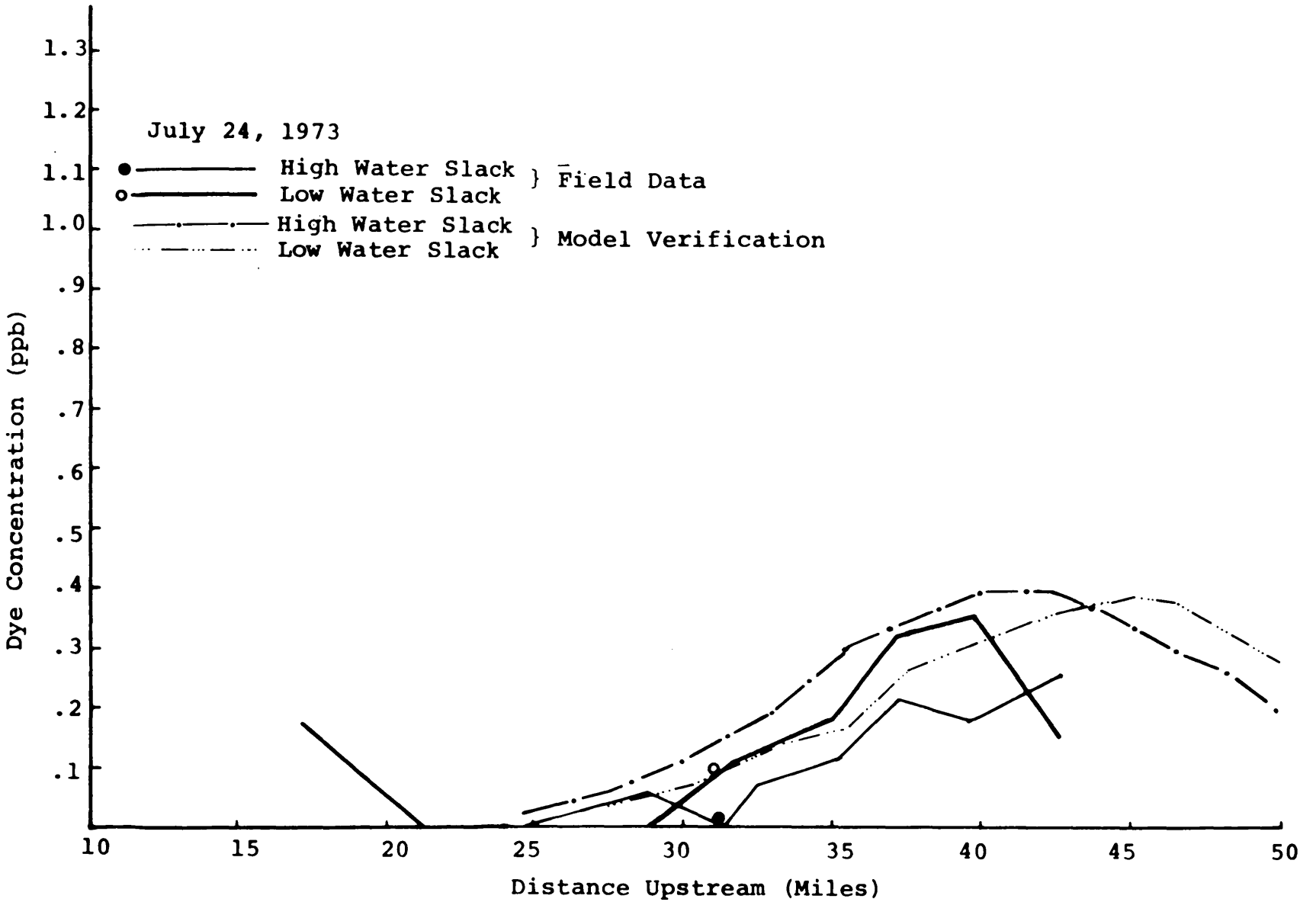

Figure B6. Longitudinal Dye Distribution, July 24.

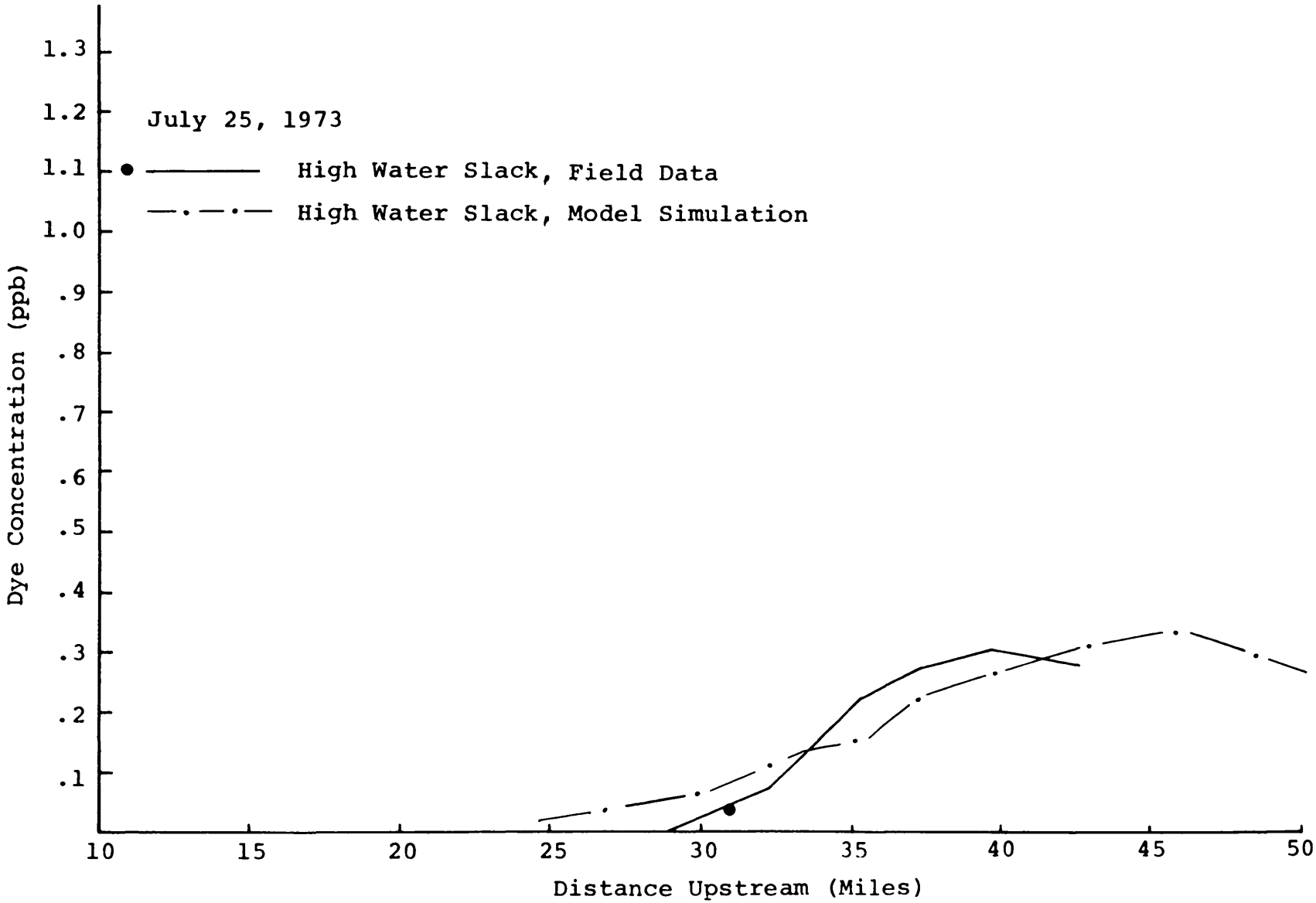

Figure B7. Longitudinal Dye Distribution, July 25.

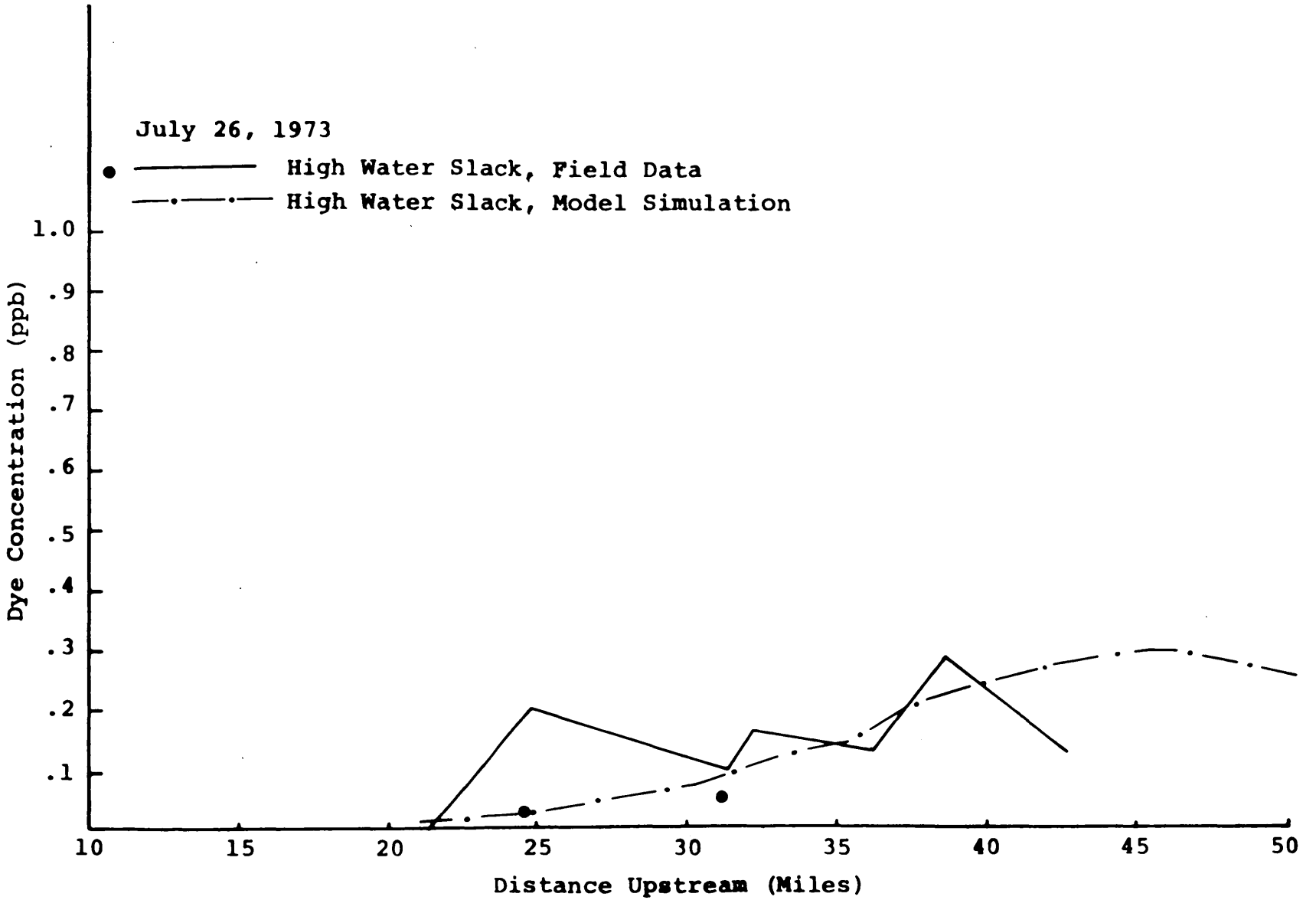

Figure B8. Longitudinal Dye Distribution, July 26.

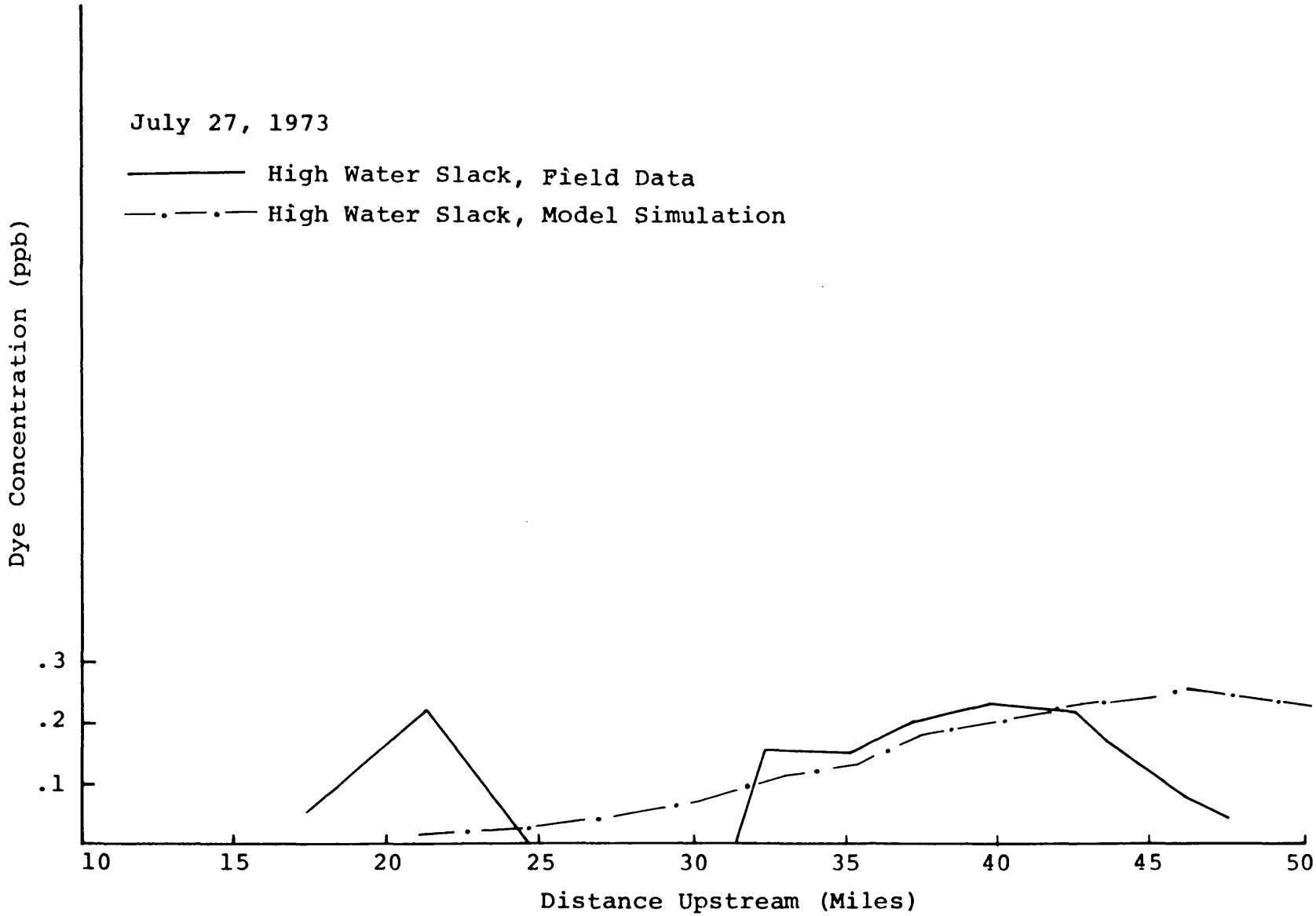

Figure B9. Longitudinal Dye Distribution, July 27.

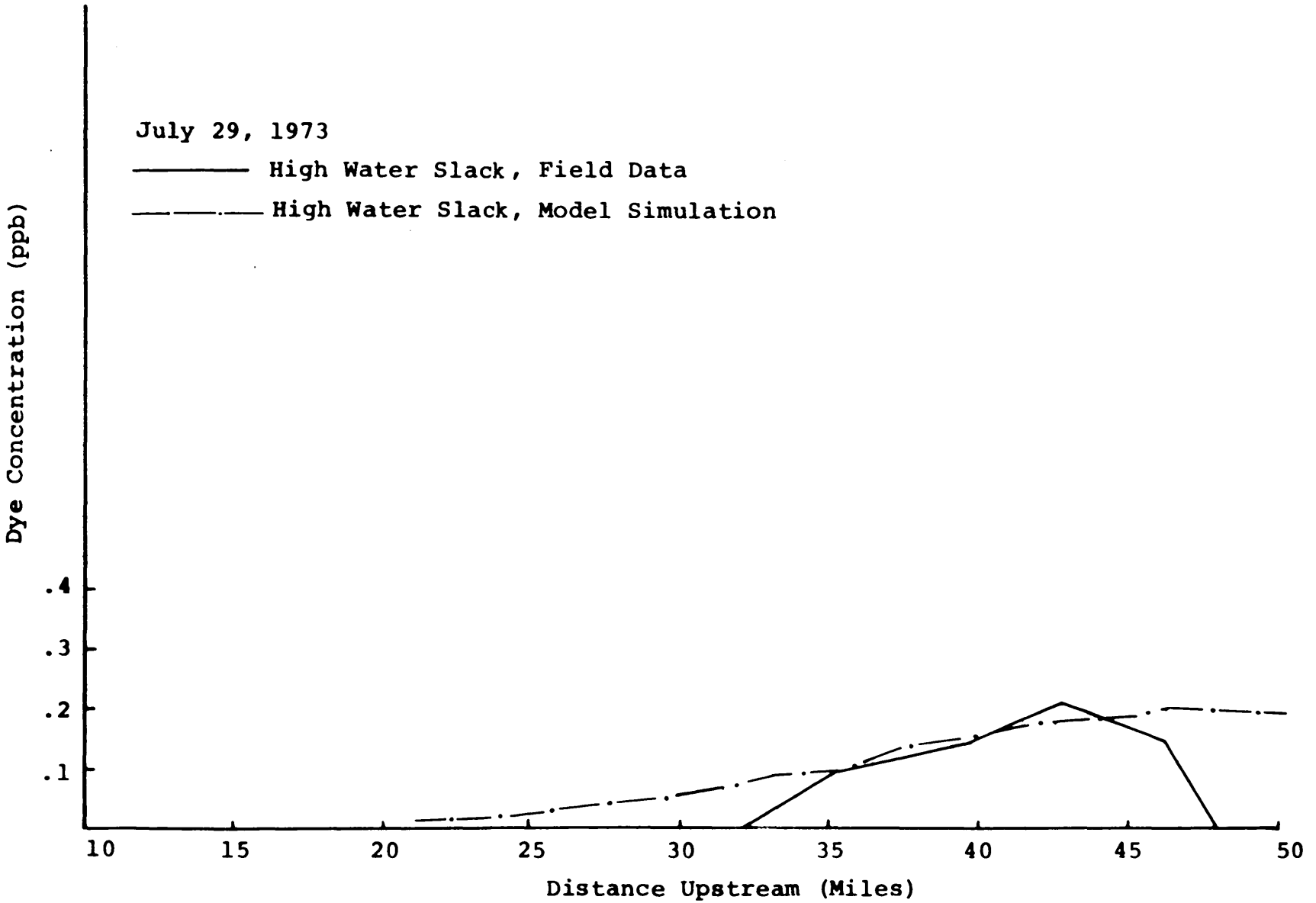

Figure B10. Longitudinal Dye Distribution, July 29.

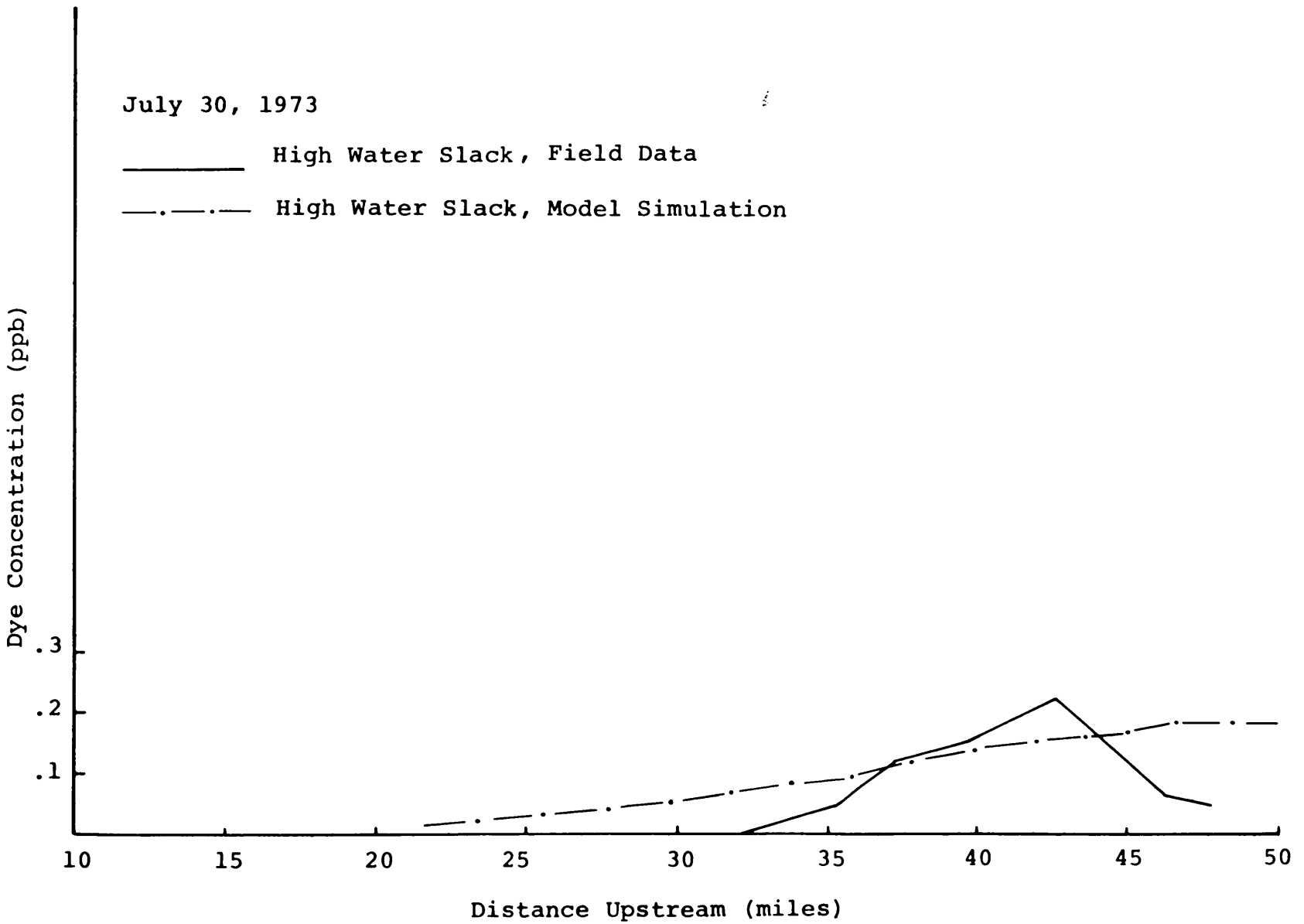

Figure B11. Longitudinal Dye Distribution, July 30.

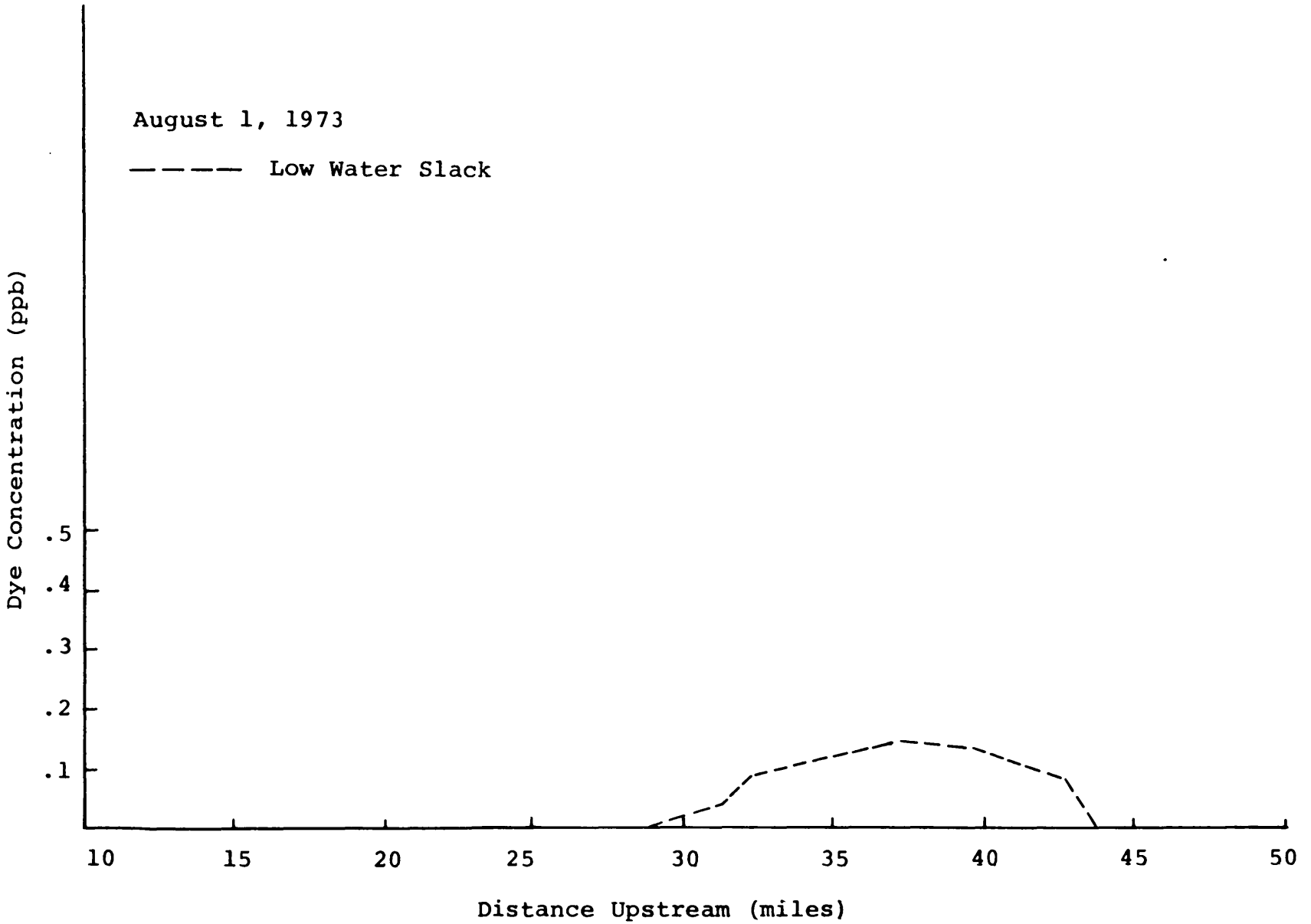

Figure B12. Longitudinal Dye Distribution, August 1.

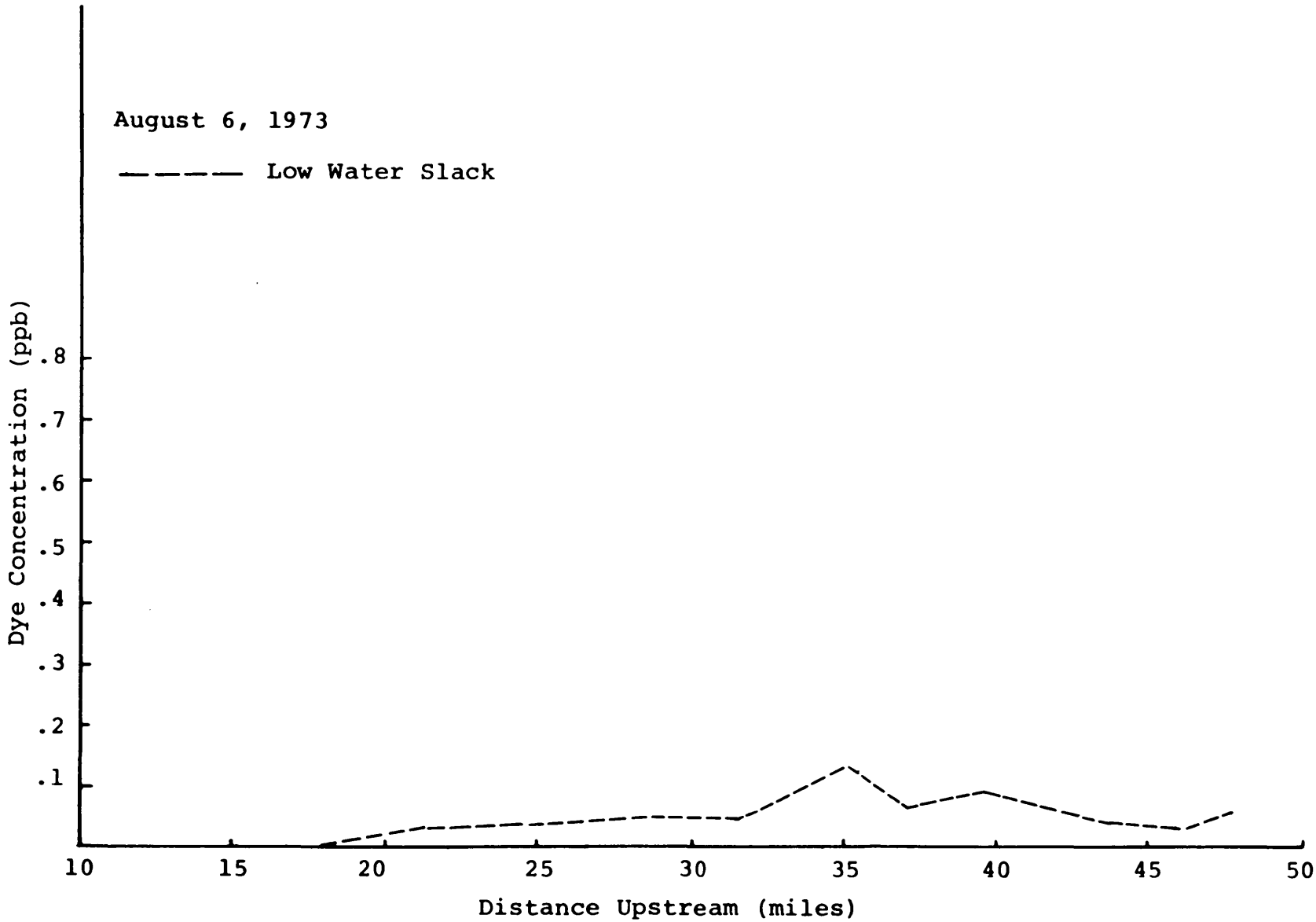

Figure B13. Longitudinal Dye Distribution, August 6.

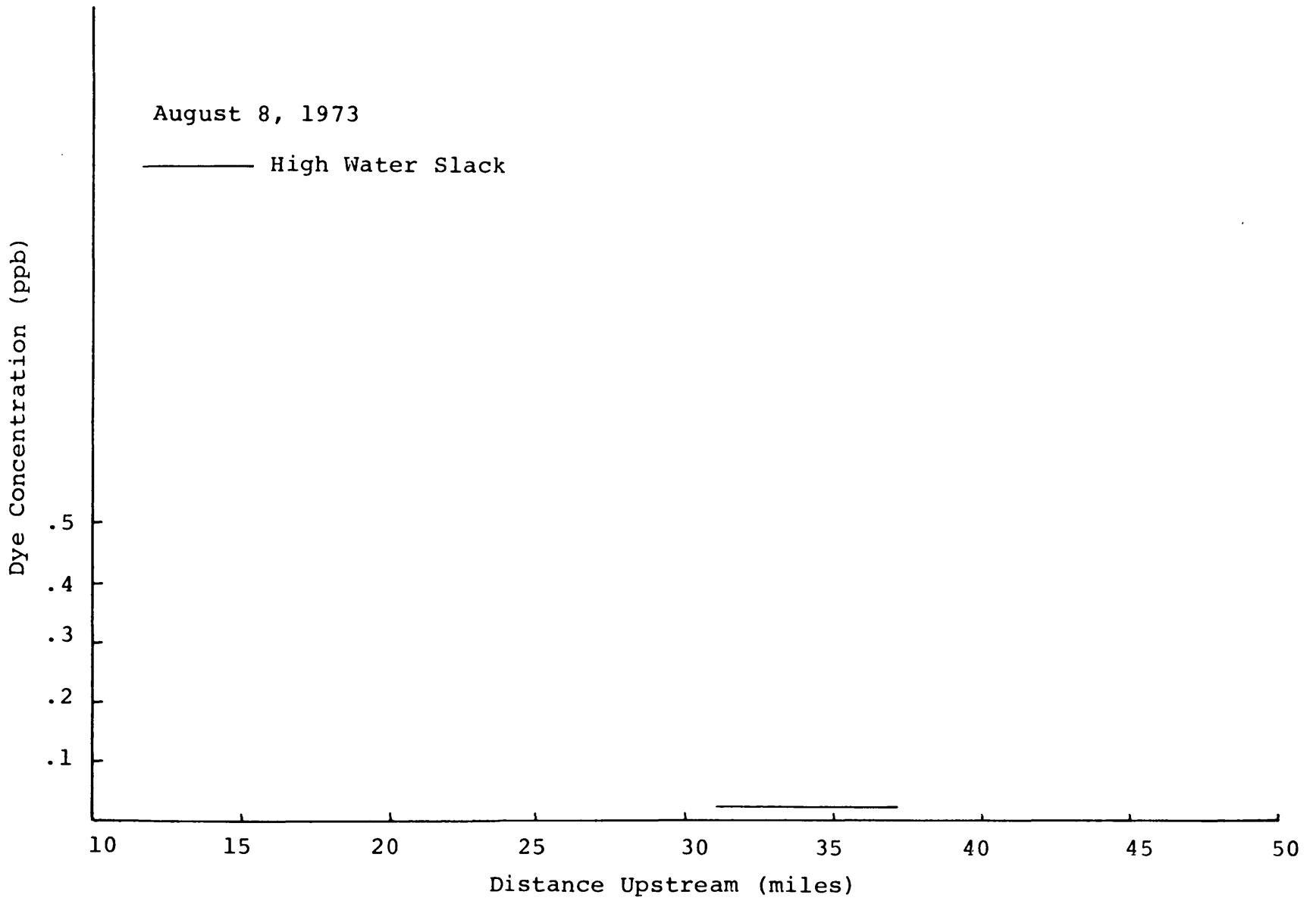

Figure B14. Longitudinal Dye Distribution, August 8.

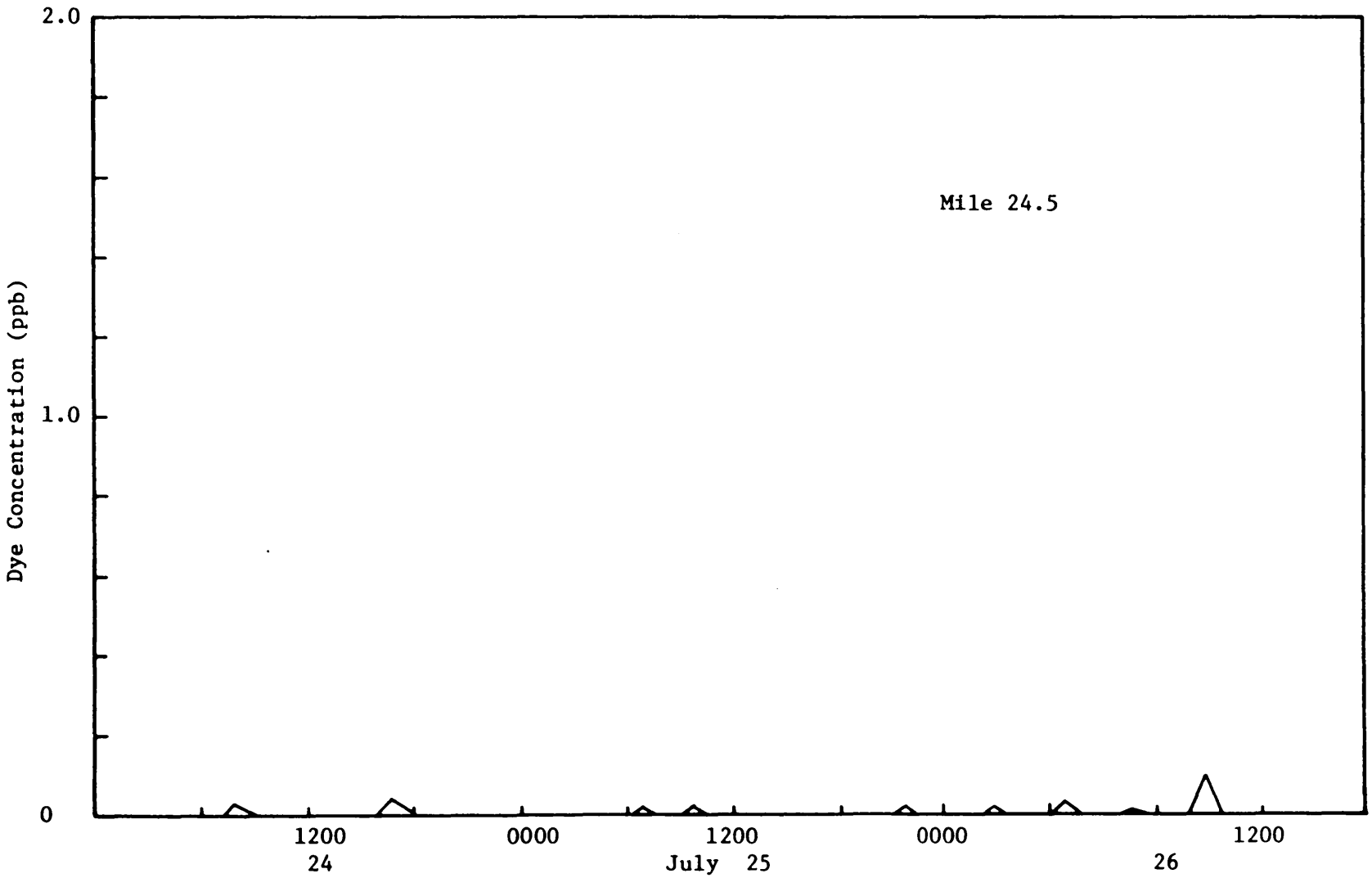

Figure B15. Observed Dye Concentration at Mile 24.5.

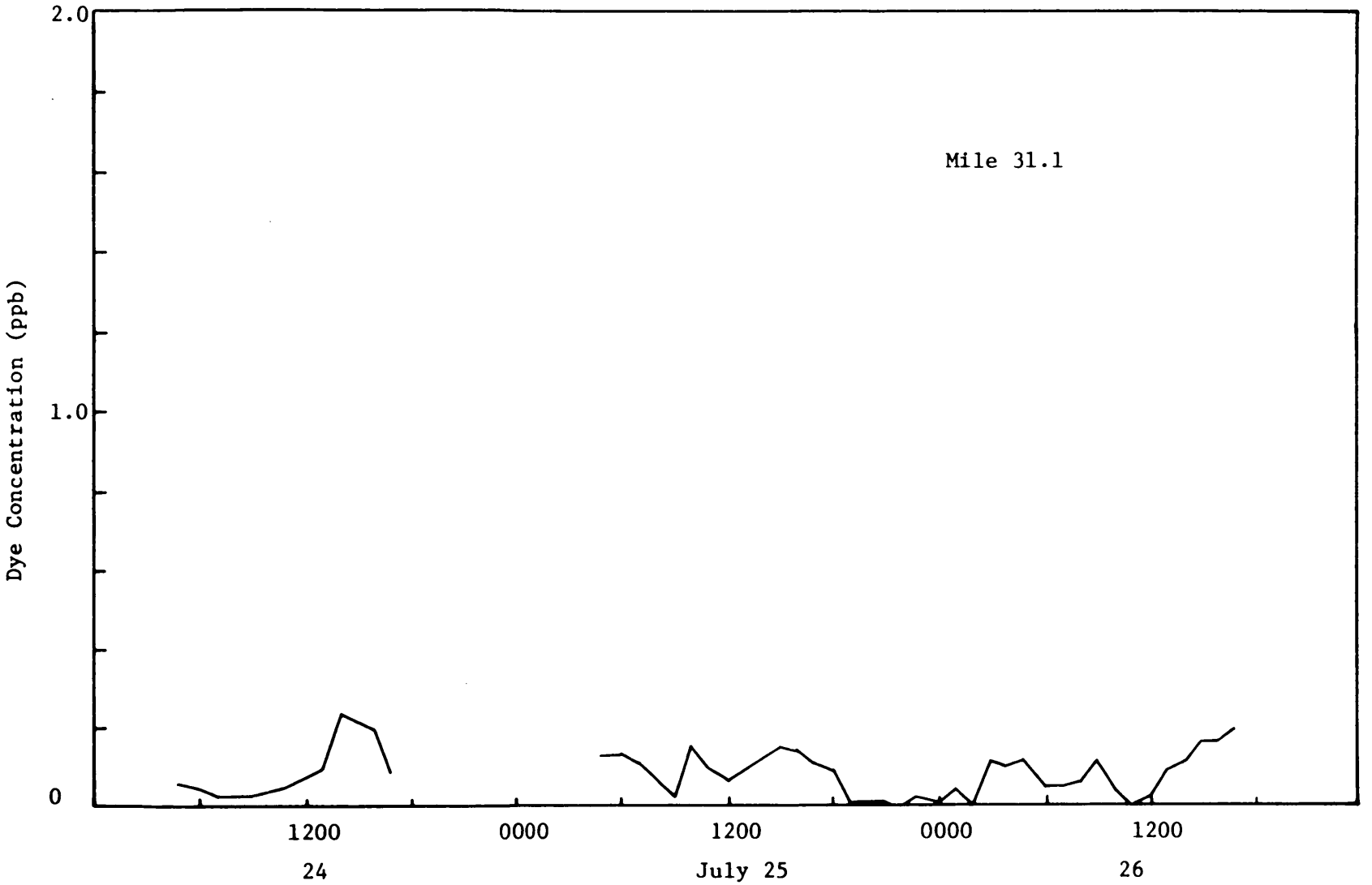

Figure B16. Observed Dye Concentration at Mile 31.1.

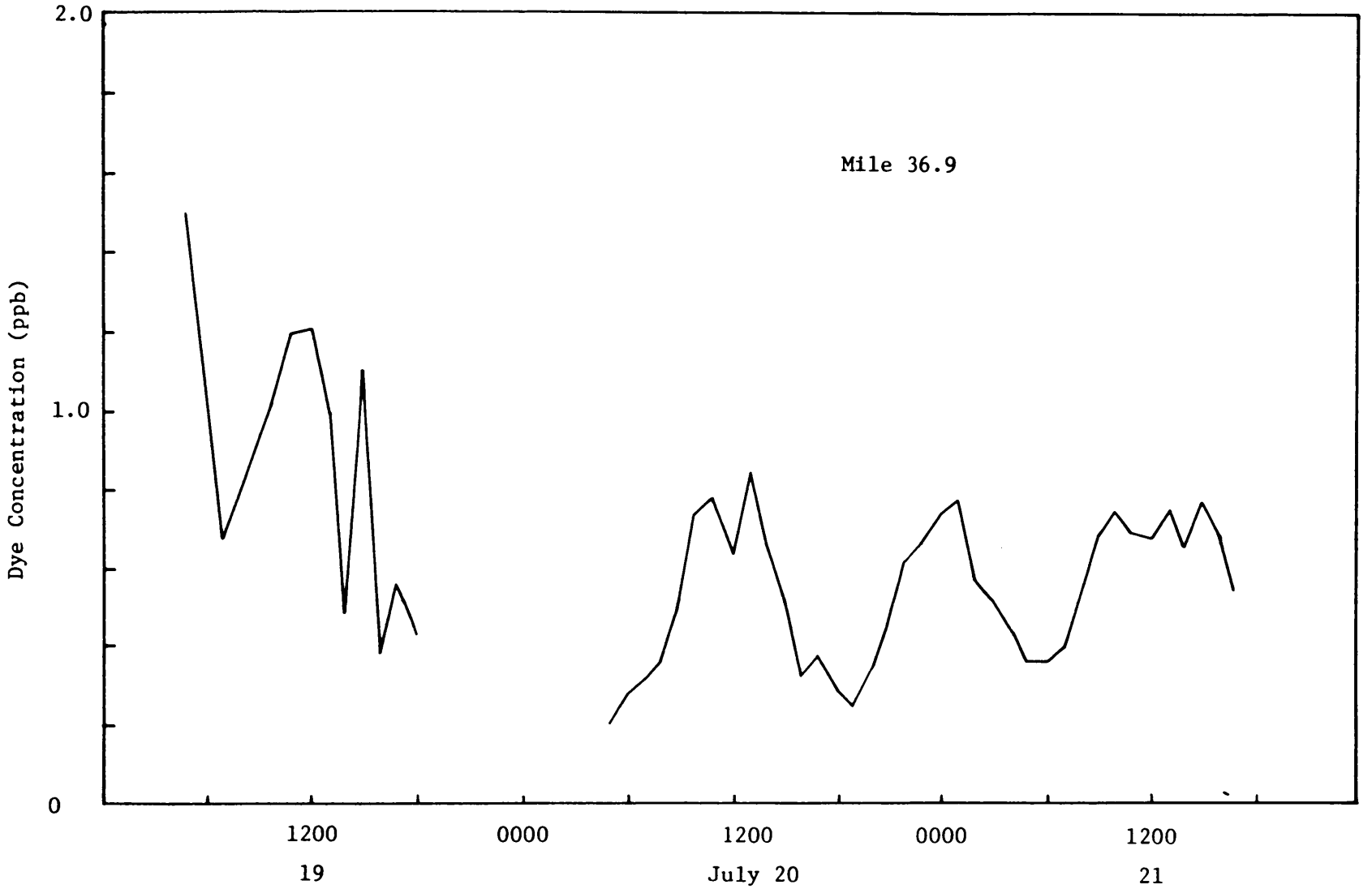

Figure B17. Observed Dye Concentration at Mile 36.9.

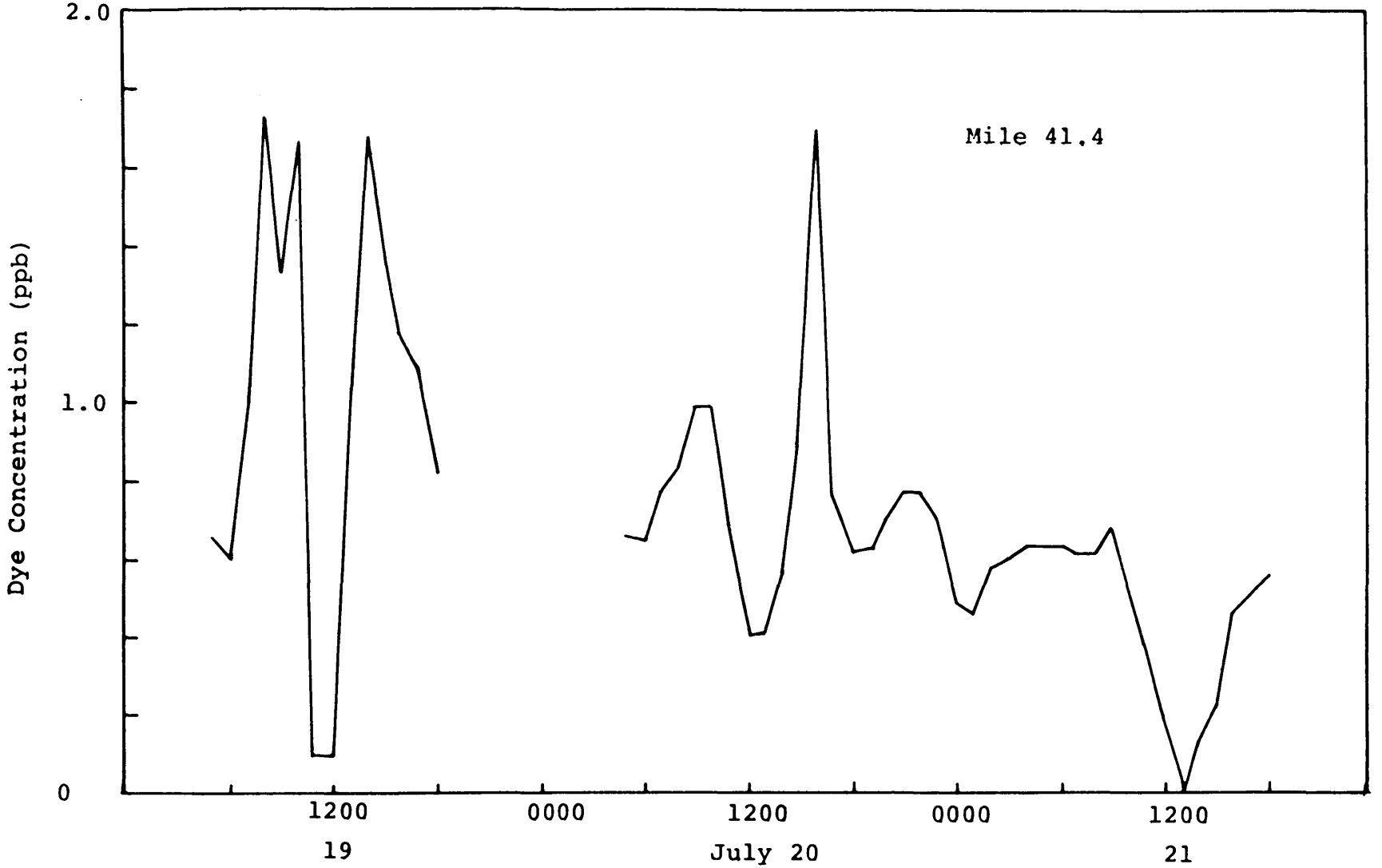

Figure B18. Observed Dye Concentration at Mile 41.4.

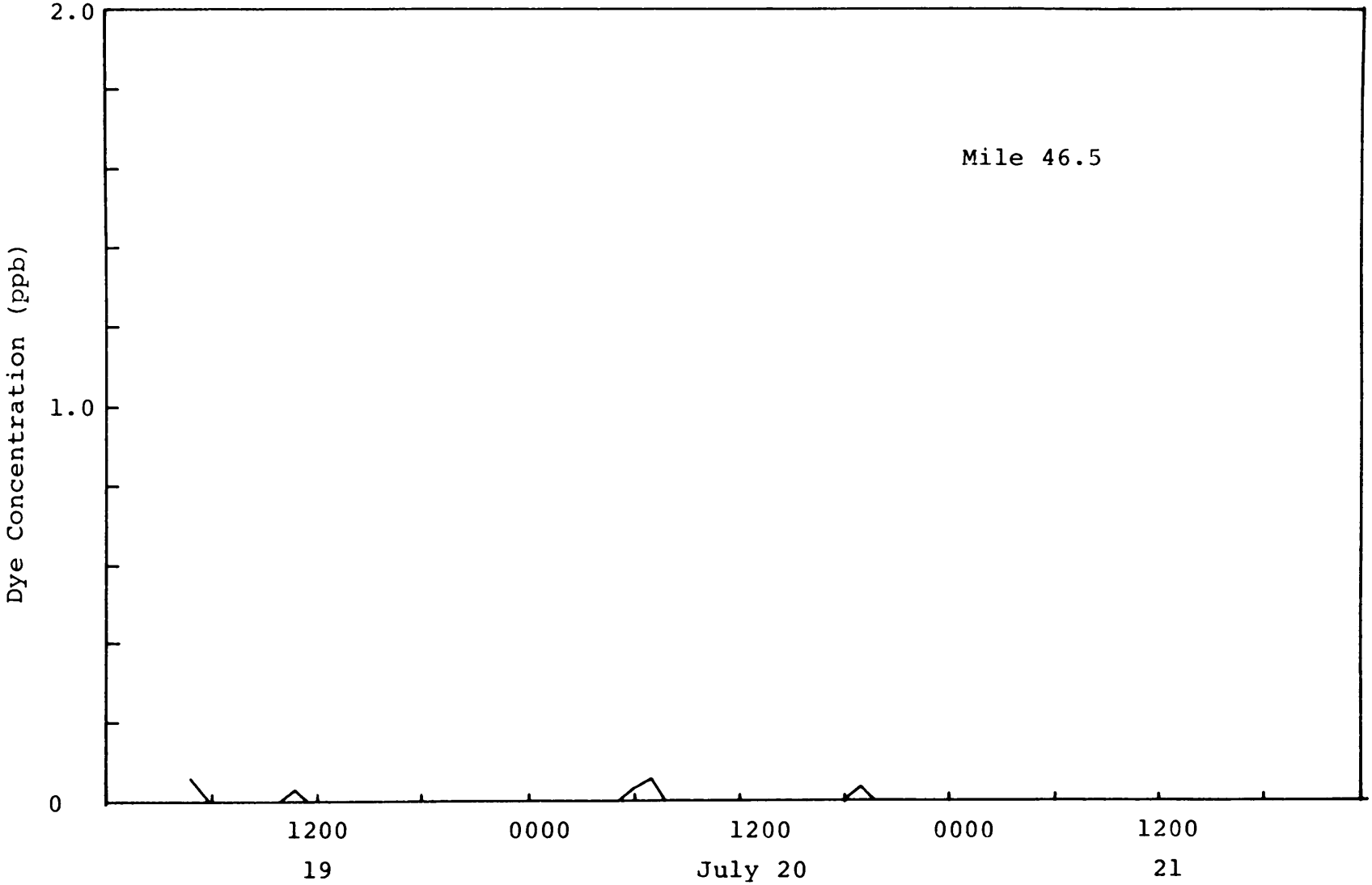

Figure B19. Observed Dye Concentration at Mile 46.5.

APPENDIX C

Observed Tidal Currents and Tidal Heights

July, 1973

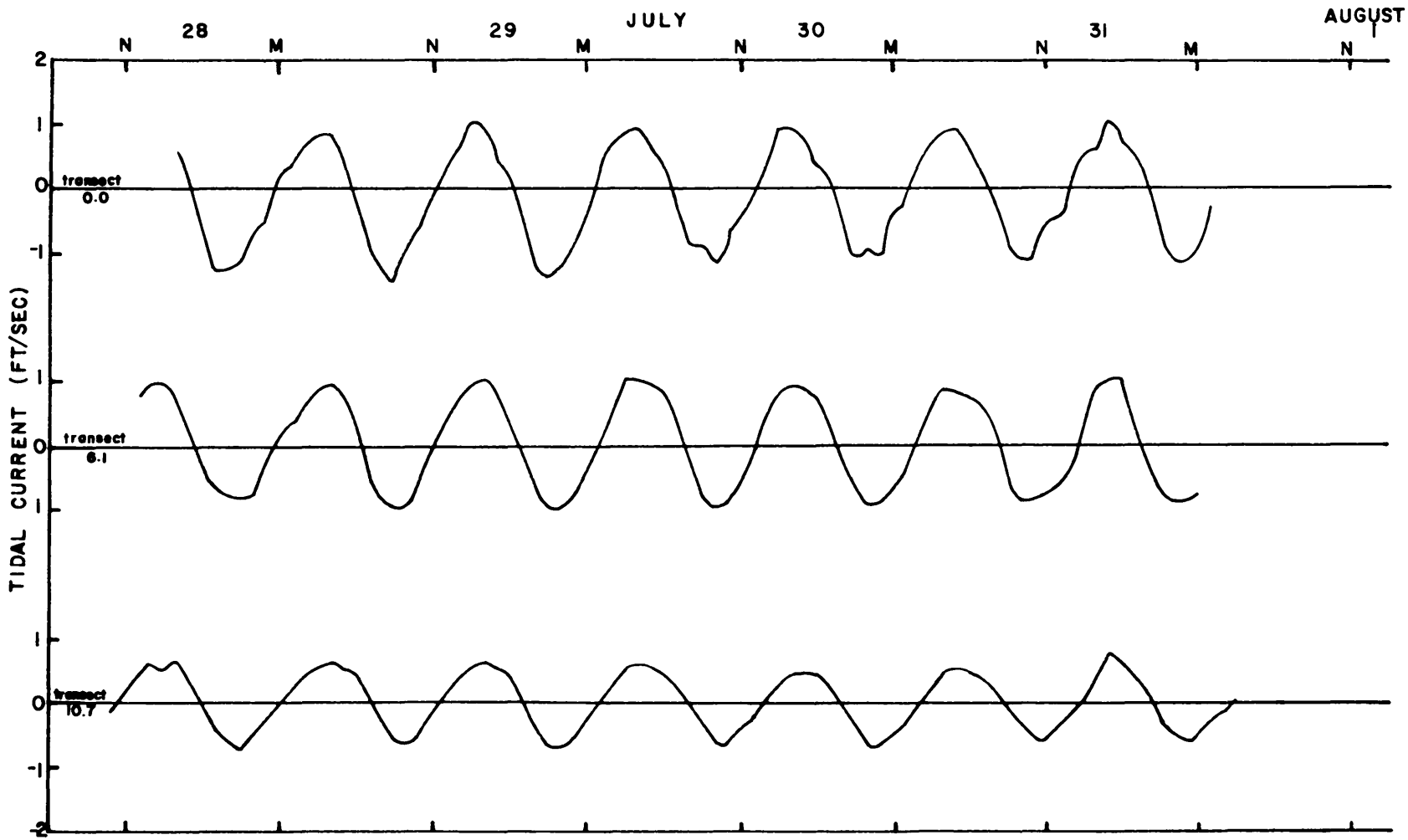

Figure C1. Cross-Section Average of Tidal Current at Mile 0, Mile 6.1, Mile 10.7.

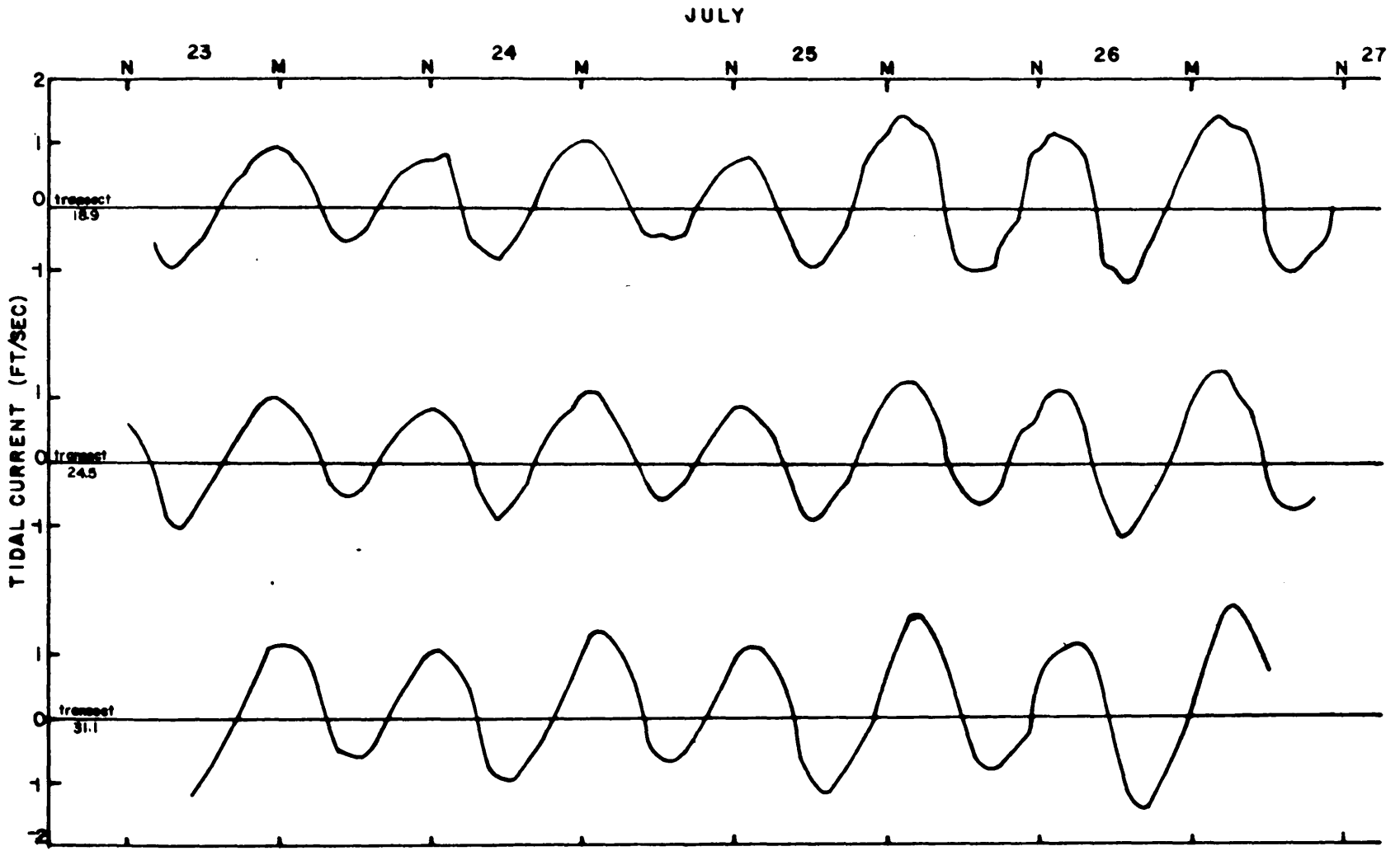

Figure C2. Cross-Section Average of Tidal Current at Mile 18.9, Mile 24.5, Mile 31.1.

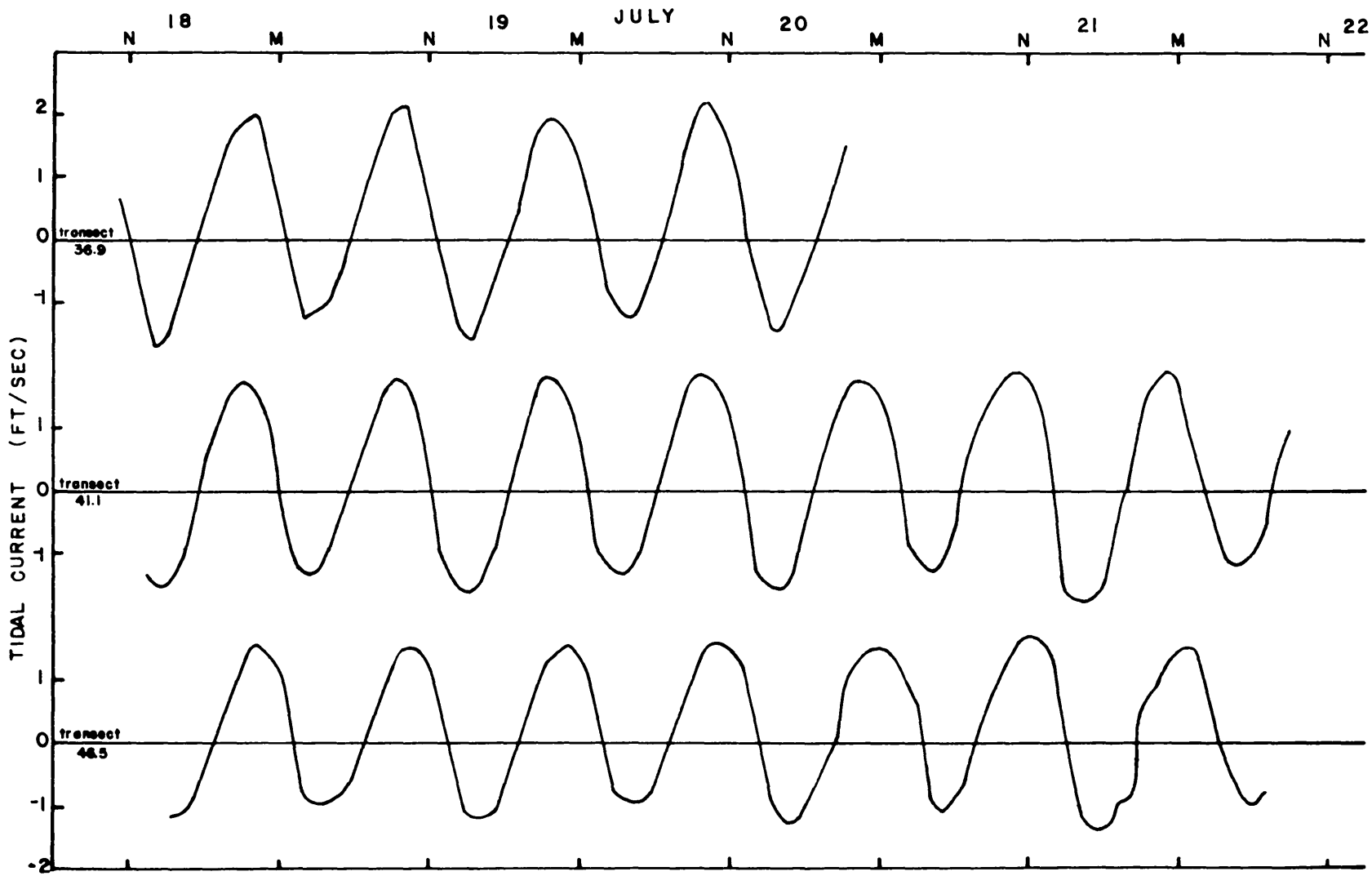

Figure C3. Cross-Section Average of Tidal Current at Mile 36.9, Mile 41.1, Mile 46.5.

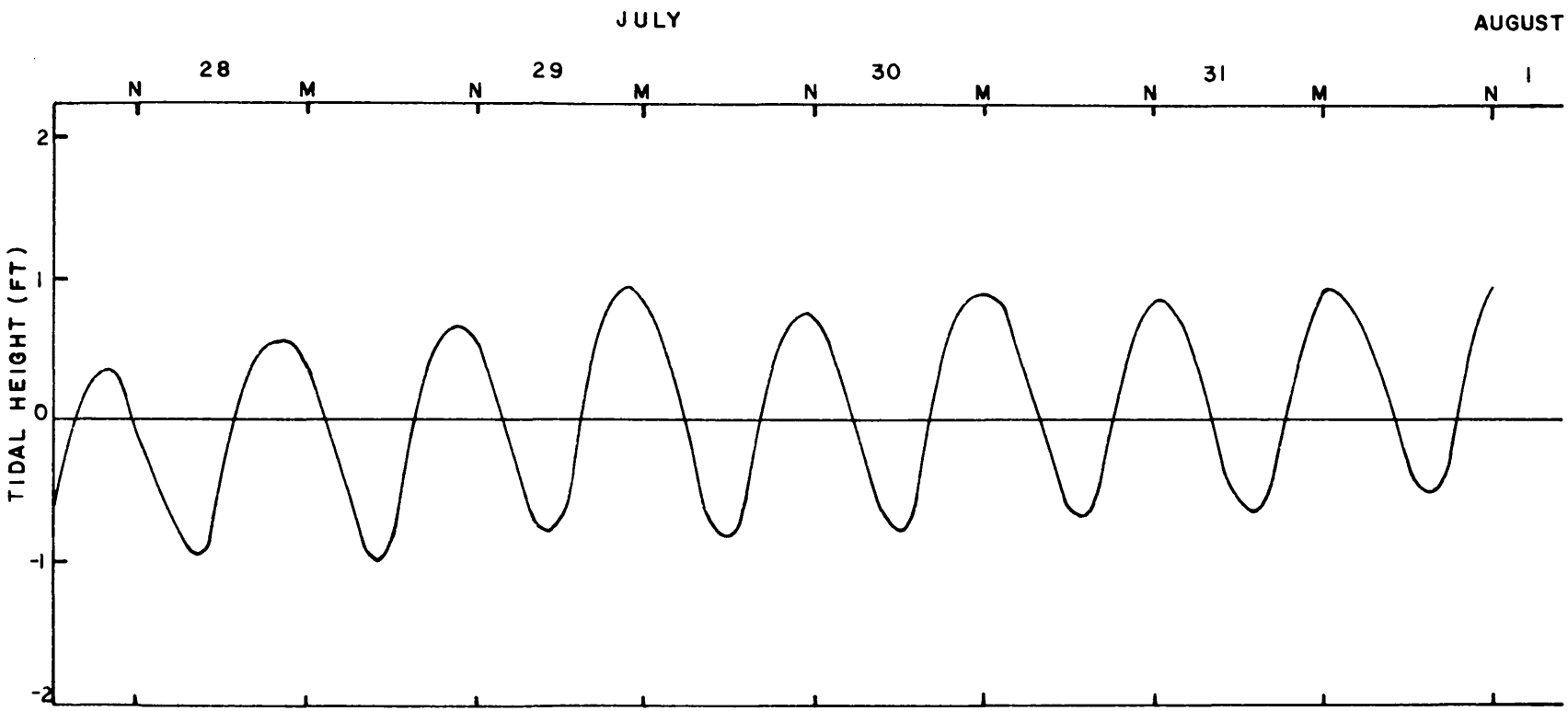

Figure C4. Tidal Height above Mean Sea Level at Grey's Point.

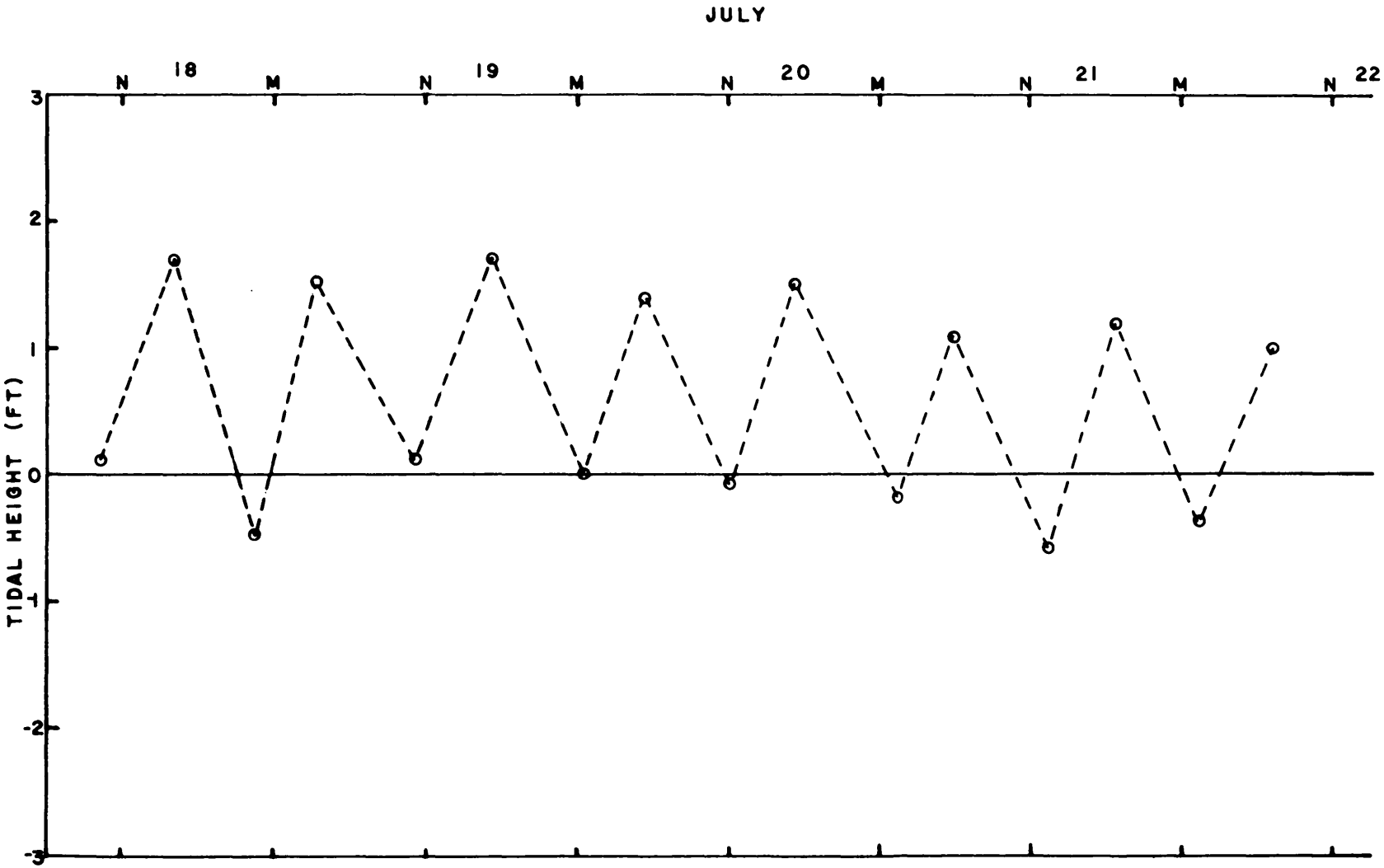

Figure C5. Tidal Height above Mean Sea Level at Tappahannock.